BRNO UNIVERSITY OF TECHNOLOGY
VYSOKÉ UČENÍ TECHNICKÉ V BRNĚ

FACULTY OF MECHANICAL ENGINEERING
FAKULTA STROJNÍHO INŽENÝRSTVÍ

ENERGY INSTITUTE
ENERGETICKÝ ÚSTAV

COMPACT SENSORS FOR EVALUATION THE THERMAL COMFORT
KOMPAKTNÍ SENZORY PRO HODNOCENÍ TEPELNÉ POHODY

DOCTORAL THESIS
DIZERTAČNÍ PRÁCE

AUTHOR Eng. Mohammad Kazkaz
AUTOR PRÁCE

SUPERVISOR prof. Eng. Milan Pavelek, CSc.
ŠKOLITEL

BRNO 2017

ABSTRACT

The air temperature is most often used to assess the thermal state of an internal environment. However, air temperature alone is insufficient in many cases to evaluate the environmental thermal state. The main objective of the thesis is evaluating the thermal state of an indoor environment and specifying the parameters that influence on it. Air temperature, mean radiant temperature, air velocity, and humidity are the four fundamental environmental parameters that determine the thermal state of an interior environment.

Given that the thermal state of an environment depends on many parameters, so it has been derived quantities which include the combined effect of several or all these parameters to determining the thermal state of the environment. Some of these quantities for example are: Effective temperature, globe temperature (temperature measured by globe thermometer), operative temperature, equivalent temperature, *PMV* and *PPD* indices… etc.
Nowadays there are a lot of high accuracy sensors which can evaluate the environmental thermal state, and due to their high price, they are primarily used for purpose of research.

The presented work is focused mainly on development of a compact plate sensor for evaluating the thermal state of an interior environment. Mainly focus was on the low cost of the sensor together with a sufficient accuracy.

To achieve the objective of the thesis, the following proceedings were carried out:

- Analysis the environmental factors affect the thermal state of an environment.
- Study the impact of the air temperature, mean radiant temperature, and air velocity on thermal indexes, the globe temperature and operative temperature.
- The theoretical comparison between globe temperature and operative temperature.
- Design, developing, and constructing a new plate sensor for assessment the thermal state of an interior environment.
- Design and constructing a testing chamber to make comparison between sensors of the thermal state of an environment.
- Calibrating the constructed sensor by measuring the physical quantities characterizing the thermal state of the environment.
- Test the developed plate sensor and comparing it with the globe thermometer in test chamber.
- Make a comparison between the theoretical solutions and the measurements in test chamber.

The results of this work are own theoretical comparison between the globe temperature and the operative temperature in the selected range of mean radiant temperature, air velocity, and air temperature for evaluating the thermal state of an internal environment.

The main output of this work is designing and constructing a simple plate sensor, which would be accurate enough to measure the thermal state of the internal environment.

Further, the testing chamber has been constructed to test the developed sensor using new measuring system INNOVA.

Keywords

Thermal state, internal environment, thermal comfort, globe temperature, operative temperature, plate temperature, environmental factors, thermal indexes.

ABSTRAKT

Teplota vzduchu je nejčastěji používaná k posouzení tepelného stavu vnitřního prostředí. Avšak teplota vzduchu sama o sobě, je v mnoha případech pro toto posouzení nedostatečná.
Hlavním cílem disertační práce je vyhodnotit tepelný stav vnitřního prostředí a specifikovat parametry, které na něj mají vliv. Teplota vzduchu, střední radiantní teplota, rychlost vzduchu a vlhkost vzduchu jsou čtyři základní parametry, které určují tepelný stav vnitřního prostředí.

Vzhledem k tomu, že tepelný stav prostředí závisí na mnoha aspektech, byly odvozeny veličiny, které zahrnují kombinovaný účinek několika nebo všech těchto parametrů k určení tepelného stavu prostředí. Jedná se např. o efektivní teplotu, teplotu kulového teploměru, operativní teplotu, ekvivalentní teplotu, *PMV* a *PPD* indexy... aj.
V dnešní době existuje spousta vysoce přesných senzorů, které mohou zhodnotit tepelný stav vnitřního prostředí. Z důvodu jejich vysoké ceny jsou používané převážně pro účely výzkumu.

Předkládaná práce se převážně soustředí na vývoj kompaktního deskového senzoru pro vyhodnocení tepelného stavu vnitřního prostředí. Zaměřuje se hlavně na nízkou cenu senzoru společně s dostatečnou přesností.

K dosažení cíle této práce jsou provedeny následující postupy:

- Analýza environmentálních faktorů ovlivňujících tepelný stav prostředí.
- Studium dopadu teploty vzduchu, střední radiantní teploty a rychlosti proudění vzduchu na tepelné indexy: teplotu kulového teploměru a operativní teplotu.
- Teoretické porovnání teploty kulového teploměru a operativní teploty.
- Navržení, rozvoj a konstrukce nového deskového senzoru pro posouzení tepelného stavu vnitřního prostředí.
- Navržení a konstrukce testovací komory pro porovnávání senzorů tepelného stavu prostředí.
- Kalibrace zkonstruovaného senzoru měřením fyzikálních veličin charakterizujících tepelný stav prostředí.
- Testy směrové závislosti vyvinutého deskového senzoru a porovnání s kulovým teploměrem v testovací komoře.
- Srovnání teoretických řešení s provedenými měřeními v testovací komoře.

Výsledkem této práce je vlastní teoretické srovnání teploty kulového teploměru a operativní teploty ve vybraném rozsahu teploty vzduchu, střední radiantní teploty a rychlosti vzduchu pro možnost hodnocení tepelného stavu vnitřního prostředí pomocí kulového teploměru.

Hlavním výstupem je však navržení a zhotovení jednoduchého deskového senzoru, který by byl dostatečně přesný pro měření tepelného stavu prostředí.

V rámci disertace byla postavena také testovací komora a bylo provedeno testování vyvinutého senzoru pomocí měřicího systému INNOVA.

Klíčová slova

Tepelný stav, vnitřní prostředí, tepelná pohoda, kulová teplota, operativní teplota, teplota desky, faktory prostředí, tepelné indexy.

BIBLIOGRAPHIC CITATION:

KAZKAZ, M. *Compact sensors for evaluation the thermal comfort*. Brno: Brno University of Technology, Faculty of Mechanical Engineering, 2017. 140 pp., Supervisor of doctoral thesis: prof. Eng. Milan Pavelek, CSc.

KAZKAZ, M. *Kompaktní senzory pro hodnocení tepelné pohody*. Brno: Vysoké učení technické v Brně, Fakulta strojního inženýrství, 2017. 140 s. Vedoucí dizertační práce prof. Ing. Milan Pavelek, CSc.

Declaration

I hereby confirm that I have written the thesis independently, under the supervision of prof. Eng. Milan Pavelek, CSc. and using the listed references

In Brno, 30. 8. 2017

Eng. Mohammad Kazkaz

Preface

The present Ph.D. thesis summarizes the author's research work performed at the Thermodynamics and Environmental Engineering, Department of Mechanical Engineering at the Brno University of Technology in the period between September 2010 and August 2017 under the supervision of Professor *Milan Pavelek*.

I would like to express my sincere gratitude to my supervisor Milan Pavelek for his guidance throughout my doctoral study. I much value all his exciting discussions of my work, his useful advice, and his help.

Warm thanks to my colleagues at the department of Thermodynamics and Environmental Engineering, I enjoyed working among you.

Special thanks to my parents and my beloved Razan: for their never-ending support.

The Ph.D. study was performed as a part of the project "Research on energy efficient systems to reach indoor environment comfort" granted by the faculty of Mechanical Engineering at the Brno University of Technology, grant no. GAČR 101/09/H050.

Table of Contents

ABSTRACT **3**

INTRODUCTION **13**

I. LITERATURE SURVEY **15**

1. BRIEF INTRODUCTION OF THE HEAT TRANSFER **15**
1.1. CONDUCTION HEAT TRANSFER 15
1.2. CONVECTION HEAT TRANSFER 15
1.2.1. Classification of Fluid Flows 16
1.2.2. Dimensionless Numbers 16
1.2.3. Forced Heat Transfer in External Flow 18
1.2.4. Natural Heat Transfer in External Flow 20
1.2.5. Combined Natural and Forced Convection 22
1.3. RADIANT HEAT TRANSFER 22
1.3.1. Blackbody Radiation 23
1.3.2. Emissivity 23
1.3.3. View Factor 24
1.3.4. Radiation Heat Transfer Between Black Surfaces 26
1.3.5. Radiation Heat Transfer Between Two Real Surfaces Enclosure 26
1.3.6. Radiation Heat Transfer Between the Globe Thermometer and Its Environment 27
2. THERMAL COMFORT **30**
2.1. ENVIRONMENTAL FACTORS 30
2.1.1. Air Temperature 30
2.1.2. Mean Radiant Temperature 32
2.1.3. Air Velocity 33
2.1.4. Humidity 33
2.2. PERSONAL FACTORS 34
2.2.1. Clothing Insulation 34
2.2.2. Metabolic Heat 36
3. HEAT BALANCE EQUATION OF THE HUMAN BODY **39**
3.1. HUMAN THERMOREGULATION SYSTEM 39
3.2. HEAT BALANCE EQUATION 40
3.2.1. Heat Production Within Human Body 42
3.2.2. Heat Loss from the Skin 42
3.2.3. Heat Loss by Respiration 44
4. THERMAL COMFORT INDICES **45**
4.1. DRY-BULB TEMPERATURE 45
4.2. WET-BULB TEMPERATURE 45

4.3. EFFECTIVE TEMPERATURE 46
4.4. GLOBE THERMOMETER TEMPERATURE 48
4.5. EQUIVALENT TEMPERATURE 49
4.6. OPERATIVE TEMPERATURE 50
4.7. WET BULB GLOBE TEMPERATURE 51
4.8. PREDICTED MEAN VOTE 52
4.9. PREDICTED PERCENTAGE DISSATISFIED 53
4.10. DRAUGHT RATE 53

II. THEORETICAL SOLUTION 54

1. INTRODUCTION TO THEORETICAL SOLUTION 54
2. MATHEMATICAL METHODS OF SOLVING THE EQUATIONS 57
2.1. METHODS OF SOLVING THE NONLINEAR EQUATION 57
2.2. NEWTON-RAPHSON METHOD 58
2.3. SECANT METHOD 59
2.4. STOPPING CRITERION 59
3. THEORETICAL SOLUTION OF GLOBE TEMPERATURE 60
3.1. FIRST THEORETICAL SOLUTION OF GLOBE TEMPERATURE 62
3.2. SECOND THEORETICAL SOLUTION OF GLOBE TEMPERATURE 65
4. THEORETICAL SOLUTION OF OPERATIVE TEMPERATURE 69
4.1. FIRST THEORETICAL SOLUTION OF OPERATIVE TEMPERATURE 70
4.2. SECOND THEORETICAL SOLUTION OF OPERATIVE TEMPERATURE 74
5. COMPARISON BETWEEN GLOBE AND OPERATIVE TEMPERATURES 77
5.1. DISCUSSION OF THE RESULTS 80
6. THEORETICAL SOLUTION OF PLATE TEMPERATURE 82
6.1. FIRST THEORETICAL SOLUTION OF SMALL PLATE TEMPERATURE 83
6.2. SECOND THEORETICAL SOLUTION OF SMALL PLATE TEMPERATURE 86
7. COMPARISON BETWEEN PLATE AND OPERATIVE TEMPERATURES 89
7.1. DISCUSSION OF THE RESULTS: 92
8. THEORETICAL SOLUTION OF LARGE PLATE SENSOR 98

III. PRACTICAL PART 104

1. CONSTRUCTION OF PLATE COMPACT SENSOR 104
2. EXPERIMENTAL EQUIPMENT 107
2.1. TESTING CHAMBER 107
2.2. CALIBRATION CHAMBER 108
2.3. INNOVA SYSTEM FOR MEASUREMENT THE THERMAL COMFORT 109
2.3.1. List of The INNOVA Sensors Used in Doctoral Measurements 111
3. EXPERIMENTAL MEASUREMENTS 115

3.1. COMPARISON BETWEEN GLOBE AND OPERATIVE TEMPERATURES IN THE TESTING CHAMBER 115
3.2. TESTING THE DESIGNED PLATE SENSOR 118
3.3. IMPACT OF THE DIRECTIONAL RADIATION ON THE TESTING SENSORS 120

CONCLUSION 123

LIST OF THE IMPORTANT SYMBOLS 127

REFERENCES 131

AUTHOR'S PUBLICATIONS 140

INTRODUCTION

The importance of the thermal comfort in an internal environment (microclimate) comes from that the body of the living person responds to the environmental variables in a dynamic interaction, which can cause discomfort, decrease of activity, damage of health, or even death if the response is unsuitable. Thus, the evaluating of the thermal state of an environment will specify the person's feeling towards his environment, in other words, will determine if a person feels cold, hot or in thermal comfort.

It has been known for a long time that the thermal comfort of a human isn't only function of air temperature. The air temperature, mean radiant temperature, air velocity, humidity, activity level, and clothing thermal resistance are the fundamental parameters affected the thermal comfort. These parameters are called the six fundamental factors that define the human thermal comfort. If the activity level and clothing thermal resistance were excluded from the previous factors, we will get the four environmental factors that define the thermal state of the environment.

In an indoor environment, to evaluate the thermal comfort it is necessary to determine the six fundamental factors, from which is calculated one quantity for evaluating the thermal comfort. Such as these quantities; the effective temperature, the globe temperature, the equivalent temperature, the operative temperature, *PMV* index, *PPD* index, etc.

In this work, it had studied the effect of the mean radiant temperature, air velocity, and air temperature on the thermal state of an environment through finding the relation between previous variables and each of operative temperature and globe temperature. Later, a comparison between globe and operative temperatures had done, where the comparison is carried out using own procedure for the application of the theoretical solutions of operative and globe temperatures in a wide range of air temperature, mean radiant temperature and air velocity. This method of applying the theoretical solution can be used later to develop the new sensors.

The second part of doctorate study is focused on development of new compact sensor for continuous and effective measurement of thermal state. The application of the new sensor is in regulation (in rooms, air-conditioned cabins and control rooms), where the sensor was constructed so that can be placed on different surfaces easily. The developed sensor was calibrated, in a special chamber by measuring the physical quantities characterizing the thermal state of the internal environment.

I. LITERATURE SURVEY

1. Brief Introduction of The Heat Transfer

Before introducing the thermal comfort, a brief overview of heat transfer by conduction, convection, and radiation (which are needed in this work) was achieved in this paragraph.

1.1. Conduction Heat Transfer

The Conduction heat transfer is defined as the energy transfer from the greater energetic particles of a matter to the adjacent less energetic ones as a result of interactions between the particles. Conduction can take place in solids, liquids, or gases (Çengel 2003).

The heat conduction rate through a medium depends on the geometry of the medium, its thickness, and the matter of the medium, as well as the temperature difference across the medium. Consider steady state of conduction heat transfer through a large plane wall of thickness dx and area A (Çengel 2003). The rate of heat transfer Q through the wall is given by Fourier's law of heat conduction as following:

$$Q_{con} = -kA\frac{dT}{dx} \tag{1}$$

where
k is the thermal conductivity of the medium, W. m^{-1}. K^{-1},
A is the heat transfer area, m^2,
dT/dx is the temperature gradient at location x, K.m^{-1}.

1.2. Convection Heat Transfer

The process of heat convection is defined as process of carrying heat away by a moving fluid. In spite of the complexity of convection, the rate of convection heat transfer is proportional to the temperature difference and is conveniently expressed by Newton's law of cooling as (Lienhard 2011):

$$Q_c = h_c A(T_s - T_\infty) \tag{2}$$

or, per unit of the surface area:

$$q_c = h_c(T_s - T_\infty) \tag{3}$$

where

h_c is the convection heat transfer coefficient, W. m^{-2}. K^{-1},
A is the heat transfer surface area, m^2,
T_s is the temperature of the surface, K,
T_∞ is the temperature of the fluid sufficiently far from the surface, K.

Despite the simple appearance of the Newton's law of cooling, but determination of the convection heat transfer coefficient h_c is quite complicated task, because it depends on the several of the variables such as surface geometry, the nature of the fluid motion, and an assortment of fluid thermodynamic and transport properties.

Thus, the study of convection heat transfer reduces to a study of means by which the convection heat transfer coefficient h_c may be determined (Incropera et al. 2007).

1.2.1. Classification of Fluid Flows

- *Laminar and Turbulent Flow*: Flows can be distinguished into two types. The highly-ordered fluid motion characterized by smooth streamlines is called *laminar*. The second type is the highly-disordered fluid motion that typically occurs at high velocities characterized by velocity fluctuations is called *turbulent*.
- *Natural and Forced Flow*: A fluid flow can be classified to natural or forced. In *natural* flows, the fluid motion is due to a natural means such as the buoyancy effect. In *forced* flow, a fluid is forced to flow by external means such as a pump or a fan.

1.2.2. Dimensionless Numbers

In the heat transfer analysis, it is common to combine the variables of one relationship into dimensionless number to reduce the number of total variables. The important dimensionless numbers used in the convection heat transfer analysis are next listed.

– Nusselt Number

The Nusselt number *Nu* is named after Wilhelm Nusselt, who made significant contributions to convective heat transfer in the first half of the twentieth century, and it is viewed as the dimensionless convection heat transfer coefficient. The Nusselt number is defined as *the ratio of heat transfer through the fluid layer by convection to heat transfer through the fluid layer by pure conduction*.

The Nusselt number is expressed as:

$$Nu = h_c \frac{L}{k} \tag{4}$$

where

k is the thermal conductivity of the fluid, $W.m^{-1}.\ K^{-1}$,

L is the characteristic length, m.

– Prandtl Number

Prandtl number *Pr* is named after Ludwig Prandtl, who introduced the concept of boundary layer in 1904 and made significant contributions to boundary layer theory. Prandtl number is defined as *the ratio of momentum diffusivity to the heat diffusivity*.

$$Pr = \frac{\text{Molecular diffusivity of momentum}}{\text{Molecular diffusivity of heat}} = \frac{\nu}{\alpha} = \frac{\mu c_p}{k} \tag{5}$$

where

υ is the kinematic viscosity, $m^2.\ s^{-1}$,

α is the thermal diffusivity, $m^2.\ s^{-1}$,

μ is the dynamic viscosity of the fluid, $kg.m^{-1}.\ s^{-1}$ or $N.\ s.\ m^{-2}$,

C_p is the specific heat capacity, $J.kg^{-1}.\ K^{-1}$,

k is the thermal conductivity of the fluid, $W.m^{-1}.\ K^{-1}$.

The Prandtl numbers of gases are about 1, which indicates that both momentum and heat dissipate through the fluid at about the same rate.

– Reynolds Number

Reynolds number *Re* is a dimensionless quantity; it is defined as *the ratio of the inertia forces to viscous forces in the fluid*. The Reynolds number is expressed as:

$$Re = \frac{\text{Inertia force}}{\text{Viscous}} = \frac{wL}{\nu} = \frac{\rho w L}{\mu} \tag{6}$$

where

w is the upstream velocity, $m.s^{-1}$,

L is the characteristic length of the geometry, m,

ρ is the density of the fluid, $kg.m^{-3}$.

At large Reynolds numbers, the inertia forces are large relative to the viscous forces, so the viscous forces cannot prevent the random and rapid fluctuations of the fluid, and thus the flow is turbulent. At small Reynolds numbers, the viscous forces are large enough to keep the fluid in line. Thus, in this case the flow is laminar.

The Reynolds number at which the flow becomes turbulent is called the critical Reynolds number Re_{cr}. The value of the critical Reynolds number is different for different geometries. For flow over a flat plate, the generally accepted value of the critical Reynolds number is $Re_{cr} = 5\times10^5$, and for flow over a cylinder or sphere $Re_{cr} = 2\times10^5$.

– Grashof Number

It is known that the flow regime in heat transfer is characterized by the Reynolds number, which represents the ratio of inertial forces to viscous forces acting on the fluid. In the natural convection heat transfer the flow regime is characterized by the dimensionless Grashof number *Gr*, which represents the *ratio of the buoyancy force to the viscous force acting on the fluid*:

$$Gr = \frac{g\beta(T_s - T_\infty)L^3}{\nu^2} \tag{7}$$

where

g is the gravitational acceleration, $m.s^{-2}$,

β is the coefficient of volume expansion, K^{-1} ($\beta = 1/T$ for ideal gas),

υ is the kinematic viscosity of the fluid, $m^2.\ s^{-1}$,

T_s is the temperature of the surface, K,

T_∞ is the temperature of the fluid sufficiently far from the surface, K,

L is the characteristic length of the geometry, m.

Usually, for the external flow, the both natural and forced heat transfer are presented. In such cases, it is important to determining the relative value of each mode of heat transfer, the relative importance of each mode is evaluated by the following ratio: Gr / Re^2, where

for $Gr / Re^2 \ll 1$ the natural convection effects are negligible,
for $Gr / Re^2 \gg 1$ the forced convection effects are negligible and free convection dominates, and
for $Gr / Re^2 \approx 1$ the both effects are significant and must be considered.

– Rayleigh Number

For natural convection heat transfer with the same fluids, it is possible to use the Rayleigh number *Ra* which is the product of the Grashof and Prandtl numbers:

$$Ra = GrPr = \frac{g\beta(T_s - T_\infty)L^3}{\nu^2}Pr \tag{8}$$

1.2.3. Forced Heat Transfer in External Flow

- Parallel Flow Over Flat Plates:

Consider the parallel flow of a fluid over a flat plate of length L, as shown in Figure 1, where w and T_∞ are the velocity and temperature of the free stream. The flow starts out as laminar, but if the plate is sufficiently long, the flow will become turbulent at a distance x_{cr} from the leading edge where the Reynolds number reaches its critical value for transition.

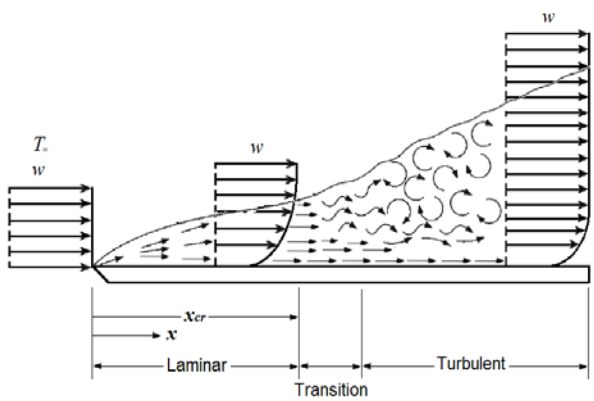

Figure 1. Laminar and turbulent flow over a flat plate

The average Nusselt number for laminar and turbulent flow over a flat plate is determined from the following equation (Çengel 2003; Pohlhausen 1921):
for laminar flow

$$Nu = \frac{h_c L}{k} = 0.664 Re^{0.5} Pr^{1/3} \tag{9}$$

$$Re < 5 \times 10^5$$

$$Pr \geq 0.6$$

for turbulent flow

$$Nu = \frac{h_c L}{k} = 0.037 Re^{0.8} Pr^{1/3} \tag{10}$$

$$5 \times 10^5 \leq Re \leq 10^7$$

$$0.6 \leq Pr \leq 60$$

For a wide range of Prandtl number, the average Nusselt number for turbulent flow over a flat plate can be determined by using the following correlation (Schlichting 1958):

$$Nu = \frac{h_c L}{k} = \frac{0.037 Re^{0.8} Pr}{1 + 2.44 Re^{-0.1}(Pr^{2/3} - 1)} \tag{11}$$

$$5 \times 10^5 < Re < 10^7$$

$$0.5 \leq Pr \leq 2000$$

All properties in the previous equations must be evaluated at the film temperature T_f, where $T_f = (T_s + T_\infty) / 2$.

- <u>Flow Across Sphere</u>

The characteristic length of a sphere is taken to be the external diameter D. The critical Reynolds number for flow across a sphere is $Re_{cr} \approx 2\times10^5$. The average Nusselt number for flow over a sphere is recommended to calculate from the following relation (Whitaker 1972):

$$Nu = \frac{h_c D}{k} = 2 + \left[0.4 Re^{0.5} + 0.06 Re^{2/3}\right] Pr^{0.4} \left(\frac{\mu_\infty}{\mu_s}\right)^{0.25} \tag{12}$$

$$3.5 \leq Re \leq 7.6 \times 10^4$$

$$0.71 \leq Pr \leq 380$$

The fluid properties in this case are evaluated at the free-stream temperature T_∞, except for μ_s, which is evaluated at the surface temperature T_s.

- <u>The Combined Laminar and Turbulent Flow Over a Flat Plate</u>

For mixed laminar and turbulent flow, the average Nusselt number over the entire plate is determined from the following equation (Çengel 2003):

$$Nu = \frac{h_c L}{k} = (0.037 Re^{0.8} + 871) Pr^{1/3} \tag{13}$$

$$5 \times 10^5 \leq Re \leq 10^7$$

$$0.6 \leq Pr \leq 60$$

All properties in the equation must be evaluated at the film temperature T_f, and the critical Reynolds number in this relation to be $Re_{cr} = 5 \times 10^5$.

A comprehensive correlation presented by Schlunder which provide the average Nusselt number for mixed laminar and turbulent flow (Schlünder 1975):

$$Nu = minNu + \sqrt{Nu_{lam}^2 + Nu_{turb}^2} \tag{14}$$

where

$$Nu_{lam} = 0.664 Re^{0.5} Pr^{1/3}$$

$$Nu_{turb} = \frac{0.037Re^{0.8}Pr}{1 + 2.44Re^{-0.1}(Pr^{2/3} - 1)}$$

$$0 < Re < 10^7$$

$$0.5 \leq Pr \leq 2500$$

Where min $Nu \leq 2$ is the minimum Nusselt number, and its value related to the shape of the body. Generally, every three-dimensional finite body has a minimal Nu, which can't be exceeded it in any way. The sphere has the largest mini $Nu = 2$, for cylinder mini $Nu = 0.3$, and for a flat plate min $Nu = 0$ (Schlünder 1975).

The correlation (14) is plotted on the Figure 2. for $Pr = 0.7$.

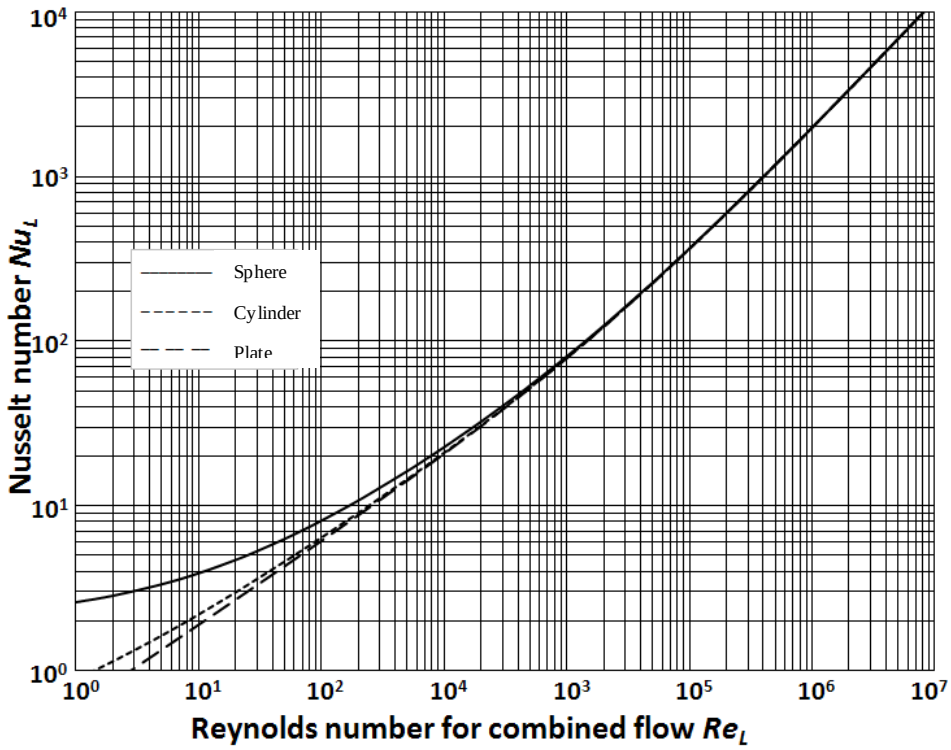

Figure 2. Nusselt number as function of Reynolds number for mixed (laminar and turbulent) flow around sphere, cylinder, and plate

1.2.4. Natural Heat Transfer in External Flow

- <u>Natural Convection Over Surfaces</u>

The heat transfer relations in natural convection are based on experimental studies. The simple empirical correlations for the average Nusselt number Nu are of the form:

$$Nu = \frac{h_c L}{k} = c(GrPr)^n = cRa^n \tag{15}$$

The values of the constants c and n depend on the geometry of the surface and the flow regime, which is characterized by the range of the Rayleigh number. The value of n is usually 1/4 for laminar flow and 1/3for turbulent flow. The value of the constant C is normally less than 1.

For natural convection over vertical plate Churchill and Chu are recommended to use the following relation (Churchill et al. 1975):

$$Nu = \left[0.825 + \frac{0.387Ra^{1/6}}{[1 + (0.492/Pr)^{9/16}]^{8/27}}\right]^2 \tag{16}$$

This relation is applicable over the entire range of Rayleigh number.

For natural convection over sphere the following correlation is recommended for $Pr \geq 0.7$ and $Ra \leq 10^{11}$ (Churchill 1983):

$$Nu = 2 + \frac{0.5897Ra^{1/4}}{[1 + (0.492/Pr)^{9/16}]^{4/9}} \tag{17}$$

all fluid properties are to be evaluated at the film temperature T_f. In Table 1. are listed the relations for the average Nusselt number of various geometries (Çengel 2003).

Table 1. Empirical correlations for the average *Nu* for natural convection (Çengel 2003)

Geometry	Characteristic length L_c	Range of Ra	Nu
Vertical plate 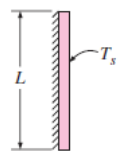	L	10^4–10^9 10^9–10^{13} Entire range	$Nu = 0.59Ra_L^{1/4}$ $Nu = 0.1Ra_L^{1/3}$ $Nu = \left\{0.825 + \frac{0.387Ra_L^{1/6}}{[1 + (0.492/Pr)^{9/16}]^{8/27}}\right\}^2$ (complex but more accurate)
Horiontal plate (Surface area A and perimeter p) (a) Upper surface of a hot plate (or lower surface of a cold plate) 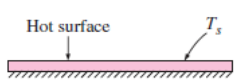 (b) Lower surface of a hot plate (or upper surface of a cold plate) 	A_s/p	10^4–10^7 10^7–10^{11} 10^5–10^{11}	$Nu = 0.54Ra_L^{1/4}$ $Nu = 0.15Ra_L^{1/3}$ $Nu = 0.27Ra_L^{1/4}$
Vertical cylinder 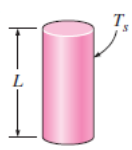	L		A vertical cylinder can be treated as a vertical plate when $D \geq \frac{35L}{Gr_L^{1/4}}$
Horizontal cylinder 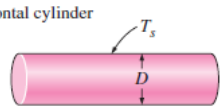	D	$Ra_D \leq 10^{12}$	$Nu = \left\{0.6 + \frac{0.387Ra_D^{1/6}}{[1 + (0.559/Pr)^{9/16}]^{8/27}}\right\}^2$
Sphere 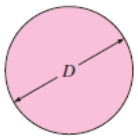	D	$Ra_D \leq 10^{11}$ ($Pr \geq 0.7$)	$Nu = 2 + \frac{0.589Ra_D^{1/4}}{[1 + (0.469/Pr)^{9/16}]^{4/9}}$

1.2.5. Combined Natural and Forced Convection

It is known that natural convection always accompanies forced convection. Therefore, it is desirable to have a criterion to estimate the relative importance of natural convection in the presence of forced convection. For a given fluid the ratio Gr / Re^2 represents the importance of natural convection relative to forced convection. Where:

for Gr / Re^2 « 1 the natural convection effects are negligible,

for Gr / Re^2 » 1 the forced convection effects are negligible and free convection dominates,

for Gr / Re^2 ≈ 1 the both effects are significant and must be considered.

Schlunder in his book (Schlünder 1975) presented a comprehensive correlation (equation (14)) for combined natural and forced convection heat transfer, which based on the same relation described the mixed laminar and turbulent flow:

$$Nu = minNu + \sqrt{Nu_{lam}^2 + Nu_{turb}^2}$$

$$Nu_{lam} = 0.664 Re_{comb.}^{0.5} Pr^{1/3} \tag{18}$$

$$Nu_{turb} = \frac{0.037 Re_{comb.}^{0.8} Pr}{1 + 2.44 Re_{comb.}^{-0.1} (Pr^{2/3} - 1)}$$

where for combined natural and forced heat transfer Schlunder suggested to use combined Reynolds number (Schlünder 1975):

$$Re_{comb.} = \sqrt{Re^2 + \frac{Gr}{2.5}} \tag{19}$$

Another expression has become widespread practice to use for the combined natural and forced convection heat transfer (Churchill 1998):

$$Nu_{comb.} = \left(Nu_{forced}^n \pm Nu_{natural}^n\right)^{1/n} \tag{20}$$

where Nu_{forced} and $Nu_{natural}$ are determined from the correlations for pure forced and pure natural convection, respectively.

The plus sign is for assisting and transverse flows and the minus sign is for opposing flows. The value of the exponent n varies between 3 and 4, depending on the geometry involved. The best correlation of data is often obtained for n = 3 for vertical plate, n = 7/2 for horizontal plate, and n = 4 for cylinders or spheres (Churchill 1998).

1.3. Radiant Heat Transfer

The fundamental of radiation was established in 1864 by the physicist James Maxwell. Maxwell postulated that accelerated changing electric currents give rise to electric and magnetic fields. These fields are called electromagnetic radiation, which represent the energy emitted by matter (Çengel 2003).

The type of electromagnetic radiation that is related to heat transfer is called the thermal radiation emitted as a result of energy transitions of molecules, atoms, and electrons of a substance. The absolute temperature is a measure of the strength of the thermal radiation.

Thermal radiation is continuously emitted by all subjects whose temperature is above absolute zero. That is, everything around us such as walls, furniture, and our bodies (Holman 2002).

1.3.1. Blackbody Radiation

Everything at a temperature above absolute zero emits radiation in all directions. The amount of radiation energy emitted from subjects depends on the material of the subject and the condition of its surface as well as the surface temperature.

An idealized body, called a blackbody is defined as a perfect emitter and absorber of radiation. The blackbody is emitted the maximum amount of radiation that can be emitted by a surface at a given temperature.

Also, a blackbody emits radiation energy uniformly in all directions per unit area normal to direction of emission. The radiation energy emitted by a blackbody per unit time and per unit surface area was determined experimentally by Joseph Stefan in 1879 and expressed as (Lienhard 2011):

$$e_b = \sigma T^4 \tag{21}$$

where:

e_b is the specific radiation energy emitted by a blackbody at absolute temperature T, W.m^{-2},

σ is the Stefan–Boltzmann constant, $\sigma = 5.67 \times 10^{-8}$ W. m^{-2}· K^{-4},

T is the absolute temperature of the surface, K.

The last equation is known as the Stefan–Boltzmann law and e_b is called the blackbody emissive power.

1.3.2. Emissivity

The radiation energy emitted by a real body at absolute temperature T does not equal to the energy emitted by a black body at the same temperature T. The ratio of the radiation emitted by the real body at a given temperature to the radiation emitted by a blackbody at the same temperature represents the emissivity of a real body. The emissivity of a body is denoted by ε, and it varies between zero and one, where the emissivity of the black body is ε =1 (Modest 1993).

The emissivity of real body (non-blackbody) can be expressed mathematically as follow:

$$\varepsilon = \frac{e}{e_b} \tag{22}$$

Then the total radiation energy emitted by a surface at the absolute temperature T is:

$$e = \varepsilon e_b = \varepsilon \sigma T^4 \tag{23}$$

The total emissivity of some surfaces at room temperature are listed in Table 2. (Sparrow et al. 1987).

1.3.3. View Factor

The radiation heat transfer between the surfaces does not depend only on the temperatures and radiation properties of the surfaces, where it depends on the orientation of the surfaces relative to each other as well as the other factors.

A new parameter called the view factor F was defined to account for the effects of orientation on the radiation heat transfer between the surfaces (Edwards 1981).

The view factor from a surface 1 to a surface 2 is denoted by F_{12}, and is defined as:

F_{12} the fraction of the radiation leaving surface 1 that strikes surface 2 directly.

The value of the view factor ranges between zero and one. When the two surfaces do not have a direct view of each other, then $F_{12} = 0$. And $F_{12} = 1$ when surface 2 surrounds surface1. The relation between the pair of view factors F_{12} and F_{21} can be expressed by the reciprocity relation as following (Siegel et al.1992):

$$A_1 F_{12} = A_2 F_{21} \tag{24}$$

where

A_1 and A_2 are the are areas of the surfaces 1 and 2, respectively, m^2.

The calculating of the view factors is very complex and difficult to perform. So, the view factors for hundreds of common geometries are evaluated and the results are listed in tables. View factors for selected geometries are given in Tables 3 and 4 (Howell 1982).

Table 2. The total emissivity for variety of substances (Sparrow et al. 1987)

Surface	ε
Aluminum	
Polished	0.03
Anodized	0.84
Foil	0.05
Copper	
Polished	0.03
Tarnished	0.75
Stainless steel	
Polished	0.60
Dull	0.21
Plated metals	
Black nickel oxide	0.08
Black chrome	0.09
Concrete	0.88
White marble	0.95
Red brick	0.93
Asphalt	0.90
Black paint	0.97
White paint	0.93
Snow	0.97
Human skin	
(caucasian)	0.97

Table 3. View factor expressions for common 3*D* geometries of finite size (Howell 1982)

Geometry	Relation
Aligned parallel rectangles 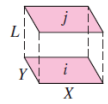	$\overline{X} = X/L$ and $\overline{Y} = Y/L$ $F_{i\to j} = \frac{2}{\pi \overline{X}\overline{Y}}\left\{\ln\left[\frac{(1+\overline{X}^2)(1+\overline{Y}^2)}{1+\overline{X}^2+\overline{Y}^2}\right]^{1/2} + \overline{X}(1+\overline{Y}^2)^{1/2}\tan^{-1}\frac{\overline{X}}{(1+\overline{Y}^2)^{1/2}} + \overline{Y}(1+\overline{X}^2)^{1/2}\tan^{-1}\frac{\overline{Y}}{(1+\overline{X}^2)^{1/2}} - \overline{X}\tan^{-1}\overline{X} - \overline{Y}\tan^{-1}\overline{Y}\right\}$
Coaxial parallel disks 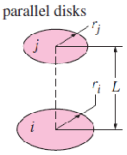	$R_i = r_i/L$ and $R_j = r_j/L$ $S = 1 + \frac{1+R_j^2}{R_i^2}$ $F_{i\to j} = \frac{1}{2}\left\{S - \left[S^2 - 4\left(\frac{r_j}{r_i}\right)^2\right]^{1/2}\right\}$
Perpendicular rectangles with a common edge 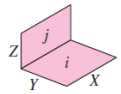	$H = Z/X$ and $W = Y/X$ $F_{i\to j} = \frac{1}{\pi W}\left(W\tan^{-1}\frac{1}{W} + H\tan^{-1}\frac{1}{H} - (H^2+W^2)^{1/2}\tan^{-1}\frac{1}{(H^2+W^2)^{1/2}} + \frac{1}{4}\ln\left\{\frac{(1+W^2)(1+H^2)}{1+W^2+H^2} \times \left[\frac{W^2(1+W^2+H^2)}{(1+W^2)(W^2+H^2)}\right]^{W^2} \times \left[\frac{H^2(1+H^2+W^2)}{(1+H^2)(H^2+W^2)}\right]^{H^2}\right\}\right)$

Table 4. View factor expressions for some infinitely long 2D geometries (Howell 1982)

Geometry	Relation
Parallel plates with midlines connected by perpendicular line 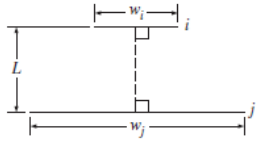	$W_i = w_i/L$ and $W_j = w_j/L$ $F_{i\to j} = \frac{[(W_i+W_j)^2+4]^{1/2} - (W_j-W_i)^2+4]^{1/2}}{2W_i}$
Inclined plates of equal width and with a common edge 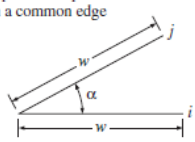	$F_{i\to j} = 1 - \sin\frac{1}{2}\alpha$
Perpendicular plates with a common edge 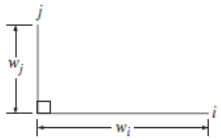	$F_{i\to j} = \frac{1}{2}\left\{1 + \frac{w_j}{w_i} - \left[1 + \left(\frac{w_j}{w_i}\right)^2\right]^{1/2}\right\}$
Three-sided enclosure 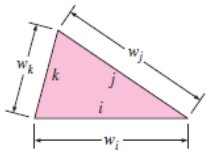	$F_{i\to j} = \frac{w_i + w_j - w_k}{2w_i}$

1.3.4. Radiation Heat Transfer Between Black Surfaces

Consider *n* black surfaces at specified temperatures. The net radiation heat transfer from any surface *i* is determined by using the view factor as following:

$$Q_i = \sum_{j=1}^{n} Q_{ij} = \sum_{j=1}^{n} A_i F_{ij} \sigma \left(T_i^4 - T_j^4\right) \tag{25}$$

where

Q_i is the net radiation heat transfer from surface *i*, W,

A_i is the area of the surface *i*, m^2,

F_{ij} is the view factor from a surface *i* to a surface *j*,

T_i, T_j are the absolute temperatures of the surfaces *i* and *j*, respectively, K.

The equation (25) can be simplified for two black surfaces 1 and 2

$$Q_1 = Q_{12} = A_1 F_{12} \sigma (T_1^4 - T_2^4) \tag{26}$$

$$Q_2 = Q_{21} = A_2 F_{21} \sigma (T_2^4 - T_1^4)$$

$$Q_1 = -Q_2$$

1.3.5. Radiation Heat Transfer Between Two Real Surfaces Enclosure

The net rate of radiation transfer between two real surfaces at one space is expressed as:

$$Q_{12} = \frac{\sigma (T_1^4 - T_2^4)}{\frac{1-\varepsilon_1}{A_1 \varepsilon_1} + \frac{1}{A_1 F_{12}} + \frac{1-\varepsilon_2}{A_2 \varepsilon_2}} \tag{27}$$

The view factor F_{12} depends on the geometry of the surfaces. Simplified forms of equation (27) for some familiar arrangements that form a two-surface are given in Table 5. (Çengel 2003).

Table 5. The radiation heat transfer between two real surfaces (Çengel 2003)

Small object in a large cavity 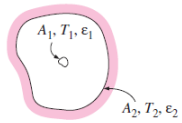	$\frac{A_1}{A_2} \approx 0$ $F_{12} = 1$	$\dot{Q}_{12} = A_1\sigma\varepsilon_1(T_1^4 - T_2^4)$
Infinitely large parallel plates 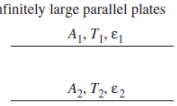	$A_1 = A_2 = A$ $F_{12} = 1$	$\dot{Q}_{12} = \frac{A\sigma(T_1^4 - T_2^4)}{\frac{1}{\varepsilon_1} + \frac{1}{\varepsilon_2} - 1}$
Infinitely long concentric cylinders 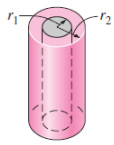	$\frac{A_1}{A_2} = \frac{r_1}{r_2}$ $F_{12} = 1$	$\dot{Q}_{12} = \frac{A_1\sigma(T_1^4 - T_2^4)}{\frac{1}{\varepsilon_1} + \frac{1-\varepsilon_2}{\varepsilon_2}\left(\frac{r_1}{r_2}\right)}$
Concentric spheres 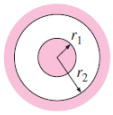	$\frac{A_1}{A_2} = \left(\frac{r_1}{r_2}\right)^2$ $F_{12} = 1$	$\dot{Q}_{12} = \frac{A_1\sigma(T_1^4 - T_2^4)}{\frac{1}{\varepsilon_1} + \frac{1-\varepsilon_2}{\varepsilon_2}\left(\frac{r_1}{r_2}\right)^2}$

1.3.6. Radiation Heat Transfer Between the Globe Thermometer and Its Environment

The globe thermometer can be considered as a small object in large cavity (the first case in Table 5). Thus, the heat transfer by radiation to or from the globe thermometer can be expressed as follow:

$$Q_r = \varepsilon\sigma A_g\left(T_r^4 - T_g^4\right) \tag{28}$$

The specific heat transfer per unit of surface area is:

$$q_r = \varepsilon\sigma\left(T_r^4 - T_g^4\right) \tag{29}$$

where

Q_r is the net radiation heat transfer to the globe thermometer, W,
q_r is the specific radiation heat transfer to the globe thermometer, W.m^{-2},
A_g is the surface area of the globe thermometer, m^2,
ε is the emissivity of the globe thermometer surface. For matt black surface $\varepsilon = 0.95$.
T_g is the absolute temperatures of the thermometer (globe temperature), K,
T_r is the mean absolute temperatures of surfaces surrounding the globe thermometer, K. It is called the mean radiant temperature and it is defined as: *The temperature of a uniform enclosure with which a small black sphere at the examination point would have the same radiation exchange as it does with the actual environment.*

The equation (29) presents the heat radiation exchange between the globe thermometer and its surroundings as a function of the difference between the fourth powers of the absolute temperatures (T_r and T_g). The fourth powers function makes some algebraic complications, especially when it

requires calculating one of the two temperatures consistent with a certain total heat exchange, or when the heat radiation transfer is compared with heat transfer by convection, since the last depends on the difference between the first powers of the temperatures the algebra become cumbersome. In such cases, it is often acceptable to use a first power approximation for the radiant heat transfer (Kerslake 1972). Then the equation (29) can be re-expressed as a first power relation as follow:

$$q_r = h_r\left(T_r - T_g\right) \tag{30}$$

where

h_r is the first power radiation coefficient, and it correspondent with h_c convection heat transfer coefficient, W. m^{-2}. K^{-1}.

The radiation coefficient h_r can be expressed as following:

$$h_r = \varepsilon\sigma\left(T_r^3 + T_r^2 T_g + T_r T_g^2 + T_g^3\right) \tag{31}$$

If the mean radiant temperature and globe temperature are too close, then h_r reduces to:

$$h_r = 4\varepsilon\sigma T^3 \tag{32}$$

The relation between the radiation coefficient h_r, the mean radiant temperature, and globe temperature was shown in Figure 3.

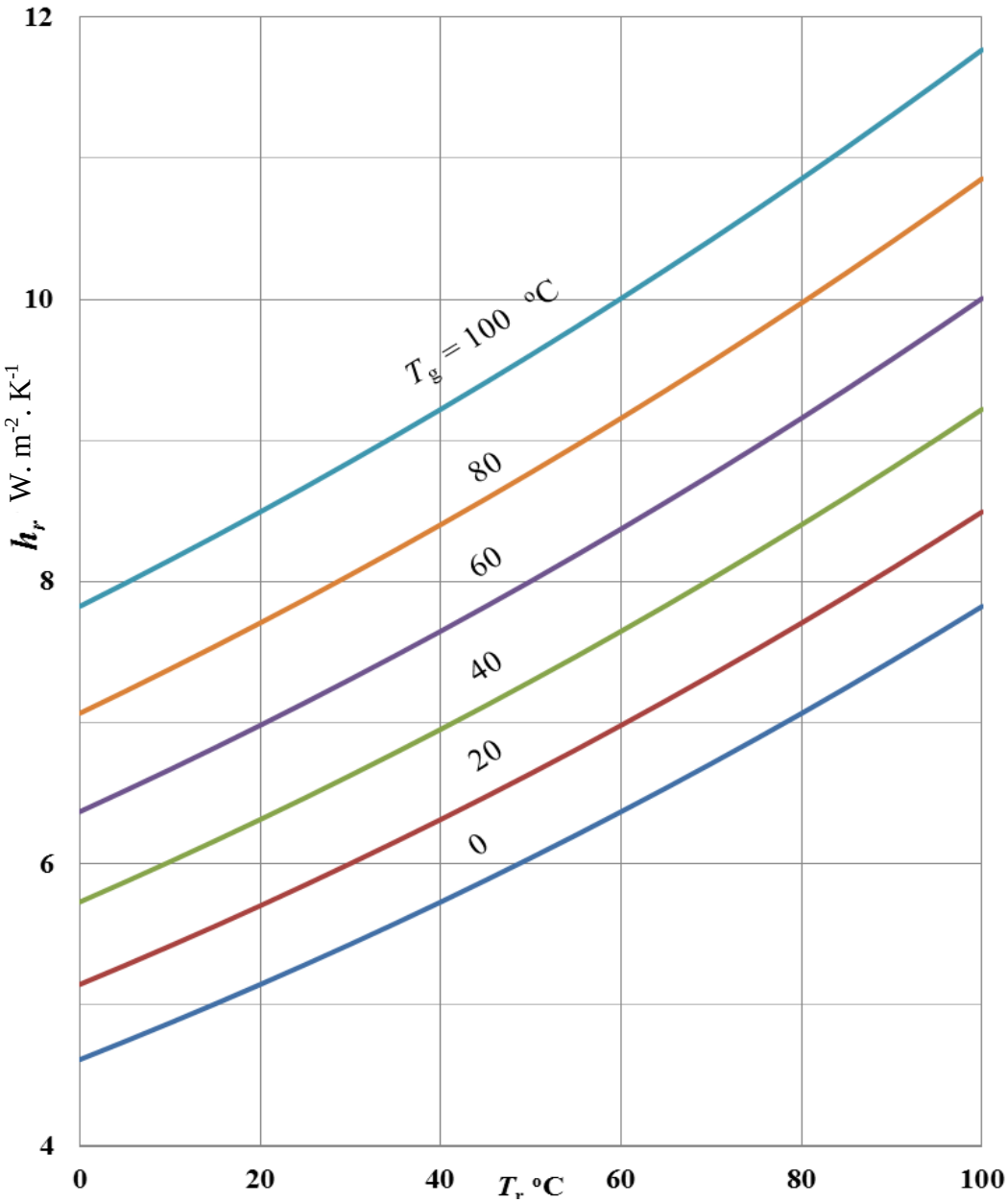

Figure 3. The radiation coefficient h_r

2. Thermal Comfort

At the present, a modern man spends most of the day indoors, and it is necessary to create a comfortable thermal environment to his stay. Due to that the thermal comfort is an important aspect of building design. The Thermal comfort is defined as '*that condition of the mind in which satisfaction is expressed with the thermal environment*' (ASHRAE 1966).

The definition of the thermal comfort is easily understood, but it is difficult to apprehend in physical parameters. There are extensive modeling and standardization for thermal comfort, which are depend both on physical and physiological parameters, as well as on psychology (ISO 7730 1994). The properties of an environment that affect the heat exchange between the human body and its surrounding it can be defined as the thermal environment state (Hoof et al. 2010). Thermal comfort is bipolar phenomena; i.e. they range from uncomfortably cold to uncomfortably hot with comfort or neutral sensations being somewhere around the middle of these (Parsons 2003).

Many factors affect the thermal comfort of the human body such as body temperature, skin moisture, and behavioral actions like clothing, activity, opening a window, changing the thermostat setting, changing location (Djongyang et al. 2010). However, the fundamental factors affect thermal comfort can be classified into two main groups; The environmental variables that affect human response, which include air temperature, mean radiant temperature, air velocity, and air humidity. The second group is the personal factors include the metabolic heat generated by human activity and clothing worn by person. The two groups together provide the six fundamental factors that define the human thermal comfort (Parsons 2003).

Two strategies were developed for assessment of thermal comfort: heat balance model and the adaptive model (Kwok et al. 2010). The heat balance model depends on the data from climate chamber studies to support its theory, best description for this strategy by the works of Fanger (Fanger 1994), while the adaptive model uses data from field studies of people in building, this way represented by the work of Humphreys and Nicol and de Dear and Brager (Humphreys et al. 1995; De Dear et al. 1998).

2.1. Environmental Factors

The air temperature, mean radiant temperature, and air velocity are the four basic parameters which effect on the thermal state of an environment. The definition and means of measurements of these parameters are presented next.

The recommended characteristics of the measuring instruments for measuring the parameters of the thermal state of the indoor environment are given for the Czech Republic and the European Union in the norm ISO 7726 (ISO 7726 1998)

2.1.1. Air Temperature

The air temperature T_a [°C] is the most important parameter affected on the thermal state of the environment. Practically, the air temperature is defined as the temperature of ambience surrounding the human body which is representative of that part of the surroundings which determines heat flow between the human body and the air (Parsons 2003).

Many instruments have been developed for measuring air temperature. One of the most common instruments for measuring the ambient temperature is the *ordinary thermometer*, which consists of a glass tube filled with mercury (Since 2005, in the European Union is no longer producing for environmental engineering) or other liquid.

Nowadays many types of the thermometer for measuring the temperature is developed such as thermocouples, thermistors or platinum resistance thermometer. Table 6. provides a comparison between the properties of measuring air temperature methods, while Table 7. gives the requirements for an instrument for measuring air temperature in the assessment of human thermal environments.

Table 6. Instrumentation for temperature measurement (Bohs 1990)

Property	Thermocouple	Thermistor	Platinum resistance thermometer	Semiconductor junction	Mercury thermometer
Signal for 1°C change	10 – 60 µV	1 % of resistance	40 µV	2.3 mV	-
Speed of response	fast	fast	moderate	moderate	slow
Relative cost (1: cheap; 5: expensive)	1	4	5	2	3
Mechanical stability	robust	moderate	moderate	robust	poor
Reproducibility	moderate	good	very good	poor	very good
Linearity	moderate	linearized	good	good	good
Accuracy	± 2 K	± 1 K	± 0.1 K	± 1 K	± 0.1 K

Table 7. Requirements for an instrument for measuring air temperature in the assessment of human thermal environments air (Parsons 2003).

Long term stability **Signal for 1°C**	Stable; the ability to recalibrate quickly an advantage as high above 'noise' as possible; ability to digitize useful; visual signal on mercury-in-glass thermometer not always easy to read
Speed of response	Depends upon study; high compared with rate of change of environmental conditions
Cost	Depends upon study; in most applications, moderate cost will provide satisfactory equipment
Mechanical stability	Moderate to high desirable
Linearity	Should be good, otherwise calibration required; may be possible to provide linearity within software; for example, in a spreadsheet
Accuracy	High and within ±0.3°C. Depends upon application. There will be measurement errors in addition to sensor accuracy
Other	Thermometers should be easy to use and not interfere with the environment or other measuring instruments (e.g. anemometers); shielding from radiation is important, particularly outdoors; must be able to measure at the point of interest

2.1.2. Mean Radiant Temperature

The heat is transferred by radiation from a hot to a cold body. The amount of heat flow by radiation between bodies is related to the difference between the fourth powers of the absolute temperatures of the bodies. The radiation field in space can be defined in terms of radiant temperature. Radiant temperature is defined as '*the temperature of a black-body source that would give the same value of some measured quantity of the radiation field as exists in reality*' (Mc Intyre 1980). Two radiant temperatures are usually used to describe the radiant heat exchange between the human body and the environment; The mean radiant temperature T_r, which gives an overall average value and the plane radiant temperature, which provides information about the direction of radiation (Parsons 2003).

The mean radiant temperature T_r, is one of the most important environmental parameters affecting on the thermal comfort (Thorsson 2007). The mean radiant temperature is defined *as the temperature of a uniform enclosure with which a small black sphere at the examination point would have the same radiation exchange as it does with the actual environment* (Parsons 2003). The use of the sphere in the definition produces the average value of mean radiant temperature in three dimensions, and this value will not depend on its orientation in the environment.

ISO 7726 gives an alternative definition of mean radiant temperature related to the human body: '*The mean radiant temperature is defined as the uniform temperature of an imaginary enclosure in which the radiant heat transfer from the human body is equal to the radiant heat transfer in the actual non-uniform enclosure*' (ISO 7726 1998).

The mean radiant temperature T_r is determined by using the globe thermometer, where the mean radiant temperature can be calculated from the following relation (Bedford 1934):

$$T_r = \left[T_g^4 - \frac{h_{cg}}{\sigma\varepsilon}\left(T_g - T_a\right)\right]^{0.25} \tag{33}$$

where

T_r is the mean absolute temperatures of surfaces surrounding the globe thermometer, K,

T_g is the absolute temperatures of the thermometer (globe temperature), K,

T_a is the air temperature, K,

h_{cg} is the convection heat transfer coefficient between air and globe thermometer, W. m^{-2}. k^{-1},

σ is Stefan – Boltzmann's constant, $\sigma = 5.67\times10^{-8}$ [W.m^{-2}. K^{-4}],

ε is the emissivity of the globe thermometer surface. For matt black surface ($\varepsilon = 0.95$).

The mean radiant temperature can be defined with respect to the human body, in this case the mean radiant temperature can be calculated from the temperatures of the surrounding surfaces, view factors and the shape, size and relative position of the surface in relation to a person (Parsons 2003).

By assuming all surfaces have high emissivity then mean radiant temperature can be estimated using the following relation (ISO 7726 1998):

$$T_r^4 = T_1^4 F_{p1} + T_2^4 F_{p2} + \cdots + T_n^4 F_{pn} \quad (34)$$

where:
T_r is the mean radiant temperature, K,
T_n is the absolute temperature of surface n (n = 1, 2, …, N), K,
F_{pn} is the view factor between a person p and surface n.

For a small difference between the temperatures of surfaces the equation (34) can be simplified to linear form (ISO 7726 1998), as follow:

$$T_r = T_1 F_{p1} + T_2 F_{p2} + \cdots + T_n F_{pn} \quad (35)$$

The mean radiant temperature and directional radiant temperature can also be measured using radiometers, thermovisions, or radiation thermometers.

2.1.3. Air Velocity

The Air velocity w is the movement of air rate of change of position with time in a specified direction (Trott et al. 2000). The air movement across the human body affects heat flow to and from the body and thus temperature of the body. Based on the definition, the air velocity will vary in time, space and direction. For more suitability, the air velocity is present the 'mean' air velocity intensity over an exposure time of interest and integrated over all directions (e.g. square root of the sum of squares of air velocity in each direction) (Parsons 2003; ISO 7726 1998).
For measuring the air velocity, usually is used instruments that work on different principles, such as cup or vein anemometers, hot wire anemometers, or kata thermometers.
The air velocity in the indoor environment is relatively low (from 0.01 up to 1m. s^{-1}), therefor in this range devices based on the mechanical principle (cup, fan blades, etc.) may be inappropriate. The hot wire anemometers, or kata thermometers are suitable to measure such low air velocity. Kata thermometers are however cumbersome and time consuming to use in practical applications (Wilson et al. 2015)

2.1.4. Humidity

The air humidity is the amount of water vapor in air and it affects human comfort (Posudin 2014). Evaporation of sweat is a function of air temperature and air humidity. Sweat heated by the human body evaporates and absorbs in the air. The perspiration allows heat transfer from the body to environment and cooling the body (Lecher 1990).

The humidity can be expressed in several terms:

- Absolute humidity: It is the mass of water vapor present per unit volume of air. Its unit is grams per cubic meter of air.
- Relative Humidity RH: It is the ratio of the partial pressure of water vapor to the saturated water vapor pressure.
- Dew Point Temperature T_{Dp}: It is the temperature at which dew would begin to form if the air was slowly cooled (Kerslake 1972).

- Wet Bulb temperature *WBT*: It is the temperature indicated by a moistened thermometer bulb exposed to the air flow. It can be measured by using an ordinary thermometer with the bulb covered by wet muslin.
- Specific humidity: It is the ratio of the mass of water vapor to the total mass of the moist air.

In the thermal comfort, the relative humidity is commonly used, and it is recommended to be above 20% all year, below 60% in the summer and below 80% in the winter (Lecher 1990).

Air humidity is most often measured by psychrometers, condensation hygrometers, electrolytic hygrometers, or dilatation hygrometers.

2.2. Personal Factors

The personal factors include the insulation of the clothing and the rate of the heat metabolic.

2.2.1. Clothing Insulation

The clothes are used for several functions in human life such as decoration, social status, protection and modesty (Song 2011). Otherwise clothing has a significant impact on the ability of person to maintain thermal comfort (Nikolaos 2013). Clothing provides a layer of thermal insulation between the human body and its environment (Smith et al. 1983).

The insulation of clothing is a property of the clothes and represents the resistance to heat transfer between the skin and the clothing surface. In other words, the rate of heat transfer through the clothing is by means of conduction, which depends on the surface area A [m^2], the temperature gradient [°C], between the human skin and the clothes surface, and the thermal conductivity of the clothing [$W.\ m^{-2}.\ {}^{o}C^{-1}$]. The Insulation of clothes is the reciprocal of clothing conductivity with units of $m^2.\ °C.\ W^{-1}$ (Parsons 2003).

In 1941 Gagge introduced the *Clo* unit, where one *Clo* represent the thermal insulation required to keep a sedentary person comfortable at 21°C. It has an average value of $0.155 m^{2.}\ °C.\ W^{-1}$ and it is approximately the insulation afforded by a man's suit (Gagge 1941).

- **Evaluating the dry thermal insulation of clothing I_{cl}:**

There are many methods to assess the thermal insulation of clothing materials. Standardized equipment is used to measuring the thermal insulation of clothing which usually involves placing a sample of clothes material on the equipment and, by measuring heat flows or temperature, the thermal insulation can be calculated. Another method is used to determining thermal insulation of clothing by involving heated manikins with a temperature distribution across the body like that of a human subject. By using thermal manikins, the values of the thermal insulation have been determined for many types of clothes, and these values have been listed in tables (Parsons 2003; Mc Cullough et al. 1985). Table 8. provides examples of the values of I_{cl} for whole clothing ensembles, and in Table 9. provides the values of I_{cl} for individual clothing garments. By simply adding the *Clo* values for garments (which is obtained from Table 8) gives a realistic estimate of ensemble I_{cl} values (Olesen et al. 1988).

Table 8. The thermal insulation values for work clothing ensembles (Olesen et al. 1988).

Work clothing	I_{cl} Clo	$m^2.K.W^{-1}$
Underpants, boiler suit, socks, shoes	0.70	0.110
Underpants, shirt, trousers, socks, shoes	0.75	0.115
Underpants, shirt, boiler suit, socks, shoes	0.80	0.125
Underpants, shirt, trousers, jacket, socks, shoes	0.85	0.135
Underpants, shirt, trousers, smock, socks,	0.90	0.140
Underwear with short sleeves and legs, shirt, trousers, jacket, socks, shoes	1.00	0.155
Underwear with short sleeves and legs, shirt, trousers, socks, shoes	1.10	0.170
Underwear with long legs and sleeves, thermo-jacket, socks, shoes	1.20	0.185
Underwear with short sleeves and legs, shirt, trousers, jacket, thermos-jacket, socks, shoes	1.25	0.190
Underwear with short sleeves and legs, boiler suit, thermos-jacket + trousers, socks, shoes	1.40	0.220
Underwear with short sleeves and legs, shirt, trousers, jacket, thermo-jacket and trousers, socks, shoes	1.55	0.225
Underwear with short sleeves and legs, shirt, trousers, jacket, heavy quilted outer jacket and overalls, socks, shoes	1.85	0.285
Underwear with short sleeves and legs, shirt, trousers, jacket, heavy quilted outer jacket and overalls, socks, shoes, cap, gloves	2.00	0.310
Underwear with long sleeves and legs, thermos jacket + trousers, outer thermos jacket + trousers, socks, shoes	2.20	0.340
Underwear with long sleeves and legs, thermos jacket + trousers, parka with heavy quilting, overalls with heavy quilting, socks, shoes, cap, gloves	2.55	0.395

For a clothed body, the heat transfer surface is increased by an amount depending on the thickness of the clothing layer. This increasing is taken into account using the term f_{cl}, which is defined as the ratio of the clothed surface area of the body to the nude surface area of the body.

Determining the value of f_{cl} is difficult, so an approximation based on the clothing insulation value can be made. For example, the following equation is an approximation to determining the f_{cl} (Mc Cullough et al. 1984):

$$f_{cl} = 1 + 0.31 I_{cl} \tag{36}$$

Table 9. The values of the thermal insulation of typical garment (ASHRAE 2004)

Garment description	I_{cl} [Clo]	**Garment description**	I_{cl} [Clo]
Underwear		*Footwear*	
Bra	0.01	Ankle-length athletic socks	0.02
Panties	0.03	Pantyhose /stockings	0.02
Men's briefs	0.04	Sandals/thongs	0.02
T-shirt	0.08	Shoes	0.02
Half-slip	0.14	Slippers (quilted, pile lined)	0.03
Long underwear bottoms	0.15	Calf-length socks	0.03
Full slip	0.16	Knee socks (thick)	0.06
Long underwear top	0.20	Boots	0.10
Shirts and Blouses		*Suit Jackets and Vests*	
Sleeveless/scoop-neck blouse	0.13	Sleeveless vest (thin)	0.10
Short-sleeve knit sport shirt	0.17	Sleeveless vest (thick)	0.17
Short-sleeve dress shirt	0.19	Single-breasted (thin)	0.36
Long-sleeve dress shirt	0.25	Single-breasted (thick)	0.42
Long-sleeve flannel shirt	0.34	Double-breasted (thin)	0.44
Long-sleeve sweatshirt	0.34	Double-breasted (thick)	0.48
Trousers and Coveralls		*Sleepwear and Robes*	
Short shorts	0.06	Sleeveless short gown (thin)	0.18
Walking shorts	0.08	Sleeveless long gown (thin)	0.20
Straight trousers (thin)	0.15	Short-sleeve hospital gown	0.31
Straight trousers (thick)	0.24	short-sleeve short robe (thin)	0.34
Sweatpants	0.28	Short-sleeve pajamas (thin)	0.42
Overalls	0.30	Long-sleeve long gown (thick)	0.46
Sleeveless vest (thin)	0.13	Long-sleeve pajamas (thick)	0.57
Sleeveless vest (thick)	0.22	Long-sleeve long warp robe (thick)	0.69
Long-sleeve (thin)	0.25	Sleeveless, scoop neck (thin)	0.23
Long-sleeve (thick)	0.36	Sleeveless, scoop neck (thick)	0.27
Skirt (thin)	0.14	Short-sleeve shirtdress (thin)	0.29
Skirt (thick)	0.23	Long-sleeve shirtdress (thin)	0.33

2.2.2. Metabolic Heat

The metabolic heat production in the human body has important effect on the human thermal comfort. The energy is produced by the process in the cells of the living body. Most of this energy is released as heat which is distributed, mainly by blood, around the body (Guyton 1974).

The integration of the heat released from the all cells in the human body provides the total metabolic heat production of the body *H*. The total production of the metabolic heat of the human body is expressed by the following relation (Parsons 2003):

$$H = M - W \tag{37}$$

where
M is the metabolic heat rate, and *W* is the mechanical work performed by the human body.

The unit of metabolic heat production is usually related to surface area of the human body or the body mass. However, the average value of human surface of 1.84 m^2 and the average value of the weight 65–70 kg for a man or 55kg for a woman. Thus, units of W. m^{-2} or kcal/min/kg are used for the metabolic heat production. The surface area of the body can also be estimated from the Du Bois surface area relation (Du Bois et al. 1916), where:

$$A_D = 0.202w^{0.425}h^{0.725} \tag{38}$$

where
A_D: is the Du Bois surface area m^2;
w, *h*: are the weight (kg), and the height (m) of the human body, respectively.
The metabolic heat production could be expressed by the unit of *Met* (ASHRAE 2004), where:
1 Met = 50 kcal. m^2. h = 58.15 W. m^{-2}
The values of metabolic rate for various type of the activity are listed on Table 10.

Table 10. The metabolic heat rate for different activity (ASHRAE 2004)

Activity	**Metabolic Rate**		**Activity**	**Metabolic Rate**	
	Met	W.m^{-2}		Met	W.m^{-2}
Walking (on level surface)			*Miscellaneous Occupational Activities*		
0.9 m. s^{-1}	2.0	115	Cooking	1.6-2.0	95-115
1.2 m. s^{-1}	2.6	150	House cleaning	2.0-3.4	115-200
1.8 m. s^{-1}	3.8	220	Seated, heavy limb movement	2.2	130
Resting			*Machine work*		
Sleeping	0.7	40	Sawing (table saw)	1.8	105
Reclining	0.8	45	Light (electrical industry)	2.0-2.4	115-140
Seated, Quite	1.0	60	Heavy	4.0	235
Standing	1.2	70	Handling 50Kg bags	4.0	235
Office Activities			*Miscellaneous Leisure Activities*		
Seated, reading, or writing	1.0	60	Dancing, social	2.4-4.4	140-255
Typing	1.1	65	Calisthenics/ exercise	3.0-4.0	175-235
Filing, seated	1.2	70	Tennis, single	3.6-4.0	210-270
Filing, standing	1.4	80	Basketball	5.0-7.6	290-440
Walking about	1.7	100	Wrestling, competitive	7.0-8.7	410-505

There are many methods for estimating the metabolic heat production, In Table 11 are presented the principles of measurement and advantages and disadvantages of the most important of these methods.

Table 11. Principles of measurement of metabolic heat production (Parsons 2003; ISO 8996 1990; Murgatroyd et al. 1993)

Method	**Principle**	**Advantages**	**Disadvantages**
Whole-body direct calorimetry	Measures rate at which heat is lost from a person in a room where all avenues of heat exchange can be measured	Accurate Fast responding Direct energy measurement Good environment for strictly controlled studies	Expensive Complex Provides no information about substrates from which energy is derived Artificial environment
Whole-body indirect calorimetry	Measures rate at which heat is produced in the body by a person in a room, from analysis of CO2 and O2 content and rate of, ingoing and outgoing air in the room	Accurate and precise Worldwide expertise Fast responding Provides information about substrates from which energy is derived	Requires careful design, engineering and computing Requires best possible instruments Expensive Artificial environment
Douglas bag method	Measures rate at which heat is produced in the body by collection of a person's expired air into an impermeable bag and measurement of its O2 and CO2 content and volume over a fixed time	Relatively simple and robust Yields reliable results Relatively inexpensive	Diffusion of CO_2 and chances of leakage of expired air Prompt analysis of expired air required after collection Suitable for short periods of activity only
K-M respirometer	Portable system which measures rate at which heat is produced in the body from expired air volume through a low resistance valve meter and mouthpiece and analysis of expired gas in a small rubber collection sample bag	Smaller, more compact and lighter than Douglas bag apparatus Useful for light to moderate activity Relatively simple and robust Yields reliable results	Suitable only for short periods of light activity Requires separate analysis of gases Prompt analysis of expired air samples required after collection
Oxylog system	Portable digital system recording cumulative oxygen consumption (using polarographic cells) and inspiratory volume (meter and mouthpiece)	Smaller, more compact and lighter than Douglas bag Can be used for light, moderate and even strenuous activity Does not require separate gas analyzers	Suitable only for short periods of activity Prolonged use leads to discomfort with mask or mouthpiece and nose clip Not simple to operate
Activity diaries and time budget determinations	Recording of activity performed over time for estimate of variation in metabolic rate and cumulative or average (time-weighted) energy production	Inexpensive for large population groups (retrospective) Provide useful data on patterns of activity	Expensive May influence habitual activity pattern Validity of energy expenditure data variable

3. Heat Balance Equation of The Human Body

It is well known that the core temperature of human body should be maintained at physiological set point around 37 °C. Humans have a powerful way to interact with environmental changes is behavioral; put on or take off clothes, change posture, move, take shelter, etc. In addition to the behavioral reaction, humans possess a developed physiological thermal control system, thermoregulation system. Both systems constantly interact and respond to changing environments to ensure maintenance of internal body temperatures near a physiological set point under a broad range of environmental conditions and metabolic rate activities (Parsons 2003; Kreith 2000).

3.1. Human Thermoregulation System

The main thermal control system center of the human is located in the hypothalamus of the brain, from which multiple reflex responses work to keep the body temperature within a limited range (Ganong 1993). The signals that activate the hypothalamic temperature-regulating centers come from two sources: the temperature-sensitive cells and cutaneous temperature receptors (Webb 1995).

The human thermoregulatory system is very complicated, where it contains multiple sensors, multiple feedback loops, and multiple outputs (Hensen 1990). The techniques by which the human body responds to the change of its energy (increase or decrease) include the evaporation of sweat, shivering of the muscles, and vasoconstriction and vasodilation of the blood vessels (Ganong 1993).

The human thermoregulatory system can induce responses to correct departure from homeothermy through six effector nervous pathways. One of these pathways, the sympathetic adrenomedullary system provides a widely-distributed network of noradrenergic terminals activating metabolic and vascular responses and a motor supply to the adrenal medulla for the release of adrenaline into the circulation (Edholm et al. 1981). Six nervous pathways and the effects are described in Table 12.

Table 12. The thermoregulatory effector pathways (Edholm et al. 1981)

Pathway	Effect
Adrenergic non-medullated nerve fibres of the sympathetic system	Vasoconstriction of skin blood vessels, possible inhibition of sympathetic vasodilator nerves and pilomotor reaction.
Sympathetic nerves	Cutaneous vasodilation and inhibition of vasoconstrictor tone
Ordinary skeletal nerve supply	Shivering
Sympathetic supply to the adrenal medulla releases adrenaline and catecholamines	Increases heat production, cardiac output and enhances skin vasoconstriction while tending to dilate blood vessels in the muscles. Glucose and free fatty acid utilization shivering thermogenesis
Sympathetic adreno-medullatory system	Non-shivering thermogenesis
Non-medullated (cholinergic) sympathetic nerves	Sweating

3.2. Heat Balance Equation

Maintain the internal temperature of human body at around 37°C, requires that there is a heat balance between the human body and its environment. Thus, the heat transfer into the body and the heat generation inside the body must be balanced by the heat transfer from the body. If the sum of the heat transferred and generated in the human body are greater than the heat transferred from the body, the internal temperature of human body would increase and if the heat transferred from the body are greater the internal body temperature would decrease (Arens et al. 2006).

Over time, heat gains and losses must balance to maintaining the core temperature of human body within its narrow range. Figure 4 illustrates the full range of core temperatures and environmental temperatures encountered by humans (Brooks et al. 1996).

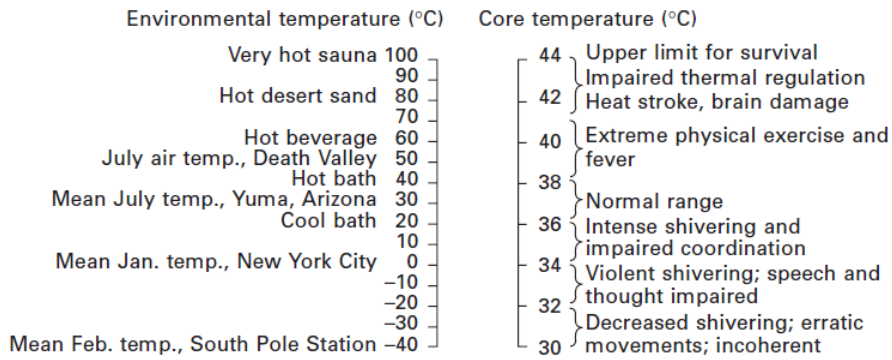

Figure 4. Ranges of environmental and human body temperatures (Arens et al. 2006)

The heat balance equation can be expressed in many forms. However, all forms have the same implicit concept and include three terms:

1- The heat generation in the body: The metabolic rate of the body supply energy to enable the body to do mechanical work and the remainder is released as heat.
2- The heat transfer between human body and its environment: It can be by conduction, convection, radiation, and evaporation.
3- The heat storage: When combined all the rates of heat production and loss provide a rate of heat storage.

In case of the human body (i.e. constant temperature), the rate of heat storage is zero. If there is a net heat gain, storage will be positive and body temperature will rise. If there is a net heat loss, storage will be negative and body temperature will fall (Parsons 2003; Fanger 1982).

The heat balance equation can be expressed as follow:

$$M - W = C + R + E + K \tag{39}$$

where

M is the metabolic heat rate,
W is the external work performed by the body,
C, R, E and K are the rates of heat loss from the body by convection, radiation, evaporation, and conduction, respectively.

In order to analysis the heat exchange between the human body and its environment, it is necessary to identify the means of the heat production and exchange for the human body, and determine the equations to calculate the heat production and the heat exchange.

Many models of the heat balance equation have developed, ASHRAE introduced the following equation of heat balance (ASHRAE 1989a):

$$M - W = Q_{sk} + Q_{res} \tag{40}$$

$$Q_{sk} = C + R + E_{sk}$$

$$Q_{res} = C_{res} + E_{res}$$

$$M - W = C + R + E_{sk} + C_{res} + E_{res}$$

where

M is the rate of metabolic heat production, W.m^{-2}
W is the rate of mechanical work, W.m^{-2}
Q_{sk} is the total rate of heat loss from the skin, W.m^{-2}
Q_{res} is the total rate of heat loss through respiration, W.m^{-2}
C is the rate of heat loss by convection from the skin, W.m^{-2}
R is the rate of heat loss by radiation from the skin, W.m^{-2}
E_{sk} is the rate of total heat loss by evaporation from the skin, W.m^{-2}
C_{res} is the rate of heat loss by convection from respiration, W.m^{-2}
E_{res} is the rate of heat loss by evaporation from respiration, W.m^{-2}.

The components of the heat balance equation are shown in Figure 5. (Salvendy 2006).

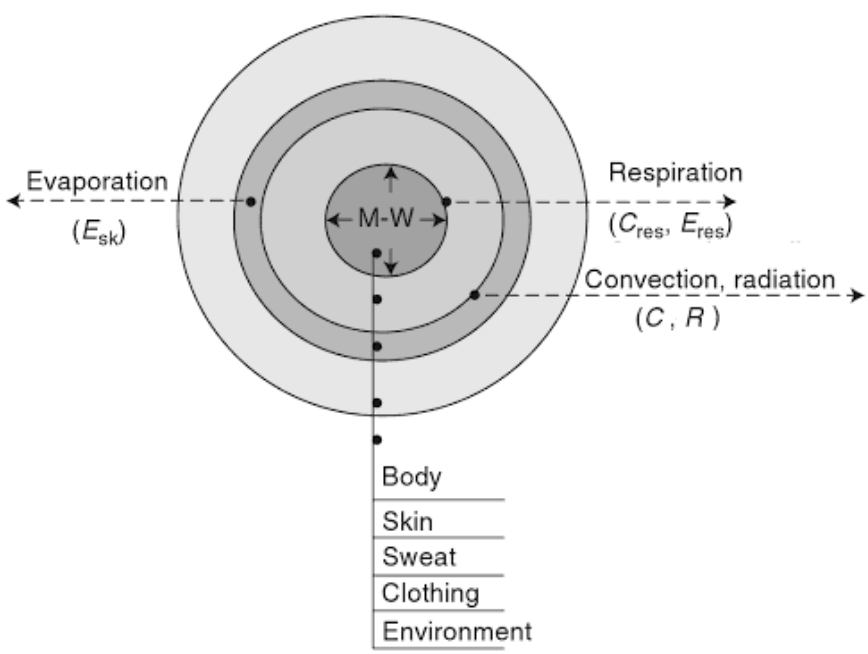

Figure 5. Heat transfer processes between human and environment (Salvendy 2006)

3.2.1. Heat Production Within Human Body

Energy obtained from metabolic processes M may be released as work, may be used to synthesis other compounds which are stored in the body for later use, or changed into heat energy (Muthayya 2002). Energy for mechanical work W will vary from about zero (for many activities) to no more than 25 per cent of total metabolic rate. The determination methods of the metabolic rate have already been mentioned.

3.2.2. Heat Loss from the Skin

The heat exchange between the human body and its environment is attained by evaporative heat loss and non-evaporative heat exchange. Non-evaporative heat exchange Q_{sk} is the sum of heat flow due to radiation, convection and conduction from a body to the environment, and it is called either dry or sensible heat loss (Clark 1998).

- *Non-Evaporative Heat Loss from the Skin*

It occurs by three physical phenomena, by conduction, convection, and radiation. In general, the heat transfer by conduction through the soles of the feet or to a chair is small, and it is often assumed to be negligible (Mc Intyre et al. 1972).

The sensible heat loss by convection and radiation can be expressed by the following relations (AHRAE 1997):

$$C = f_{cl} h_c (T_{cl} - T_a) \tag{41}$$

$$R = f_{cl} h_r (T_{cl} - T_r)$$

$$C + R = f_{cl} h (T_{cl} - T_o)$$

$$T_o = \frac{h_r T_r + h_c T_a}{h_r + h_c}$$

$$h = h_r + h_c$$

where

f_{cl} is the clothing area factor. It is defined as the surface area of the clothed body A_{cl}, divided by the surface area of the nude body A_D,
h_c is the convective heat transfer coefficient, W. m^{-2}. K^{-1},
h_r is the linear radiative heat transfer coefficient, W. m^{-2}. K^{-1},
h is the combined heat transfer coefficient, W. m^{-2}. K^{-1},
T_o is the operative temperature, K,
T_r is the mean radiant temperature, K,
T_a is the air temperature, K,
T_{cl} is the mean temperature over the clothed body, K.

The heat transfer through clothing is combined into a single thermal resistance value R_{cl}. So, the sensible heat loss by convection and radiation can wright as follow:

$$C + R = \frac{T_{sk} - T_{cl}}{R_{cl}} \tag{42}$$

Combining equations (41) and (42) to remove T_{cl} the final form is:

$$C + R = \frac{T_{sk} - T_o}{R_{cl} + \frac{1}{f_{cl} h}} \tag{43}$$

where

T_{sk} is the mean skin temperature, K,
R_{cl} is the thermal resistance of clothing, m^2. K. W^{-1}.

The convective heat transfer coefficient h_c is related to the type of heat flow (natural or forced), and there are many formulations which used to determine it. For example, for a seated person the fallowing equation can be used (Mitchell 1974):

$h_c = 8.3w^{0.6}$ for $0.2 < w < 4.0$ m. s^{-1}

$h_c = 3.1$ for $0.0 < w < 0.2$ m. s^{-1}

where

w is the air velocity in m. s^{-1}

Also, the convective heat transfer coefficient h_c can be determined using equation provided in ISO 8996 (ISO 7933 1989):

$h_c = 2.38(|T_{sek} - T_a|)^{0.25}$ for natural convection

$h_c = 3.5 + 5.2w$ for $w < 1$ m. s^{-1}

$h_c = 8.7w^{0.6}$ for $w > 1$ m. s^{-1}

The linearized radiative heat transfer coefficient h_r can be given by the following equation (Fanger 1967):

$$h_r = 4\varepsilon\sigma \frac{A_r}{A_D}\left[273 + \frac{T_{cl} - T_r}{2}\right]^3$$

where

ε is the emissivity of the clothing body surface, it is often assumed to be between 0.95 to 1.0,
σ is Stefan-Boltzmann constant, 5.67×10^{-8} [W m^{-2} K^{-4}],
A_r is the effective radiative area of the body, m^2,
A_D is the surface area of the nude body, m^2.

For typical indoor conditions, a reasonable approximate value of $h_r = 4.7$ W m^{-2} K^{-1} (AHRAE 1997).

- *Evaporative heat loss from the skin E_{sk}*

The heat transfer by evaporation is a process of mass transfer (water vapor) and is determined by physical laws related to the convective heat transfer process. The evaporative heat exchange is determined by the amount of water (sweat) evaporated at the skin surface and transported as vapor to the environment (Vernon et al. 2011).

The evaporative heat loss to the environment may be calculated using an evaporative heat exchange coefficient and the water vapor pressure difference between the skin and the ambient air by the following equation (AHRAE 1997):

$$E_{sk} = \frac{w\left(P_{sk,s} - P_a\right)}{R_{e,cl} + \frac{1}{f_{cl} h_e}} \tag{44}$$

where

P_a is the water vapor pressure in the ambient air, Pa,
$P_{sk,s}$ is the saturated water vapor at skin temperature T_{sk}, Pa,
$R_{e,cl}$ is the evaporative heat transfer resistance of the clothing layer, m^2 Pa W^{-1},
h_e is the evaporative heat transfer coefficient, in W m^{-2} Pa^{-1}. It is calculated using the Lewis Relation $h_e = LR\, h_c$. The Lewis number LR, defined as the ratio of mass transfer coefficient by evaporation to heat transfer coefficient by convection,
w is the skin wetness.

The skin wetness was first introduced by Gagge (Gagge 1937) and is defined *as the ratio between the actual evaporative heat loss and the maximum possible evaporative heat loss for a given environmental condition* (Havenith et al. 2002). In other words, it represents the fraction of total body surface area covered with sweat. The value of skin wettedness varies from a value of 0.06 when only natural diffusion of water through the skin occurs, to 1.0 when skin is completely wet and maximum evaporation occurs.

3.2.3. Heat Loss by Respiration

The heat loss in respiration ($C_{res} + E_{res}$) can be expressed as the sum of two terms, the first by dry convective heat transfer (C_{res}), when the cool air inhaled, then is heated to core temperature in the lungs, thus the heat is transferred in exhaled air to the environment. And the other is relating to the gain in enthalpy of dry air (E_{res}), where the inhaled air is moistened (to saturation) by the lungs (Blaxter 1989).

ASHRAE (AHRAE 1997) gives the following equation for total respiratory heat loss:

$$C_{res} + E_{res} = 0.0014M(34 - T_a) + 0.0173M(5.87 - P_a) \tag{45}$$

4. Thermal Comfort Indices

Given that the thermal comfort of the environment depends on the six fundamental factors (air temperature, mean radiant temperature, air velocity, humidity, the metabolic heat generated by human activity, and clothing worn by person), many attempts have been carried out to find a single index by integrating some or all the six fundamental factors that could be used to determine thermal comfort conditions (Kazkaz et al. 2013). The most common of the thermal indices are next discussed:

4.1. Dry-Bulb Temperature

The dry-bulb temperature T_{db} is the temperature measured by an ordinary thermometer (which consists of a glass tube filled with mercury). The dry-bulb temperature does not agree to the definition of an index as an instrument which produces one value from two or more factors, nevertheless, it remains the most important single measure of thermal stress (Macpherson 1962).

4.2. Wet-Bulb Temperature

The wet-bulb temperature T_{wb} is the temperature which considers the amount of moisture in the air. Its value can be obtained by rotating a thermometer with a moistened cotton or wet wick encasing the bulb through the air (Figure 6) (Bobenhausen 1994).

The psychrometer (Figure 7) usually used to measurement the wet bulb temperature. It comprises two thermometers. One thermometer its bulb is covered with a moistened cotton or linen wick and is called the wet bulb, whereas the other thermometer its bulb is uncovered and is referred to as the dry bulb thermometer (Blair et al. 1972).

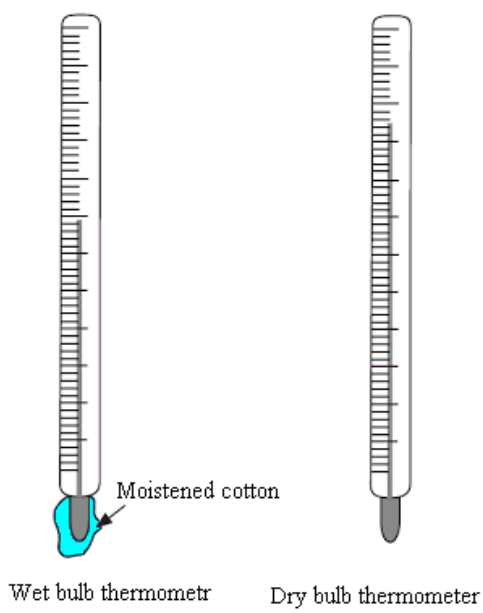

Figure 6. The wet and dry bulb thermometers

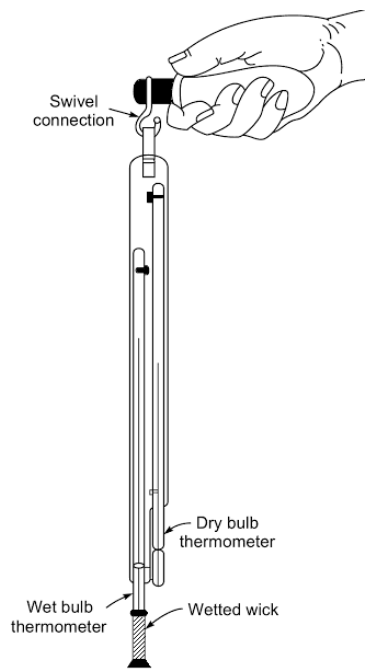

Figure 7. Sling Psychrometer (Ananthanarayanan 2013)

The wet-bulb temperature can be called a thermal comfort index because it is an integration of two factors, the air temperature and the air humidity; the effect of air velocity and radiation is ignored. Haldane (1905) was the first who used the wet bulb temperature as an index of thermal stress. He was sure that the wet bulb temperature provides the best measure of the physiological effects of hot environments (Macpherson 1962).

4.3. Effective Temperature

The effective temperature T_e is not a real temperature in the meaning that it can be measured by a thermometer. It is an index which combines the effects of dry bulb and wet bulb temperatures with air movement to give equivalent sensation of warmth or cold. In other words, the effective temperature index combines the effects of air temperature and humidity (Asimakopoulos 2001).

The T_e index was developed by Houghten and Yagloglou at the ASHVE (American Society of Heating and Ventilating Engineers) Pittsburgh research laboratories. Mathematically, the effective temperature can be expressed as follows (Houghton et al. 1923):

$$T_e = T_{db} - 0.4(T_{db} - 10)(1 - \frac{RH}{100}) \tag{46}$$

All temperatures in the equation are in ^{o}C

In1923 Houghten and Yagloglou represented the effective temperature index by a series of equal comfort lines drawn on the psychrometric chart (Figure 8.). Houghten and Yagloglou emphasized that, these lines of equal comfort did provide a valid measure of physiological effect. That is to say, all points on the same line of equal comfort provide the same degree of physiological strain (Houghton et al. 1923). Later, Houghten and Yagloglou replaced the equal comfort lines in terms of effective temperature (because at high temperatures and humidity there is no comfort) (Macpherson 1962).

The original effective temperature index was developed for people wearing 1 col clothing (Yglou 1947). A comprehensive series of methods of correction of the effective temperature were proposed to allow air velocity, clothing, and radiation to be considered. ASHVE published a nomogram representation of the effective temperature index, which included air velocity effects (Houghton et al. 1924).

In year 1932 Vernon and Warner included the effect of radiation by using globe temperature values (temperature measured by 150 mm diameter globe thermometer) in place of the dry bulb temperature and the index is then termed Corrected Effective Temperature T_{ce} (Vernon et al. 1932).

As clothing has a large effect on radiation, Bedford (Bedford 1946) produced two nomograms: one for persons stripped to the waist (Basic Effective Temperature Figure 9.) and another for persons '*normally clad*' (Normal Effective Temperature (NET) Figure 10.). Both effective and corrected effective temperatures have been influential and widely used as a comfort index. They are still used but not generally recommended now (Parsons 2003).

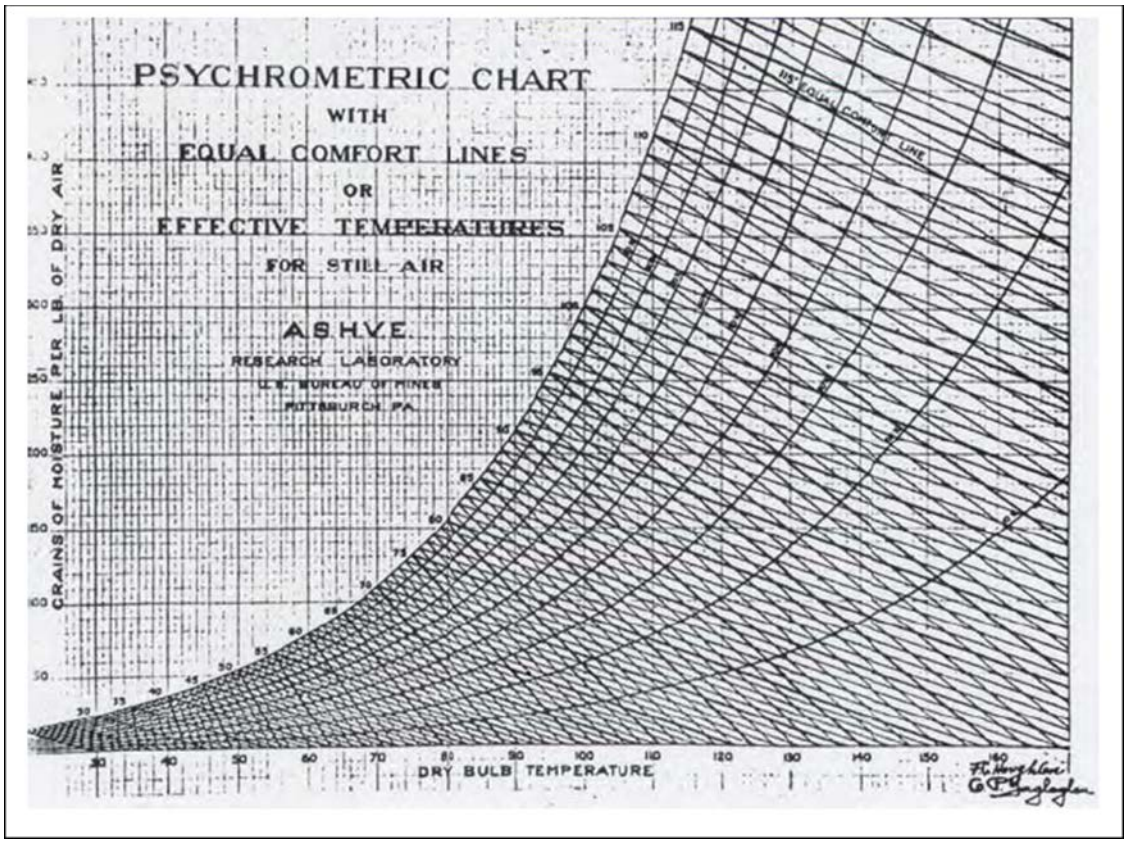

Figure 8. Yagloglou's original representation of the effective temperature (Houghton et al. 1923)

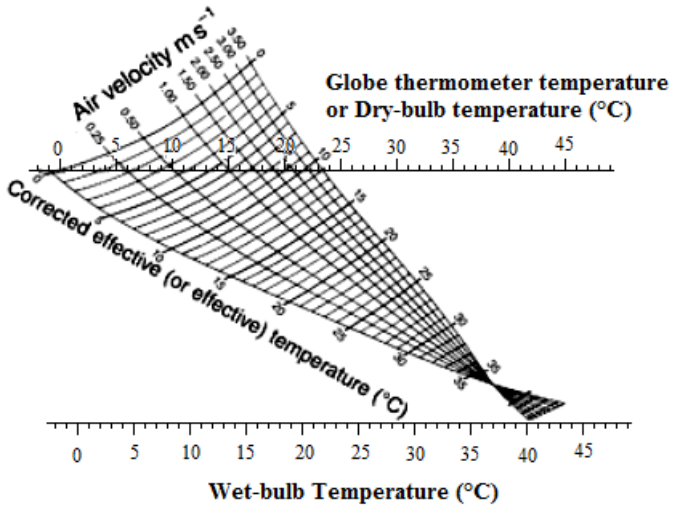

Figure 9. Chart of the basic scale of corrected effective (or effective) temperature (Bedford 1946)

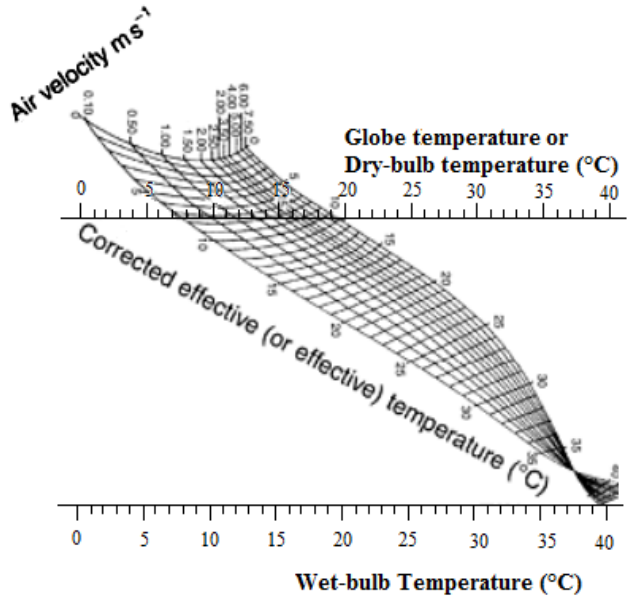

Figure 10. Chart of the normal scale of corrected effective (or effective) temperature (Bedford 1946)

4.4. Globe Thermometer Temperature

The globe thermometer is a device introduced by Vernon. It consists of a hollow copper sphere of diameter 150 mm, coated with matt black paint and containing an ordinary thermometer with its bulb fixed at the center of the sphere, without source of heat (see Figure 11) (Vernon 1930).

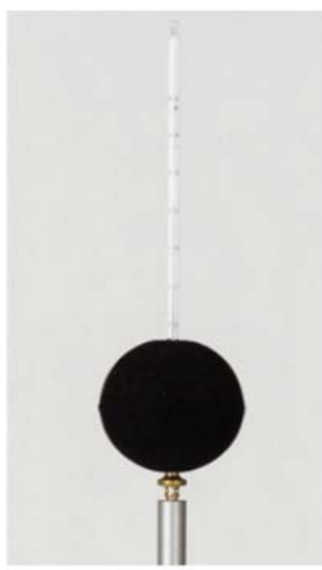

Figure 11. The globe thermometer

Vernon's choice of 150 mm sphere was a succeeded one, because this size of globe weights the air temperature and mean radiant temperature nearly correctly for a human subject (Kerslake 1972).

New modification of Vernon's globe thermometer is a Vernon-Jokl globe thermometer, which is an ordinary globe thermometer its surface is covered by polyurethane.

For purpose of research have been purchased number of globe thermometers (INNOVA, DOMAT, and SPEKTRUM) (LumaSense Technologies 2007; Domat control system 2017; Spektrum 2017). These thermometers were tested for use in dissertation.

The globe thermometer measures the combined effect of air temperature, air movement, and mean radiant temperature in a single index, that the globe temperature T_g, which provides a convenient method of assessment the thermal environment (Macpherson 1962).
In year 1934 Bedford and Warner has introduced the globe thermometer as a device for determining the mean radiant temperature of the surroundings, and it is now widely and successfully used for this purpose (Bedford 1934).
When the globe thermometer is in equilibrium with its environment the effects of radiation and convection balance each other. The men radiant temperature can be calculated by the following equations (ISO 7726 1998):

For natural convection

$$T_r = \left[(T_r + 273)^4 + \frac{0.25 \times 10^8}{\varepsilon}\left(\frac{|T_a - T_g|}{D}\right)^{0.25}(T_g - T_a)\right]^{0.25} - 273 \qquad (47)$$

For forced convection

$$T_r = \left[(T_r + 273)^4 + \frac{1.1 \times 10^8}{\varepsilon}\frac{w^{0.6}}{D^{0.4}}(T_g - T_a)\right]^{0.25} - 273 \qquad (48)$$

where:

T_r is the mean radiant temperature, °C,
T_a is the air temperature, °C,
T_g is the Globe temperature, °C,
D is the diameter of globe thermometer, m,
w is the air velocity, m.s^{-1},
ε is the emissivity of the clothing body surface, it is often assumed to be between 0.95 to 1.0,
σ is Stefan-Boltzmann constant, 5.67×10^{-8} (W. m^{-2}. K^{-4}).

4.5. Equivalent Temperature

The equivalent temperature T_{eq} is introduced by Dufton, where he developed a device a heated black copper cylinder to imitate the thermal behavior of the human body (it is called eupatheoscope) to measure this index. The equivalent temperature combines the effect of the air temperature, air velocity, and the temperature of the surroundings (Dufton 1929; Dufton 1932).

Bedford derived an equation for calculating the equivalent temperature index from the measurements of the individual thermal factors (Bedford 1951):

$$T_{eq} = 0.522T_a + 0.478T_r - 0.21\sqrt{w}(37.8 - T_a) \qquad (49)$$

where temperatures are in °C and air velocity w in m s^{-1}.

ASHRAE defined the equivalent temperature *as the temperature of an imaginary enclosure with the mean radiant temperature equal to air temperature and still air in which a person has the same heat exchange by convection and radiation as in the actual conditions* (ASHRAE 1989). The equivalent temperature is used to express the thermal state in small thermally homogeneous areas, such as cab of cars (Fišer et al. 2014).

4.6. Operative Temperature

The operative temperature T_o is one of several environmental temperature indices, which are used to assist with the quantification of thermal comfort (Kreith 2000).

The index of operative temperature was introduced by Winslow, Herrington, and Gagge (Winslow et al. 1936), as result of the work intended to measure the physical effect of the surrounding walls and ambient air temperature.

The operative temperature index provides a physical measure of thermal environment. The index integrates the air temperature and mean radiant temperature into a single temperature. This is achieved by using the heat coefficients to relate the heat exchange by radiation and convection to differences between skin temperature, on the first side, and mean radiant and air temperature, on the other (Ingram et al. 1975).

Although the heat exchange by radiation is determined by the difference between the fourth powers of the absolute temperatures (Stefan – Boltzmann's law), when the temperature differences are small the simple temperature difference itself can be used with only a small error (Burton et al. 1955).

The operative temperature is defined as *a uniform temperature of a radiantly black enclosure in which an occupant would exchange the same amount of heat by radiation and convection as in the actual non-uniform environment*; Mathematically operative temperature can be defined as (ASHRAE 1981):

$$T_o = \frac{T_a h_c + T_r h_r}{h_c + h_r} \tag{50}$$

or

$$T_o = A T_a + (1 - A) T_r \tag{51}$$

where

$$A = \frac{h_c}{h_c + h_r}$$

where:

h_c, h_r are the heat transfer coefficients by convection and radiation, respectively, W. m^{-2}. K^{-1},

T_a, T_r are the air and mean radiant temperature, respectively, ^{o}C,

A is the weighting coefficient. The values of the coefficient A are listed in Table 13.

Table 13. Values of the weighting coefficient A (Madsen et al. 1984)

w [m.s^{-1}]	< 0.2	0.2 - 0.6	0.6 - 1
A [-]	0.5	0.6	0.7

The coefficient A can be calculated from the following relation (ISO 7726 1998):

$$A = 0.73w^{0.2}$$

Gagge (Gagge et al. 1967) was indicated that the globe temperature is approximately equal to the operative temperature.

From the equation (50), the operative temperature can be defined as a weighted average of air temperature and mean radiant temperature by appropriate of coefficients of heat transfer by convection and radiation.

Many approximations were achieved to calculate the operative temperature. For small difference between air and man radiant temperatures (less than 4 ^{o}C) and small value of the air velocity (less than 0.2 m. s^{-1}), the operative temperature can be approximated with acceptable accuracy by the mean of the air and mean radiant temperatures (ASHRAE 1981).

$$T_o = \frac{T_r + T_a}{2}$$

4.7. Wet Bulb Globe Temperature

The wet bulb globe temperature *WBGT* is one of direct heat stress indices; it is introduced by Yaglou and Minard (1957) because of the studies in the US military centers. The index combines the effect of air temperature, radiation, air velocity, and humidity in a single value (Yaglou et al. 1957).

The *WBGT* index consists of a simple weighting of three temperatures; the temperature of globe thermometer T_g, the air temperature T_a, and the temperature of wet bulb thermometer T_{wb}.

For conditions with solar radiation:

$$WBGT = 0.7T_{wb} + 0.2T_g + 0.1T_a \tag{52}$$

For indoor conditions with no solar radiation:

$$WBGT = 0.7T_{wb} + 0.3T_g \tag{53}$$

where

T_{wb} is the temperature of a naturally ventilated wet bulb thermometer, ^{o}C,

T_a is the air temperature, ^{o}C,

T_g is the temperature of a 150 mm diameter black globe thermometer, ^{o}C.

WBGT Index was used to reduce the heat casualties between military recruits during the army training operations. Where, it was found that heat casualties and time lost due to cessation of training in the heat were both reduced by using the *WBGT* index instead of air temperature alone. The important aspect of this index is that no measurement of air velocity is required, where the effect of air velocity is on the globe temperature, and in the absence of a radiant heat load ($T_r = T_a$), air movement would not affect the index value. The *WBGT* is therefore more applicable in the open desert conditions for where the radiant heat load is high and air movement contributes to the index value through its effect on the globe thermometer (Kerslake 1972).

4.8. Predicted Mean Vote

Through the efforts for evaluating the thermal environment, Fanger proposed that the degree of discomfort will depend on the thermal load of human body which he defined as '*the difference between the internal heat production and the heat loss from the body to the actual environment for a human by activity hypothetically kept at the comfort levels of the mean skin temperature and the sweat secretion at the actual activity level*'. According to the definition the comfort conditions is provided when the thermal load equal to zero (Fanger 1970).

The *PMV* index integrates six variables; the four environmental variables (air temperature, mean radiant temperature, air velocity, and relative humidity), and two personal variables (clothing insulation and activity level) into an index that predict the average thermal sensation of a large group of people in an environment. The *PMV* index predicts the mean response of a large group of people on the following scale (ASHRAE 1993):

+3	Hot
+2	Warm
+1	Slightly warm
0	Natural
-1	Slightly cool
-2	Cool
-3	Cold

The PMV index is given by the following equation (Fanger 1970):

$$\begin{aligned} PMV = (0.303e^{-0.036M} + 0.028)\big[&(M - W) \\ &- 3.05 \times 10^{-3}\{5733 - 6.99(M - W) - P_p\} \\ &- 0.42\{(M - W) - 58.15\} - 1.7 \times 10^{-5}M(5867 - P_p) \\ &- 0.0014M(34 - T) - 3.96 \times 10^{-8}f_{cl}\{(T_{cl} + 273)^4 - (T_r + 273)^4\} \\ &- f_{cl}h_c(T_{cl} - T_a)\big] \end{aligned} \tag{54}$$

where

$$\begin{aligned} T_{cl} = 35.7 - 0.028(M - W) \\ - R_{cl}[3.96 \times 10^{-8}f_{cl}\{(T_{cl} + 273)^4 - (T_r + 273)^4\} \\ + f_{cl}h_c(T_{cl} - T_a)] \end{aligned}$$

$$f_{cl} = \begin{cases} 1.00 + 0.2I_{cl} & for \quad I_{cl} \leq 0.5clo \\ 1.05 + 0.1I_{cl} & for \quad I_{cl} > 0.5clo \end{cases}$$

and for h_c,

$$h_c = \begin{cases} 2.38(|T_{cl} - T_a|)^{0.25} & for \quad 2.38(|T_{cl} - T_a|)^{0.25} > 12.1\sqrt{w_r} \\ 12.1\sqrt{w_r} & for \quad 2.38(|T_{cl} - T_a|)^{0.25} \leq 12.1\sqrt{w_r} \end{cases}$$

where

M is the metabolic heat rate, W. m^{-2},
W is the external mechanical power, W. m^{-2},
f_{cl} is the coverage degree of body by clothing (ratio of clothed to nude surface area),
T_a is the air temperature, ^{o}C,
T_r is the mean radiant temperature, ^{o}C,
P_p is the partial water vapor pressure, Pa,
h_c is the coefficient of heat transfer by convection, W. m^{-2}. K^{-1},
T_{cl} is the surface temperature of clothing, ^{o}C,
R_{cl} is the thermal resistance of clothing, m^{2}. K. W^{-1},
w_r is the relative air velocity against the human body, m. s^{-1},
I_{cl} is dimensionless thermal resistance of clothing, $I_{cl} = R_{cl} / 0.155$ [clo].

4.9. Predicted Percentage Dissatisfied

The predicted percentage dissatisfied *PPD* index describes the percentage of occupants that are dissatisfied with the given thermal conditions. Fanger (Fanger 1970) related PPD to PMV as follows:

$$PPD = 100 - 95e^{(-0.03353PMV^4 - 0.2179PMV^2)} \tag{55}$$

Figure 12. represents the relationship between the *PMV* and *PPD*.

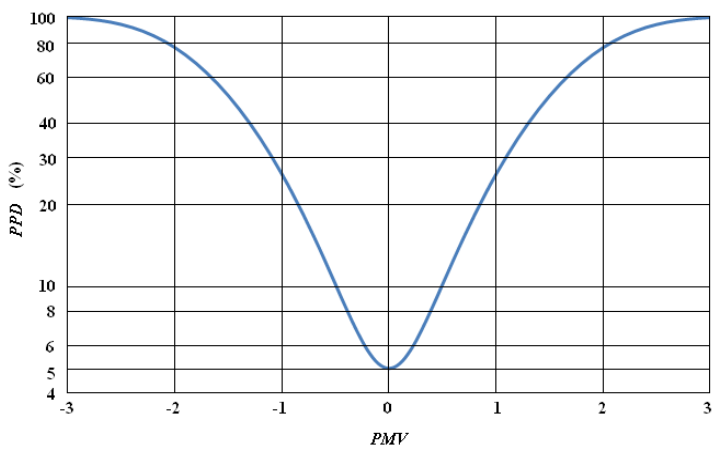

Figure 12. The predicted percentage dissatisfied *PPD* persons as a function of *PMV* index

4.10. Draught Rate

The discomfort because of draught is expressed as the percentage of people predicted to be fussed by draught. The draught rate (*DR*) is calculating using the following equation (ISO 7730 1994):

$$DR = (34 - T_a)(w - 0.05)^{0.62}(0.37w.Tu + 3.14)$$

Tu is the local air turbulence (per cent), which is defined as the ratio of the standard deviation of the local air velocity to the local mean air velocity.
T_a is the air temperature, ^{o}C,
w is the air velocity, m.s^{-1}.

II. THEORETICAL SOLUTION

The most common thermal indices are presented in the first part of the thesis. In this part of thesis two indices, that are the globe and operative temperatures, were selected to study. Choosing these two indices was due to the following reasons:

1- The term of temperature is a convenient way to represent the human thermal environment, because it is easier for us to understand how a human body would respond to a change in the temperature than how it would respond to a change in absorbed energy for example.
2- The globe temperature is direct index, that it can be measured directly by globe thermometer (Kazkaz et al. 2014).
3- The operative temperature is the simplest environmental index, because it depends on the environmental factors only, and represents a direct measure of the environmental heat stress on human body.
4- The similarity between the globe and operative temperature, where both them depend on the heat balance between the radiation and convection heat transfer (ASHRAE 1981).

Thus, it has been selected the globe and operative temperatures to be studied, where the effect of the environmental parameters on the two indices was studied, and the relations between the environmental variables and each of globe temperature and operative temperature were fund. Later, the comparison between the two indices was done, where this comparison was carried out using own theoretical solution of operative and globe temperatures in a wide range of environmental parameters (mean radiant temperature, air velocity, and air temperature).

1. Introduction to Theoretical Solution

The aim of the work is to design a new compact sensor for evaluating the thermal state in the indoor environment, which includes the working environment. According to the binding regulations and norms the operating temperature is used for designing or assessing the thermal state of the environment (see for example the Government Regulation No. 93/2012 Sb. (Nařízení vlády 2012)). For this reason, a compact sensor was developed which, in a certain range of environmental parameters (air temperature, mean radiation temperature and air velocity), will generate a directly the operative temperature.

The development of sensor is performed using different theoretical solutions. This procedure is first used for assessment the possibility of measuring the operative temperature using the globe thermometer, and after that, the procedure is used for development a new sensor suitable for both the regulation and evaluation of the thermal state of the environment.

The procedure of application of the mentioned theoretical solutions is based on the following considerations:

- The operative temperature T_o can be represented as the balanced temperature on the surface of the human body, at which affect only the heat convection from ambient air at air velocity and air temperature, and the heat radiation from the surrounding surfaces at mean radiation temperature T_r, see Figure 13a.

Note: Since the operative temperature is particularly intended for evaluating the state of the human indoor environment, in this work was not considered the metabolic heat or other metabolic effect, nor the heat capacity of the human body.

- In the theoretical solution of the operative temperature T_o, the surface of the human body is replaced by sphere, see Figure 13b, since the determination of the real surface of the human body is very complex. For calculating the convection, the sphere has the same surface A_D as the human body, and in case of radiation the surface is replaced by another sphere of smaller radius A_r. This simulation between the human bod and sphere is acceptable because the sphere has against the environment different situated surfaces, similar as human body.

  Note: For the standing person, it would be more appropriate to replace the surface of the human body with a vertical ellipsoid, but the person is present in other settings, such as sitting, lying.

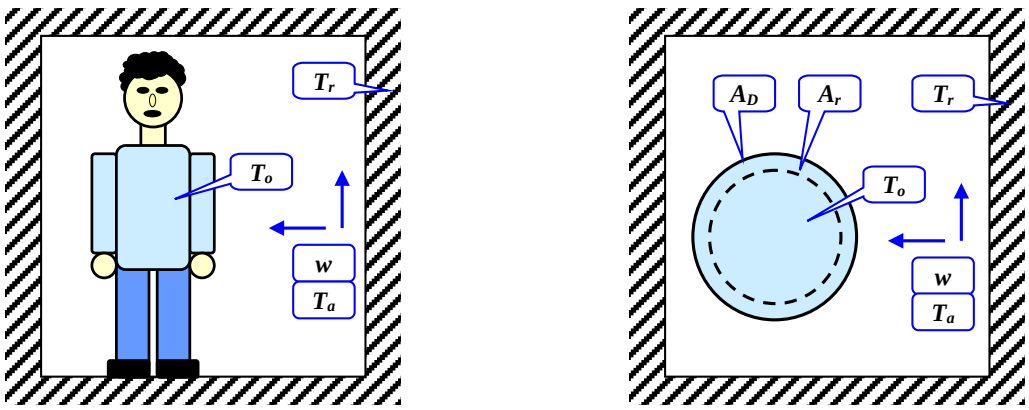

a) Human body in an indoor environment b) Globe in in an indoor environment

Figure 13. The human body in an indoor environment and his replacement globe of the same surface

- For determining the operative temperature, in practice is often used the globe thermometer with diameter D = 150 or 100 mm, (see Figure 14a). Then the temperature of the globe thermometer T_g can be approximately identified the operative temperature, but this only in a certain range of the environmental parameters, which is theoretically solved and explored in the dissertation thesis.

  Note: In the literature, there are various approximate methods for determining the operative temperature. Some manufacturers identify a globe thermometer or an unheated ellipsoid thermometer with an operative temperature sensor (LumaSense Technologies 2007). According to literature (Nařízení vlády 2002), it is possible to replace the operative temperature T_o by the globe temperature T_g, and this for air velocity $w < 0.2$ m. s^{-1} (see also chapter II / 6.1). And according to the literature (Zmrhal et al. 2010) it is possible to replace the operative temperature T_o by the globe temperature T_g for air velocity $w > 0.2$ m. s^{-1}. Therefore, these conclusions need to be clarified.

Approximate determination of the operative temperature is also given in paragraph (ASHRAE 1981) (see Chapter I / 4.6) where T_o is for $| T_a - T_r | < 4$ K calculated from the relationship $T_o = (T_a + T_r) / 2$. However, this method requires complex measurement of the radiation temperature T_r.

- The aim of thesis is designing a relatively small compact plate sensor, which measures the plate temperature T_p, (see Fig. 14b.). The plate temperature could be then, as in case of the globe thermometer, accurately identified with the operative temperature T_o, and this in widest range of the environmental parameters.

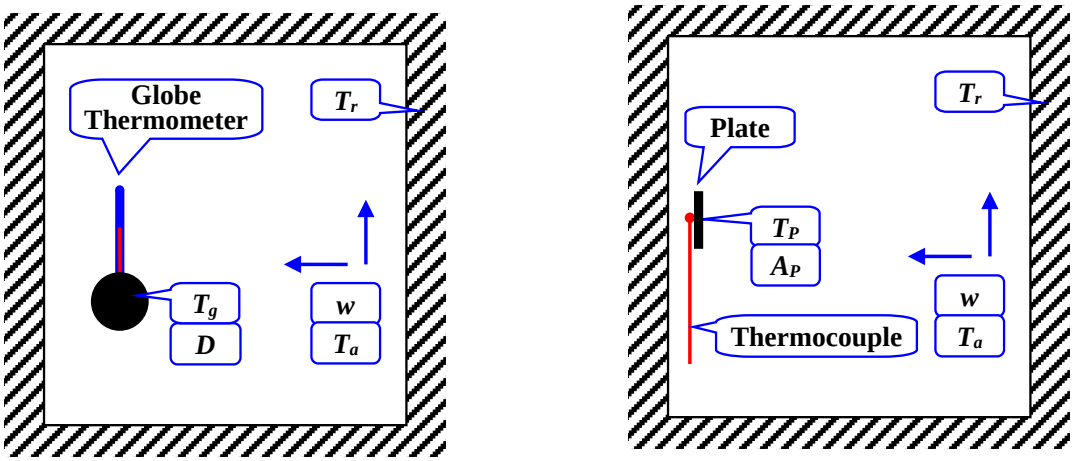

a) Measuring the operative temperature using globe thermometer

b) Measuring the *operative temperature* using plate thermometer

Figure 14. Measuring the operative temperature using the compact sensors

Note: To extend the range of environmental parameters allowing this identification, it will be appropriate to correct the plate temperature T_p.

2. Mathematical Methods of Solving the Equations

The mathematical models of a wide range of problems in science and engineering applications can be formulated as an equation of the form $f(x) = 0$. The solution of this type of the equations is achieved by finding the values of x at which the function $f(x)$ becomes zero, due to that these values are called the zeroes of the function $f(x)$ (Srivastava et al. 2011).

The equation $f(x) = 0$ can be algebraic, polynomial, transcendental equation. Where,

- *The algebraic equation*: is an equation of the form $f(x, y) = 0$, this equation has an infinite number of pairs of x and y values which satisfy it.
- *Polynomial equation*: is a simple class of algebraic equation that can be expressed as follow:

  $$a_n x_n + a_{n-1} x_{n-1} + \cdots + a_1 x + a_0 = 0$$

  This equation is called nth degree polynomial and has n roots. The roots can be real or complex numbers.
- *Transcendental equation*: is a non-algebraic equation, this type of equations containing trigonometric, hyperbolic, exponential, or logarithmic functions. A transcendental equation may have a finite or an infinite number of real or complex roots.

Any function doesn't graph as a line in two dimensions, or doesn't graph as a plane in three dimensions, is called a nonlinear function (Balagurusamy 2012).

2.1. Methods of Solving the Nonlinear Equation

There are several methods to solving the nonlinear equation and find its roots. These methods include:

- *Direct analytical method*: is used to solve the simple linear equation. By using the direct method, the exact values of the roots can be found in a finite number of steps.
- *Graphical method*: is based on plotting the function and determining the points where the function intersects the x-axis. These points represent approximate values of the roots of the function.
- *Trial and error method*: in this method, the roots of the function are found by using series of guesses for the variable x, each time evaluating the function to see whether it is closed to zero. The value of x that cases the function value closer to zero is one of the approximate roots of the solution.
- *Iterative method*: the first step in this method to choose an approximate value of the root (the initial guess), which is then successively corrected iteration by iteration. The process of iteration stops when the desired level of accuracy is obtained.

There are many methods which use the iterative technique; these methods can be classified into two categories:

1. *Bracketing methods*: start with two initial guesses that 'bracket' the root and then systematically reduce the width of the bracket until the solution is reached.
2. *Open-end methods*: use a single starting value or two values that do not necessarily bracket the root. It may be noted that the bracketing method requires finding sign changes in the function during every iteration. Open end method doesn't require this (Balagurusamy 2012).

The most common open end iterative methods:

- Newton-Raphson method
- Secant method
- Muller's method
- Fixed-point method
- Bairstow's method

In the following paragraph are briefly described Newton-Raphson method and secant method, which are the more suitable methods for solving the transcendental equations. These two methods are effective in finding the roots of the equation with the least effort and time, how to use these methods and the difference between them is mentioned later.

2.2. Newton-Raphson Method

This method is an open-end method that requires a single initial value x_0 and is based on linear approximation of the function. In this method, finding the roots of the function is achieved by constructing a tangent to the curve at the initial guess x_0. The point where the tangent intersects the x-axis represents the approximation value. The process is repeated until the value of the function is sufficiently close to zero.

Considering the function $f(x)$, the equation of tangent to the function $f(x)$ at x_0 is given by:

$$f(x) - f(x_0) = (x - x_0)f'(x_0) \tag{56}$$

Where $f'(x_o)$ is the slope of the tangent (the derivation of the function $f(x)$).

The value of x at which the tangent crosses the x-axis is taken as the next approximation value of the root x_1. Thus,

$$x_1 = x_0 - f(x_0)/f'(x_0) \tag{57}$$

The next approximation would be:

$$x_2 = x_1 - f(x_1)/f'(x_1)$$

or generally

$$x_{n+1} = x_n - f(x_n)/f'(x_n) \tag{58}$$

The equation (58) is called the Newton-Raphson formula. The process will be terminated when the difference between two successive values is within a prescribed limit (Srivastava et al. 2011).

2.3. Secant Method

When the derivative function $f'(x)$, is unavailable or difficult to evaluate, an alternative to Newton's method is required, the perfect alternative method is the secant method.

The secant method is based on the approximation of the nonlinear function $f(x)$ by linear function $g(x)$, which is the secant to $f(x)$, and the point at which the scant $g(x)$ intersects the x-axis is taken as a next approximation to the root of the nonlinear function $f(x)$. The procedure is applied repetitively to convergence (Hoffman 2001).

Secant method requires two initial values x_0 and x_1, from which the secant to the function $f(x)$ passes. The slope of the secant passing through the points x_0 and x_1 is given by:

$$g'(x) = \frac{f(x_1) - f(x_0)}{x_1 - x_0} \tag{59}$$

Thus, the next approximation value of the root is:

$$x_2 = x_1 - \frac{x_1 - x_0}{f(x_1) - f(x_0)} f(x_1) \tag{60}$$

or generally

$$x_{i+1} = x_i - \frac{x_i - x_{i-1}}{f(x_i) - f(x_{i-1})} f(x_i) \tag{61}$$

2.4. Stopping Criterion

The process of iteration stops when the desired level of accuracy is obtained. There are a few criterions which are used to determine when to terminate the process (Sakara 2007):

- $|x_{i+1} - x_i|$ $\leq E_a$ (the absolute error in x)
- $|(x_{i+1} - x_i) / x_{i+1}|$ $\leq E_r$ (the relative error in x), $x \neq 0$
- $|f(x_{i+1})|$ $\leq E$ (value of function at root)
- $|f(x_{i+1}) - f(x_i)|$ $\leq E$ (difference in function values)
- $|f(x)|$ $\leq F_{max}$ (large function value)
- $|x_i|$ $\leq$ XL (large value of x)

Here, x_i represents the estimate of the root at ith iteration and $f(x_i)$ is the value of the function at x_i.

3. Theoretical Solution of Globe Temperature

The globe temperature is thermal comfort index which combines the effect of air temperature, air movement, and mean radiant temperature. It is a direct index which can measure directly by the globe thermometer. The globe thermometer consists of a hollow copper sphere of diameter 150 mm (or 100 mm), coated with matt black paint and containing an ordinary thermometer with its bulb fixed at the center of the sphere, without source of heat, see Figure 11. (Vernon 1930).

The work principle of the globe thermometer is based on the thermal balance between the radian heat flow from (to) the sphere and the convective heat flow to (from) the sphere. The time required to the globe thermometer reaches the thermal equilibrium depends on the environmental parameters, usually (10 - 20) minutes. The globe thermometer reaches thermal equilibrium when the heat gain by radiation equals the heat loss by convection.

$$q_r = q_c \tag{62}$$

The specific heat transfer gain by radiation for the globe thermometer can be determined from Stefan – Boltzmann's law, as following:

$$q_r = \varepsilon\sigma(T_r^4 - T_g^4) \tag{63}$$

The specific heat transfer loss by convection for the globe thermometer is given by the equation:

$$q_c = h_{cg}(T_g - T_a) \tag{64}$$

where:

q_r is the specific radiation heat transfer, W.m^{-2},
q_c is the specific convection heat transfer, W.m^{-2},
ε is the emissivity of the globe thermometer surface. For matt black surface (ε = 0.95),
σ is Stefan – Boltzmann's constant, $\sigma = 5.67\times10^{-8}$ [W.m^{-2}. K^{-4}],
h_c is the convection heat transfer coefficient, W. m^{-2}. k^{-1},
T_g is the absolute temperatures of the thermometer (globe temperature), K,
T_r is the mean absolute temperatures of surfaces surrounding the globe thermometer, K,
T_a is the air temperature, K.

The coefficient heat transfer h_{cg} can be calculated by using the definition of Nusselt number as follow:

$$h_{cg} = Nu\frac{k}{D} \tag{65}$$

where

k is the thermal conductivity of the air, W.m^{-1}. K^{-1},
D is the external diameter of globe thermometer, m.

Then the heat balance equation of the globe thermometer can be rewritten as:

$$\varepsilon\sigma(T_r^4 - T_g^4) = h_{cg}(T_g - T_a) \tag{66}$$

The equation (66) represent the heat balance equation for the globe thermometer with its environment. From this equation, the globe temperature can be considered as function of the environmental parameters. The difficulty in this relation is to determine the coefficient heat transfer h_{cg} or the Nusselt number (see equation (65)).

The determination of the heat transfer coefficient (Nusselt number) is difficult and complicated, and it is required to know the type of flow (laminar, turbulent, or mixed) and kind of the convection heat transfer (natural, forced, or combined).

In this work, the combined convection heat transfer (forced and natural) has been used to calculate the Nusselt number. Two separated analysis was used to calculate the Nusselt number.

- ***<u>The first solution</u>*** is based on the comprehensive correlation (18):

$$Nu_{comb.} = minNu + \sqrt{Nu_{lam}^2 + Nu_{turb}^2}$$

$$Nu_{lam} = 0.664 Re_{comb.}^{0.5} Pr^{1/3}$$

$$Nu_{turb} = \frac{0.037 Re_{comb.}^{0.8} Pr}{1 + 2.44 Re_{comb.}^{-0.1}(Pr^{2/3} - 1)}$$

$$0 < Re_{comb.} < 10^7$$

$$0.5 < Pr < 2500$$

where for combined natural and forced heat transfer Schlunder (Schlünder 1975) suggested to use combined Reynolds number (equation (19)):

$$Re_{comb.} = \sqrt{Re^2 + \frac{Gr}{2.5}}$$

- ***<u>The second solution</u>*** analysis is based on the relation (20):

$$Nu_{comb.} = \left(Nu_{forced}^n \pm Nu_{natural}^n\right)^{1/n}$$

where Nu_{forced} and $Nu_{natural}$ are determined from the correlations for pure forced and pure natural convection, respectively.

The plus sign is for assisting and transverse flows and the minus sign is for opposing flows. The value of the exponent n depends on the geometry involved. The best correlation of data is often obtained for n = 3 for vertical plate, n = 7/2 for horizontal plate, and n = 4 for cylinders or spheres (Churchill 1998).

3.1. First Theoretical Solution of Globe Temperature

In this chapter, the equation (18) is used to calculate the Nusselt number of combined convection heat transfer. Where:

$$Nu_{comb.} = minNu + \sqrt{Nu_{lam}^2 + Nu_{turb}^2}$$

$$Nu_{lam} = 0.664 Re_{comb.}^{0.5} Pr^{1/3}$$

$$Nu_{turb} = \frac{0.037 Re_{comb.}^{0.8} Pr}{1 + 2.44 Re_{comb.}^{-0.1} (Pr^{2/3} - 1)}$$

$$Re_{comb.} = \sqrt{Re^2 + \frac{Gr}{2.5}}$$

where

$$Re = \frac{wD}{\nu}$$

$$Gr = \frac{g\beta(T_g - T_a)D^3}{\nu^2}$$

where

Re is the Reynolds number of flow,
Gr is the Grashof number,
Pr is Prandtl number,
w is the air velocity, $m.s^{-1}$,
g is the gravitational acceleration, $m.s^{-2}$,
β is the coefficient of volume expansion, K^{-1} ($\beta = 1/T$ for ideal gases),
υ is the kinematic viscosity of the fluid, $m^2.s^{-1}$,
T_g is the globe temperature, °C,
T_a is the temperature of the air sufficiently far from the globe thermometer, °C,
D is the diameter of the globe thermometer, m.

For globe thermometer, the following conditions are applied:

- Minimum Nusselt number min $Nu = 2$
- Diameter of sphere $D = 0.15$ m
- The volumetric thermal expansion coefficient $\beta = 2 / (T_g + T_a)$
- *Pr* and υ are depended on air temperature.

Thus, the Nusselt number of flow around the globe thermometer can be expressed as follow:

$$Nu_{comb.} = 2 + \left[\left(0.664 Pr^{1/3} \left(\left(\frac{Dw}{\nu} \right)^2 + \frac{2}{2.5} \frac{g(T_g - T_a)D^3}{\nu^2 (T_g + T_a)} \right)^{0.25} \right)^2 + \left(\frac{0.037 \left(\left(\frac{Dw}{\nu} \right)^2 + \frac{2}{2.5} \frac{g(T_g - T_a)D^3}{\nu^2 (T_g + T_a)} \right)^{0.4} Pr}{1 + 2.44(Pr^{2/3} - 1) \left(\left(\frac{Dw}{\nu} \right)^2 + \frac{2}{2.5} \frac{g(T_g - T_a)D^3}{\nu^2 (T_g + T_a)} \right)^{-0.05}} \right)^2 \right]^{0.5} \tag{67}$$

The convection heat transfer coefficient for the flow around the globe thermometer is:

$$h_{cg} = Nu_{comb.} \frac{k}{D} \tag{68}$$

or

$$h_{cg} = \frac{k}{D} \left\{ 2 + \left[\left(0.664 Pr^{1/3} \left(\left(\frac{Dw}{\nu} \right)^2 + \frac{2}{2.5} \frac{g(T_g - T_a)D^3}{\nu^2 (T_g + T_a)} \right)^{0.25} \right)^2 + \left(\frac{0.037 \left(\left(\frac{Dw}{\nu} \right)^2 + \frac{2}{2.5} \frac{g(T_g - T_a)D^3}{\nu^2 (T_g + T_a)} \right)^{0.4} Pr}{1 + 2.44(Pr^{2/3} - 1) \left(\left(\frac{Dw}{\nu} \right)^2 + \frac{2}{2.5} \frac{g(T_g - T_a)D^3}{\nu^2 (T_g + T_a)} \right)^{-0.05}} \right)^2 \right]^{0.5} \right\} \tag{69}$$

The equation (69) represent the convection heat transfer coefficient for the flow around the globe thermometer, and it is a function of the environmental factors.

By substituting the equation (69) in the equation (66), the globe temperature is written as follow:

$$T_g = \left(T_r^4 - \frac{h_{cg}}{\varepsilon \sigma} (T_g - T_a) \right)^{1/4} \tag{70}$$

where T_g, T_r, and T_a in unit of K.

or

$$T_g = \left((T_r + 273)^4 - \frac{h_{cg}}{\varepsilon \sigma} (T_g - T_a) \right)^{1/4} - 273 \tag{71}$$

where T_g, T_r, and T_a in unit of ^{o}C.

The equation (71) describes the globe temperature as function of the environmental factors (men radiant temperature, velocity, and air temperature).

$$T_g = f(T_r, w, T_a)$$

The equation (71) is a transcendental equation, which can be solved using one of the iterative methods, mentioned previous (chapter II/2.), and the more suitable methods are Newton-Raphson method and secant method.

However, The *MATLAB* and *SURFER* programs were used to solve and draw this equation in range of variables:

$$0 \leq T_r \leq 40\ ^{o}\text{C}$$

$$0 \leq w \leq 1\ \text{m. s}^{-1}$$

$$T_a = 15,\ 25,\ \text{and}\ 35\ ^{o}\text{C}$$

On Figure 15 and 16 are plotted the three globe temperature surfaces, each surface represents the globe temperature function for a constant air temperature.

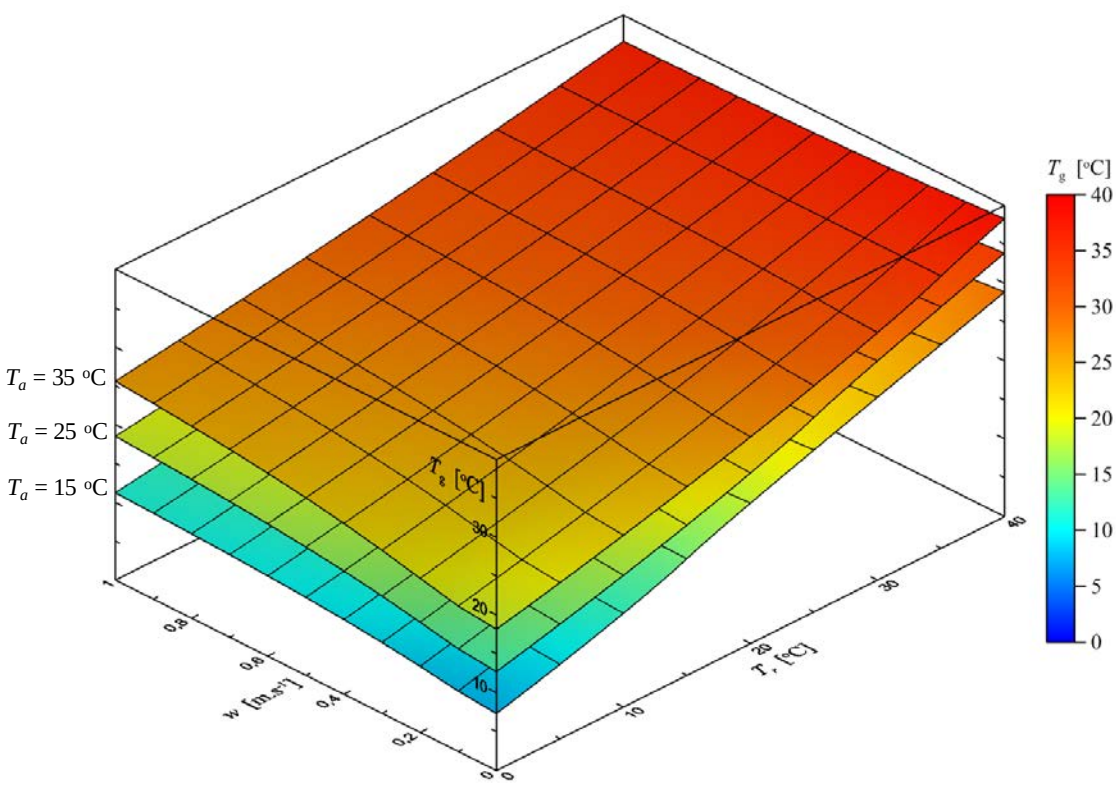

Figure 15. The globe temperature function for constant air temperature – Front view

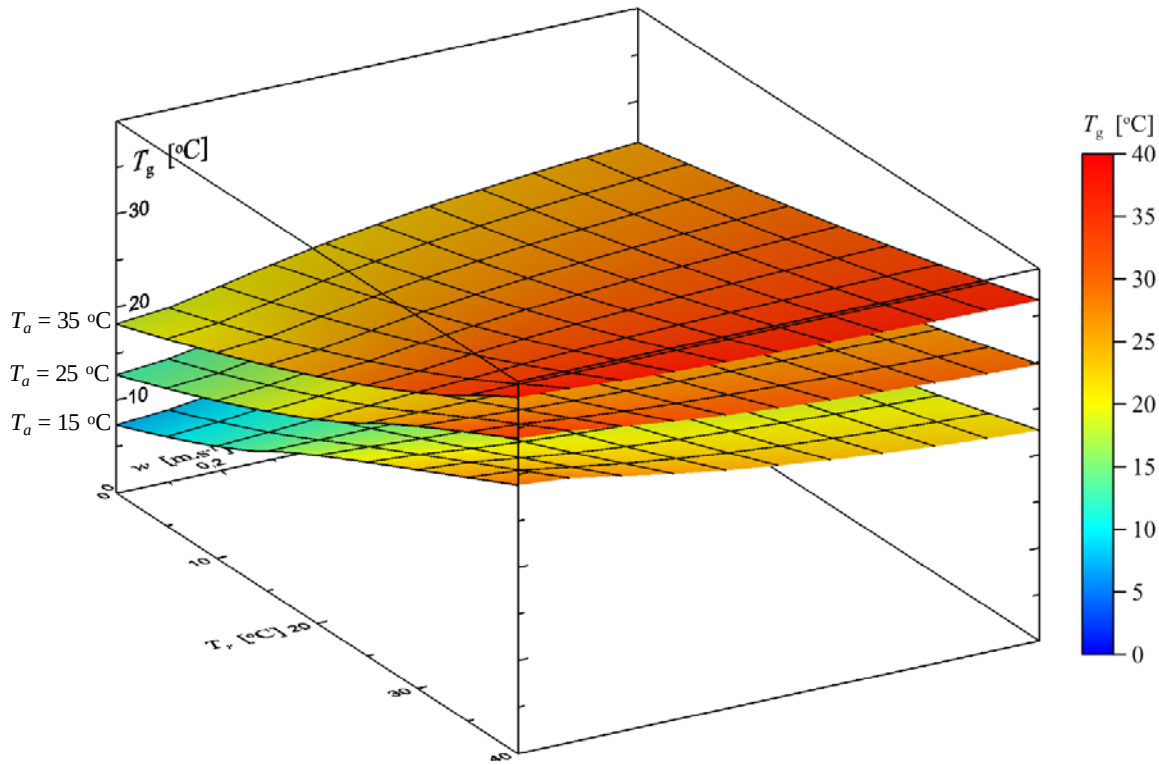

Figure 16. The globe temperature function for constant air temperature – Side view

3.2. Second Theoretical Solution of Globe Temperature

In this chapter, the equation (20) was used to calculate the Nusselt number of combined convection heat transfer. Where

$$Nu_{comb.} = \left(Nu_{forced}^{n} \pm Nu_{natural}^{n}\right)^{1/n}$$

where Nu_{forced} and $Nu_{natural}$ are determined from the correlations for pure forced and pure natural convection, respectively. The plus-minus sign is related to the direction of flow. The value of the exponent n depends on the geometry involved.

For globe thermometer $n = 4$, and for assisting and transverse flows the plus sign is used, and for Nu_{forced} and $Nu_{natural}$ the relation (12) and (17), respectively, were used (Whitaker 1972; Churchill 1983):

$$Nu_{forced} = 2 + \left[0.4Re^{0.5} + 0.06Re^{2/3}\right]Pr^{0.4}\left(\frac{\mu_\infty}{\mu_s}\right)^{0.25}$$

$$3.5 \leq Re \leq 7.6 \times 10^4$$

$$0.71 \leq Pr \leq 380$$

$$Nu_{natural} = 2 + \frac{0.5897Ra^{1/4}}{\left[1 + (0.492/Pr)^{9/16}\right]^{4/9}}$$

$$Ra \leq 10^{11}$$

$$Pr \geq 0.7$$

where

$$Re = \frac{wD}{\nu}$$

$$Ra = GrPr = \frac{g\beta\left(T_g - T_a\right)D^3}{\nu^2}Pr$$

$$h_{cg} = Nu_{comb.}\frac{k}{D}$$

where

Ra is the Rayleigh number of flow,
w is the air velocity, $m.s^{-1}$,
g is the gravitational acceleration, $m.s^{-2}$,
β is the coefficient of volume expansion, K^{-1},
υ is the kinematic viscosity of the fluid, $m^2.\ s^{-1}$,
μ_∞ is the dynamic viscosity of the air at the air temperature, $kg.m^{-1}.\ s^{-1}$,
μ_s is the dynamic viscosity of the air at glob temperature, $kg.m^{-1}.\ s^{-1}$,
T_g is the globe temperature, °C,
T_a is the temperature of the air sufficiently far from the globe thermometer, °C,
D is the diameter of the globe thermometer, m.

For globe thermometer, the following conditions are applied:

- Diameter of sphere $D = 0.15$ m
- The volumetric thermal expansion coefficient $\beta = 2 / (T_g + T_a)$
- *Pr, k, and* υ are depended on air temperature.

Thus, the coefficient of convection heat transfer for air flow around the globe thermometer can be expressed as follow:

$$h_{cg} = \frac{k}{D}\left[\left(2 + \left(0.4Re^{0.5} + 0.06Re^{2/3}\right)Pr^{0.4}\left(\frac{\mu_a}{\mu_g}\right)^{0.25}\right)^4 + \left(2 + \frac{0.5897Ra^{0.25}}{[1 + (0.469/Pr)^{9/16}]^{4/9}}\right)^4\right]^{0.25} \quad (72)$$

The equation (72) represent the convection heat transfer coefficient for the flow around the globe thermometer, and it is a function of the environmental factors.
By substituting the equation (72) in the equation (66), the globe temperature is written as follow:

$$T_g = \left((T_r + 273)^4 - \frac{h_{cg}}{\varepsilon\sigma}(T_g - T_a)\right)^{1/4} - 273 \quad (73)$$

where T_g, T_r, and T_a in unit of °C.

The equation (73) describes the globe temperature as function of the environmental factors (men radiant temperature, velocity, and air temperature).

$$T_g = f(T_a, T_r, w)$$

The equation (73) is a transcendental equation, which can be solved using one of the iterative methods, mentioned previous (chapter II/2.), and the more suitable methods are Newton-Raphson method and secant method.

However, The *MATLAB* and *SURFER* programs were used to solve and draw this equation in range of variables:

$$0 \leq T_r \leq 40\ ^{o}\mathrm{C}$$

$$0 \leq w \leq 1\ \mathrm{m.\ s^{-1}}$$

$$T_a = 15,\ 25,\ \text{and}\ 35\ ^{o}\mathrm{C}$$

On Figure 17 and 18 are plotted the three globe temperature surfaces, each surface represents the globe temperature function for a constant air temperature.

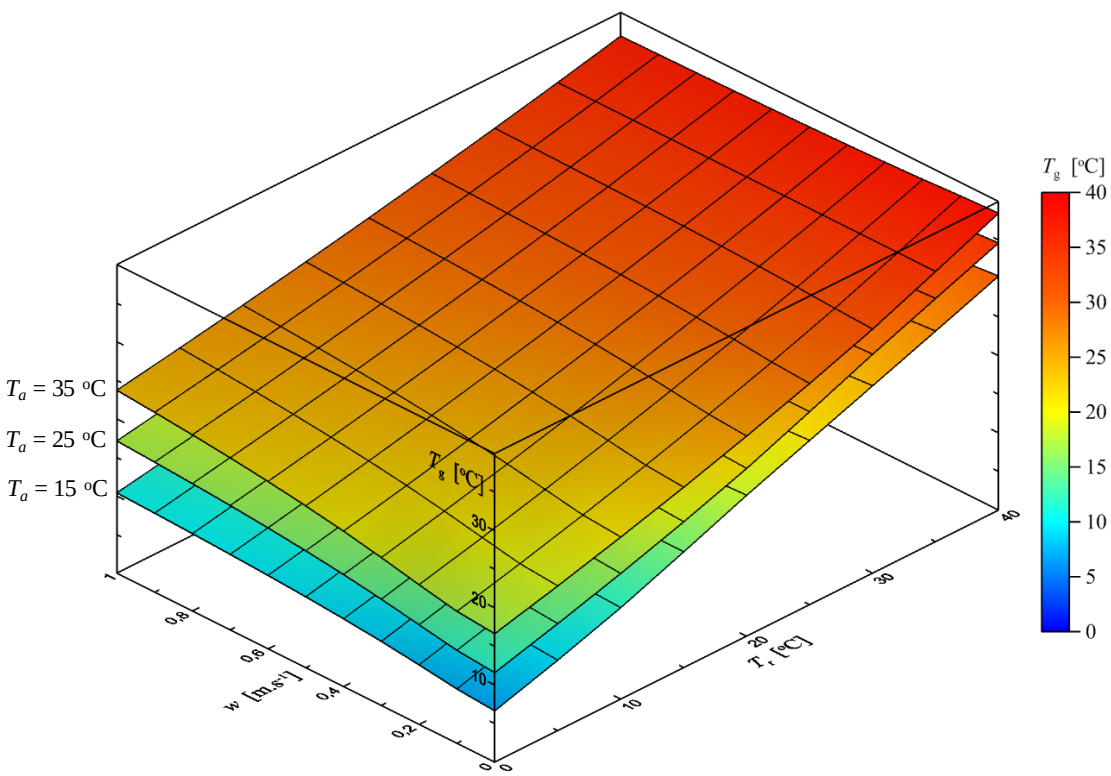

Figure 17. The globe temperature function for constant air temperature – Front view

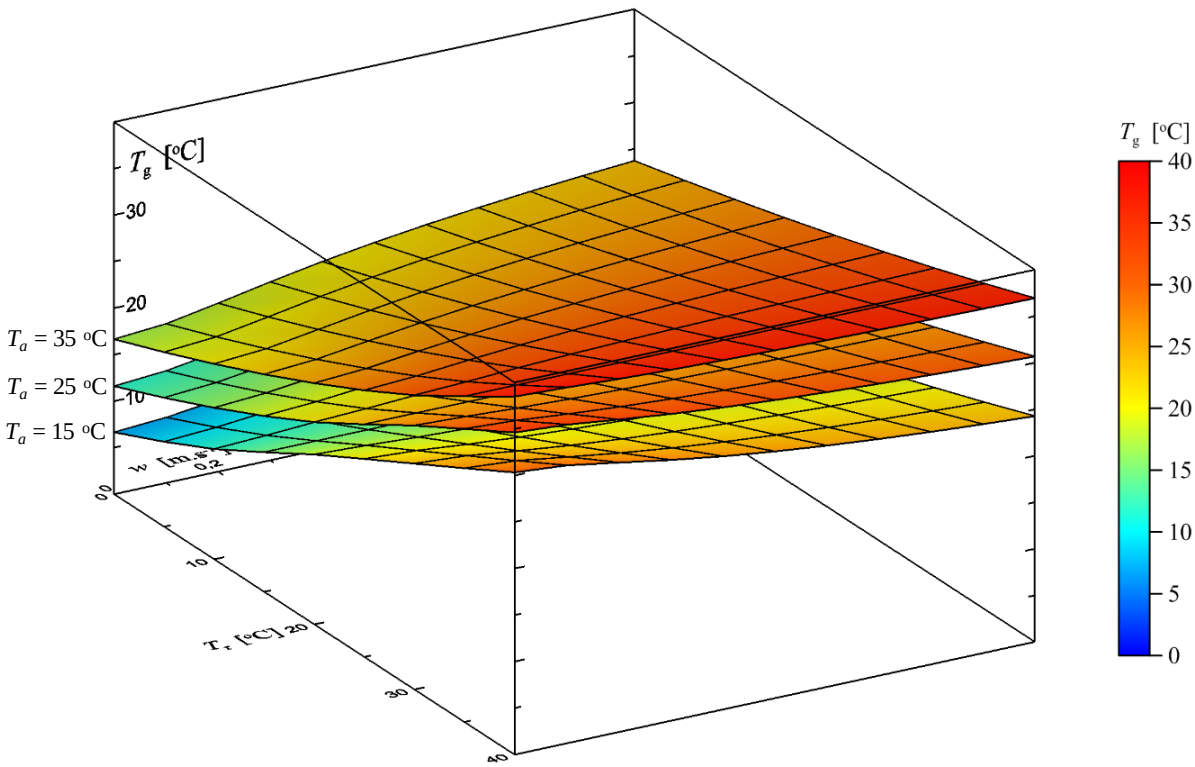

Figure 18. The globe temperature function for constant air temperature – side view

4. Theoretical Solution of Operative Temperature

The operative temperature T_o is an index that integrates the air temperature and mean radiant temperature into a single temperature. The operative temperature is defined as *a uniform temperature of a radiantly black enclosure in which an occupant would exchange the same amount of heat by radiation and convection as in the actual non-uniform environment*.

Mathematically operative temperature can be defined as (ASHRAE 1981):

$$T_o = \frac{T_a h_c + T_r h_r}{h_c + h_r} \tag{74}$$

where:
h_c is the convective heat transfer coefficient W. m^{-2}. K^{-1},
h_r is the linear radiative heat transfer coefficient on the body surface W. m^{-2}. K^{-1},
T_a is the air temperature ^{o}C,
T_r is the mean radiant temperature ^{o}C.

In this work, a simulation was performed between the human body and the globe thermometer in order to compare the two heat indexes; the globe and the operative temperatures. To achieve the simulation, it has been assumed the human body resembles a large sphere with diameter D_o (see Figure 13).

The average value of 1.84 m^2 is assumed for the surface area of the human body, then the equivalent diameter of human body is D_o = 0.757 m (Fanger 1967). In this simulation, the operative temperature of human body (large sphere with diameter D_o = 0.757 m) is calculated from the equation (74).

The coefficient of heat transfer by radiation on the body surface h_{ro}, in equation (74), is calculated from the following equation (Parsons 2003):

$$h_{ro} = \varepsilon\sigma \frac{A_r}{A_D} \frac{T_o^4 - T_r^4}{T_o + T_r} \tag{75}$$

where:
ε is the area emissivity of the human body, and it is often assumed to be between 0.95 to 1.0,
σ is Stefan-Boltzmann constant, 5.67×10^{-8} W. m^{-2}. K^{-4},
A_r is the effective radiative area of the human body, m^2,
A_D is the total body surface area, m^2.

The total body surface area A_D is conventional estimated from the following simplified equation (Du Bois et al. 1916):

$$A_D = 0.202 W^{0.425} H^{0.725} \tag{76}$$

where

W is weight of body, kg,
H is height of body, m.

An average standard value of 1.8 m^2 is used for a 70 kg man of height 1.73m. A_r/A_D can be estimated as 0.72, as average value for a person (Fanger 1967).

In this work, the combined convection heat transfer (forced and natural) has been used to calculate the convective heat transfer coefficient h_{co} (therefor the Nusselt number). Two separated analysis was used to calculate the Nusselt number.

- ***<u>The first solution</u>*** is based on the comprehensive correlation (18):

$$Nu_{comb.} = minNu + \sqrt{Nu_{lam}^2 + Nu_{turb}^2}$$

$$Nu_{lam} = 0.664 Re_{comb.}^{0.5} Pr^{1/3}$$

$$Nu_{turb} = \frac{0.037 Re_{comb.}^{0.8} Pr}{1 + 2.44 Re_{comb.}^{-0.1} (Pr^{2/3} - 1)}$$

$$0 < Re_{comb.} < 10^7$$

$$0.5 < Pr < 2500$$

$$Re_{comb.} = \sqrt{Re^2 + \frac{Gr}{2.5}}$$

- ***<u>The second solution</u>*** is based on the relation (20):

$$Nu_{comb.} = \left(Nu_{forced}^n \pm Nu_{natural}^n\right)^{1/n}$$

where Nu_{forced} and $Nu_{natural}$ are determined from the correlations for pure forced and pure natural convection, respectively.

The plus sign is for assisting and transverse flows and the minus sign is for opposing flows. The value of the exponent n depends on the geometry involved (Churchill 1998).

4.1. First Theoretical Solution of operative Temperature

As it is mentioned above, for the mixed convection heat transfer around the human body (large sphere), the combined Nusselt number is expressed as follow (see equation (18)) (Schlünder 1975):

$$Nu_{comb.} = minNu + \sqrt{Nu_{lam}^2 + Nu_{turb}^2}$$

$$Nu_{lam} = 0.664 Re_{comb.}^{0.5} Pr^{1/3}$$

$$Nu_{turb} = \frac{0.037 Re_{comb.}^{0.8} Pr}{1 + 2.44 Re_{comb.}^{-0.1} (Pr^{2/3} - 1)}$$

$$Re_{comb.} = \sqrt{Re^2 + \frac{Gr}{2.5}}$$

$$Re = \frac{D_o w}{\nu}$$

$$Gr = \frac{g\beta (T_o - T_a) D_o^3}{\nu^2}$$

where
w is the air velocity, m.s^{-1},
g is the gravitational acceleration, m.s^{-2},
β is the coefficient of volume expansion, K^{-1} ($\beta = 1/T$ for ideal gases),
υ is the kinematic viscosity of the fluid, m^2. s^{-1},
T_o is the operative temperature, °C,
T_a is the temperature of the air sufficiently far from the globe thermometer, °C,
Do is the effective diameter of the human body, m.

For human body (large sphere), the following conditions are applied:

- Minimum Nusselt number min $Nu = 2$,
- Diameter of sphere $D_o = 0.757$ m,
- The volumetric thermal expansion coefficient $\beta = 2 / (T_o + T_a)$
- Pr and υ are depended on air temperature.

Thus, the Nusselt number of flow around the human body can be expressed as follow:

$$Nu_{comb.} = 2 + \left[\left(0.664 Pr^{1/3} \left(\left(\frac{D_o w}{\nu} \right)^2 + \frac{2}{2.5} \frac{g(T_o - T_a) D_o^3}{\nu^2 (T_o + T_a)} \right)^{0.25} \right)^2 + \left(\frac{0.037 \left(\left(\frac{D_o w}{\nu} \right)^2 + \frac{2}{2.5} \frac{g(T_o - T_a) D_o^3}{\nu^2 (T_o + T_a)} \right)^{0.4} Pr}{1 + 2.44 (Pr^{2/3} - 1) \left(\left(\frac{D_o w}{\nu} \right)^2 + \frac{2}{2.5} \frac{g(T_o - T_a) D_o^3}{\nu^2 (T_o + T_a)} \right)^{-0.05}} \right)^2 \right]^{0.5} \quad (77)$$

The convection heat transfer coefficient between air and the human body is:

$$h_{co} = \frac{k}{D_o} Nu_{comb.} \tag{78}$$

or

$$h_{co} = \frac{k}{D_o}\left\{2 + \left[\left(0.664 Pr^{1/3}\left(\left(\frac{D_o w}{\nu}\right)^2 + \frac{2}{2.5}\frac{g(T_o - T_a)D_o^3}{\nu^2(T_o + T_a)}\right)^{0.25}\right)^2 + \left(\frac{0.037\left(\left(\frac{D_o w}{\nu}\right)^2 + \frac{2}{2.5}\frac{g(T_o - T_a)D_o^3}{\nu^2(T_o + T_a)}\right)^{0.4} Pr}{1 + 2.44(Pr^{2/3} - 1)\left(\left(\frac{D_o w}{\nu}\right)^2 + \frac{2}{2.5}\frac{g(T_o - T_a)D_o^3}{\nu^2(T_o + T_a)}\right)^{-0.05}}\right)^2\right]^{0.5}\right\} \tag{79}$$

By substituting the equations (79) and (75) in the equation (74):

$$T_o = \frac{T_a h_{co} + T_r h_{ro}}{h_{co} + h_{ro}} \tag{80}$$

Thus,

$$T_o = f(T_a, T_r, w)$$

The equation (80) describes the operative temperature as function of the environmental factors (men radiant temperature, velocity, and air temperature). It is a transcendental equation, which can be solved using one of the iterative methods, mentioned previous (chapter II/2.), and the more suitable methods are Newton-Raphson method and secant method. However, The *MATLAB* and *Surfer* programs were used to solve and draw this equation in range of variables:

$$0 \leq T_r \leq 40\ ^oC$$

$$0 \leq w \leq 1\ m.\ s^{-1}$$

$$T_a = 15,\ 25,\ \text{and}\ 35\ ^oC$$

On Figure 19 and 20 are plotted the three operative temperature surfaces $T_o = f(T_a, T_r, w)$, each surface represents the operative temperature function for a constant air temperature.

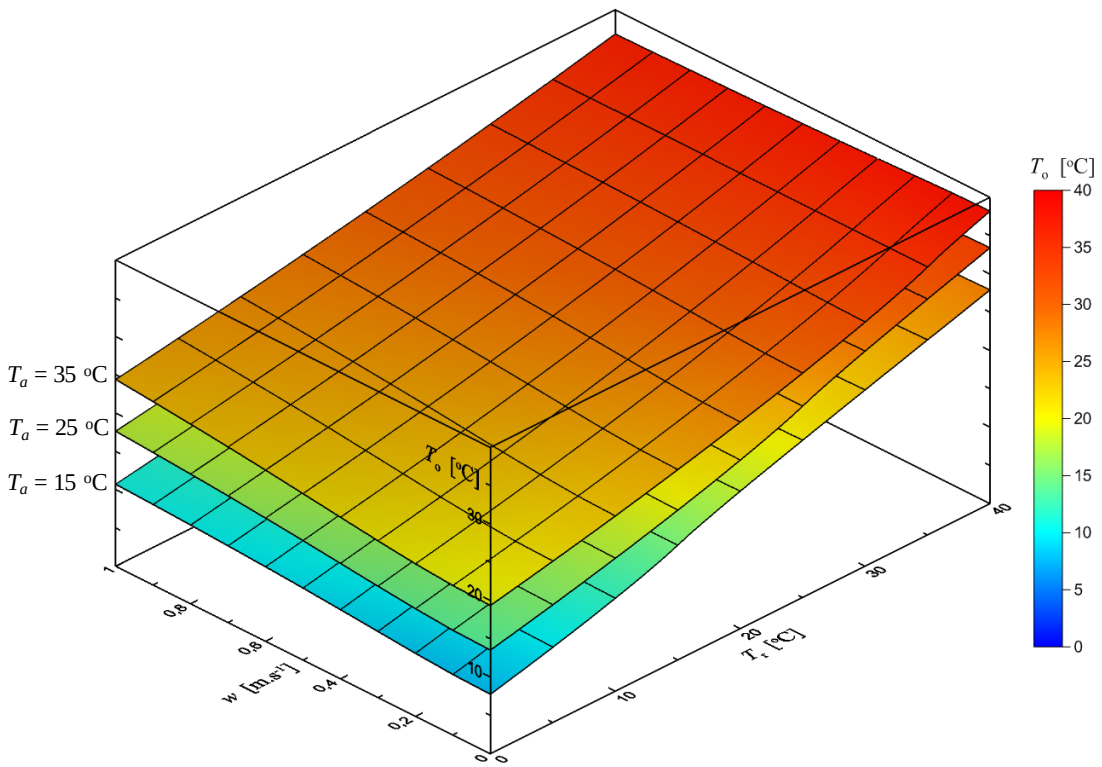

Figure 19. The operative temperature function for constant air temperature – front view

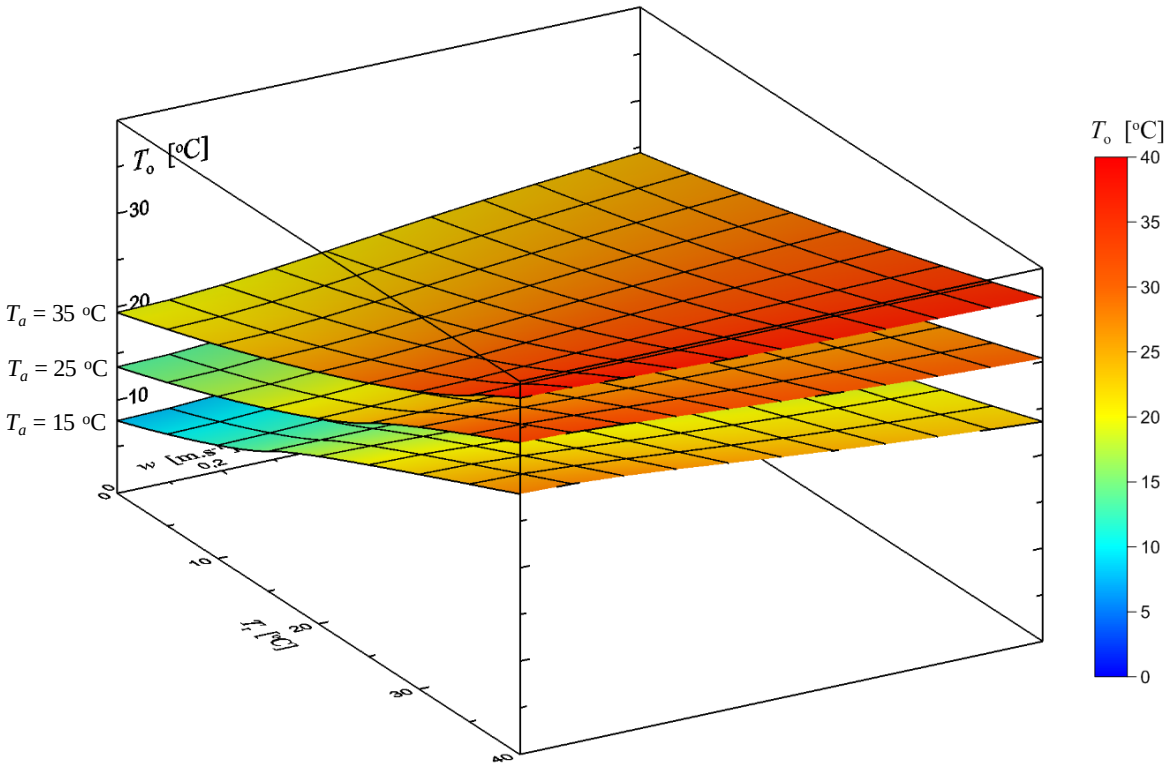

Figure 20. The operative temperature function for constant air temperature – side view

4.2. Second Theoretical Solution of Operative Temperature

In this chapter, the equation (20) was used to calculate the Nusselt number of combined convection heat transfer. Where

$$Nu_{comb.} = \left(Nu_{forced}^{n} \pm Nu_{natural}^{n}\right)^{1/n}$$

where Nu_{forced} and $Nu_{natural}$ are determined from the correlations for pure forced and pure natural convection, respectively. The plus-minus sign is related to the direction of flow. The value of the exponent n depends on the geometry involved.

For human body (big sphere) n = 4, and for assisting and transverse flows the plus sign is used, and for Nu_{forced} and $Nu_{natural}$ the relation (12) and (17), respectively, were used (Whitaker 1972; Churchill 1983):

$$Nu_{forced} = 2 + \left[0.4Re^{0.5} + 0.06Re^{2/3}\right]Pr^{0.4}\left(\frac{\mu_a}{\mu_o}\right)^{0.25}$$

$$3.5 \leq Re \leq 7.6 \times 10^4$$

$$0.71 \leq Pr \leq 380$$

$$Nu_{natural} = 2 + \frac{0.5897Ra^{1/4}}{[1 + (0.492/Pr)^{9/16}]^{4/9}}$$

$$Ra \leq 10^{11}$$

$$Pr \geq 0.7$$

where

$$Re = \frac{D_o w}{\nu}$$

$$Ra = GrPr = \frac{g\beta(T_o - T_a)D_o^3}{\nu^2}Pr$$

$$h_{co} = Nu_{comb.}\frac{k}{D_o}$$

where

Ra is the Rayleigh number of flow,
w is the air velocity, m.s^{-1},
g is the gravitational acceleration, m.s^{-2},
β is the coefficient of volume expansion, K^{-1},
υ is the kinematic viscosity of the fluid, m^2. s^{-1},
μ_a is the dynamic viscosity of the air at the air temperature, kg.m^{-1}. s^{-1},
μ_o is the dynamic viscosity of the air at the operative temperature, kg.m^{-1}. s^{-1},
T_o is the operative temperature, °C,
T_a is the temperature of the air sufficiently far from the globe thermometer, °C,
D_o is the diameter of the globe thermometer, m.

For human body, the following conditions are applied:

- Diameter of sphere D_o = 0.757 m
- The volumetric thermal expansion coefficient $\beta = 2 / (T_o + T_a)$
- *Pr, k, and υ* are depended on air temperature.

Thus, the coefficient of convection heat transfer for air flow around the human body can be expressed as follow:

$$h_{co} = \frac{k}{D_o}\left[\left(2 + \left(0.4Re^{0.5} + 0.06Re^{2/3}\right)Pr^{0.4}\left(\frac{\mu_a}{\mu_o}\right)^{0.25}\right)^4 + \left(2 + \frac{0.5897Ra^{0.25}}{[1 + (0.469/Pr)^{9/16}]^{4/9}}\right)^4\right]^{0.25} \tag{81}$$

The equation (81) represent the convection heat transfer coefficient for the flow around the human body, and it is a function of the environmental factors.

By substituting the equations (81) and (75) in the equation (74), the operative temperature is written as follow:

$$T_o = \frac{T_a h_{co} + T_r h_{ro}}{h_{co} + h_{ro}} \tag{82}$$

Thus,

$$T_o = f(T_a, T_r, w)$$

The equation (82) describes the operative temperature as function of the environmental factors (men radiant temperature, velocity, and air temperature). It is a transcendental equation, which can be solved using one of the iterative methods, mentioned previous (chapter II/2), and the more suitable methods are Newton-Raphson method and secant method.

However, The *MATLAB* and *Surfer* programs were used to solve and draw this equation in range of variables:

$$0 \leq T_r \leq 40\ ^oC$$

$$0 \leq w \leq 1\ m.\ s^{-1}$$

$$T_a = 15, 25, \text{and } 35\ ^oC$$

On Figure 21 and 22 are plotted the three operative temperature surfaces $T_o = f(T_a, T_r, w)$, each surface represents the globe temperature function for a constant air temperature.

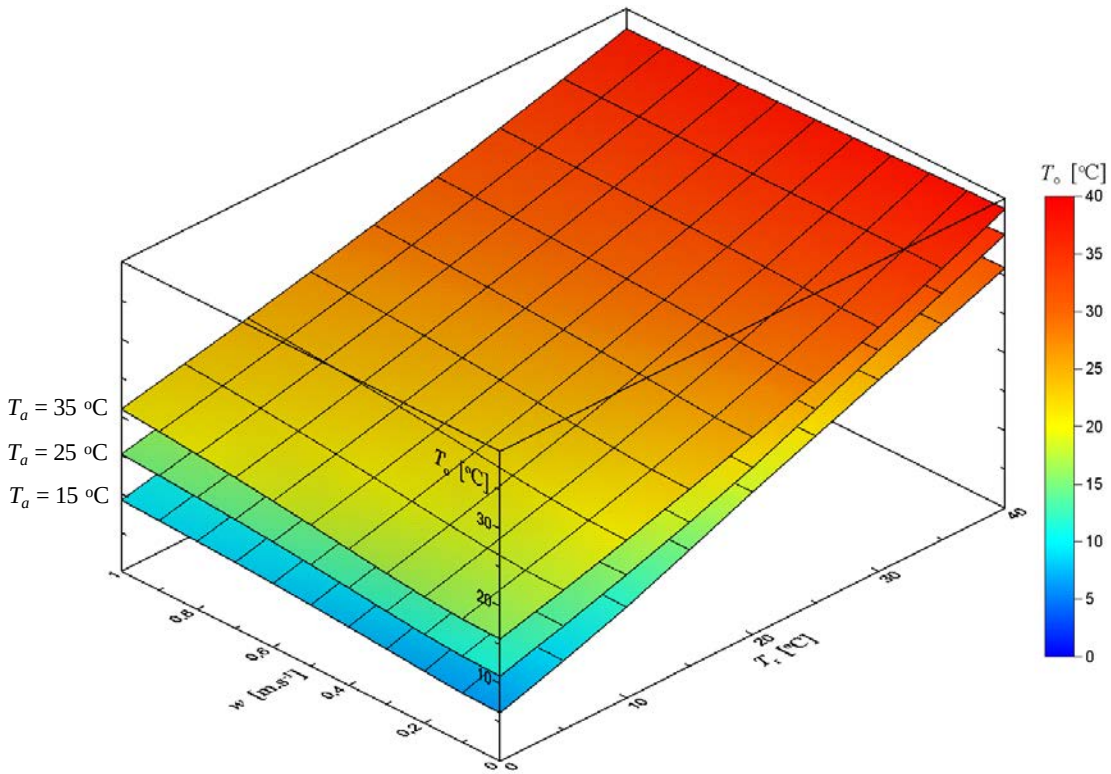

Figure 21. The operative temperature function for constant air temperature – front view

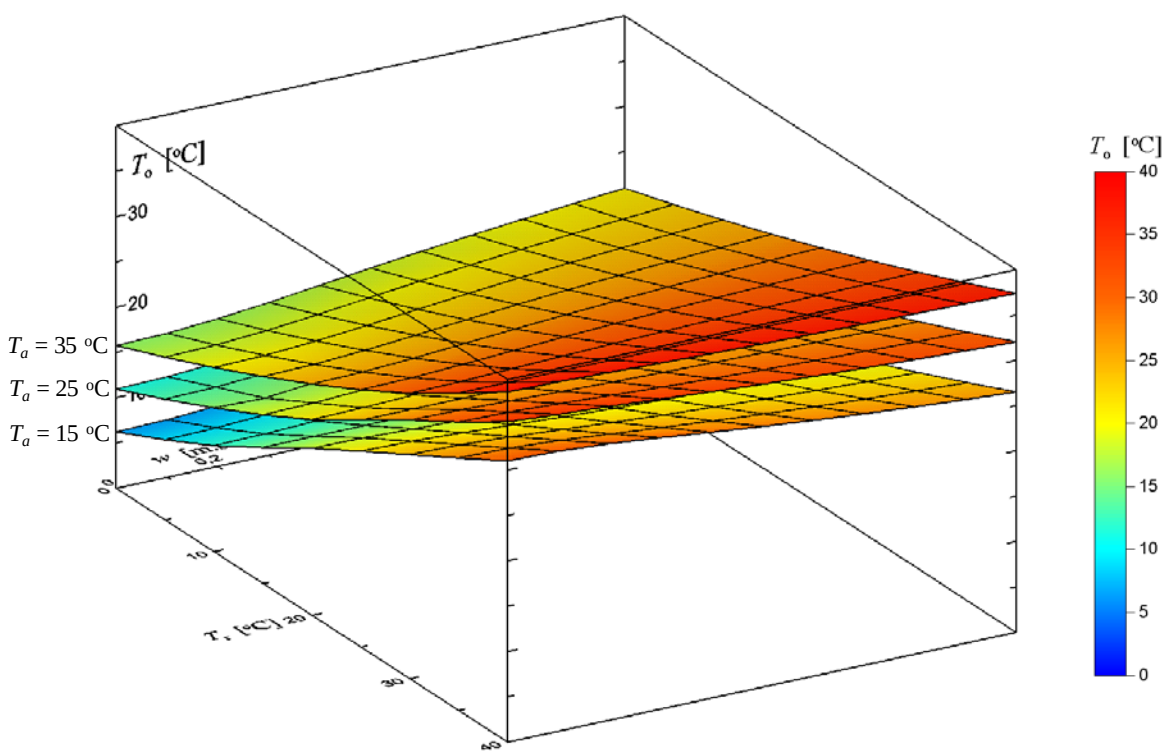

Figure 22. The operative temperature function for constant air temperature – side view

5. Comparison Between Globe and Operative Temperatures

As it mentioned earlier, the simulation of a big sphere for the human body was to make the comparison between the globe and the operative temperatures. In the previous sections, the globe and operative temperatures has been written as functions of the environmental factors (air temperature, air velocity, and mean radiant temperature), these functions were as results of the theoretical solution of the combined convection heat transfer based on the equations (18) and (20). The difference between these two functions (globe and operative temperatures) represents the difference between the globe and the operative temperatures; this difference is also function of the environmental factors as follow:

$$T_g - T_o = f_1(T_r, w, T_a) \tag{83}$$

$$T_g - T_o = f_2(T_r, w, T_a) \tag{84}$$

where

f_1: is function based of the theoretical solution of the equations (18)
f_2: is function based of the theoretical solution of the equations (20)

The difference between the globe and the operative temperatures was plotted on Figures 35, 36, and 37 for the function f_1, and on Figures 38, 39, and 40 for the function f_1.

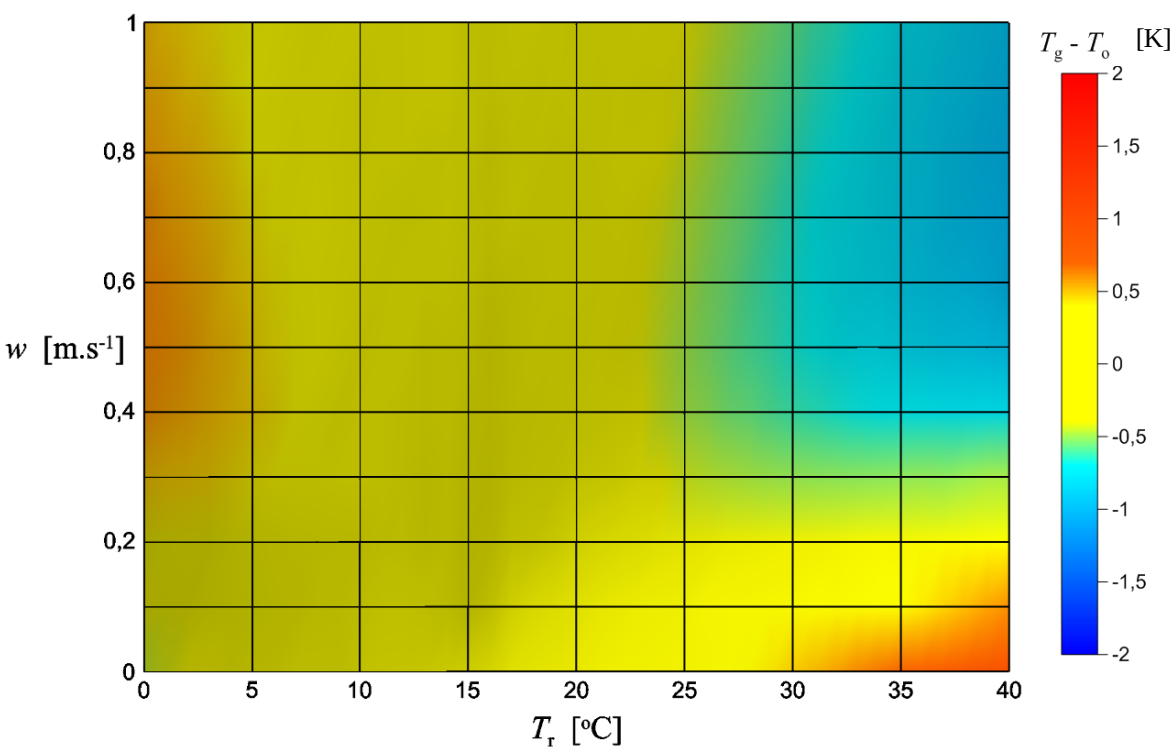

Figure 23. The difference between the globe and the operative temperatures based on the first solution (equation (18)), for constant air temperature T_a = 15 °C

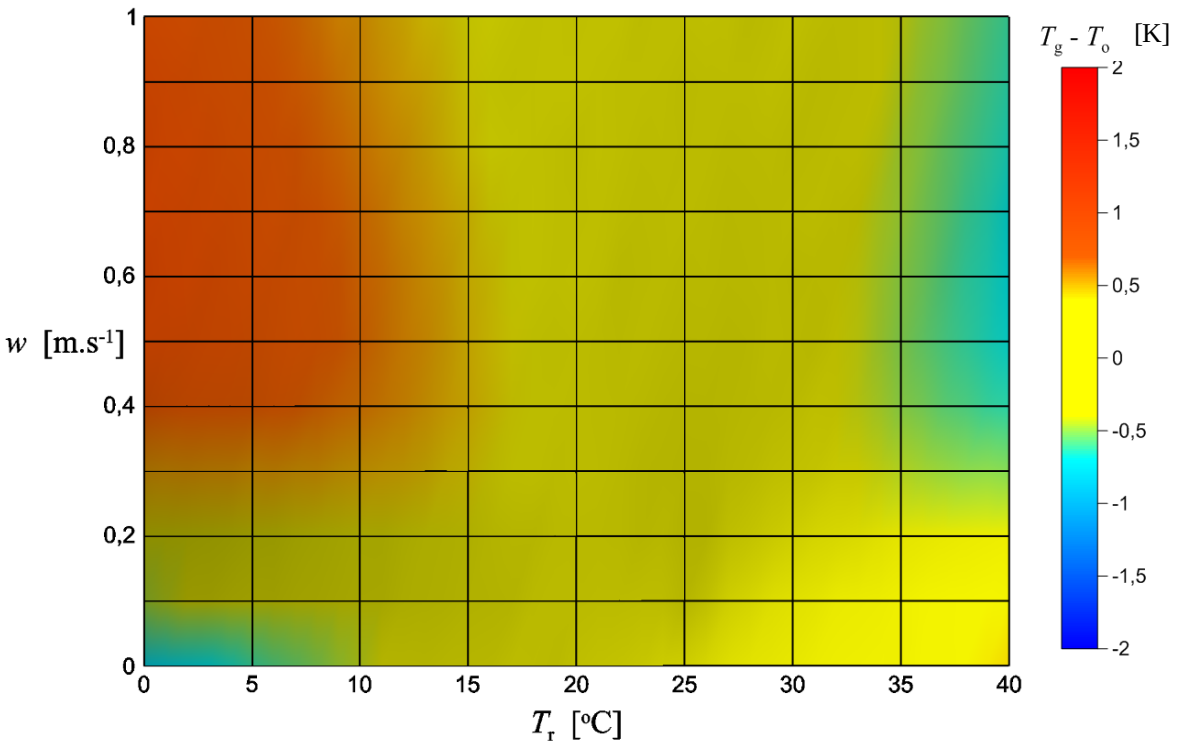

Figure 24. The difference between the globe and the operative temperatures based on the first solution (equation (18)), for constant air temperature T_a = 25 °C

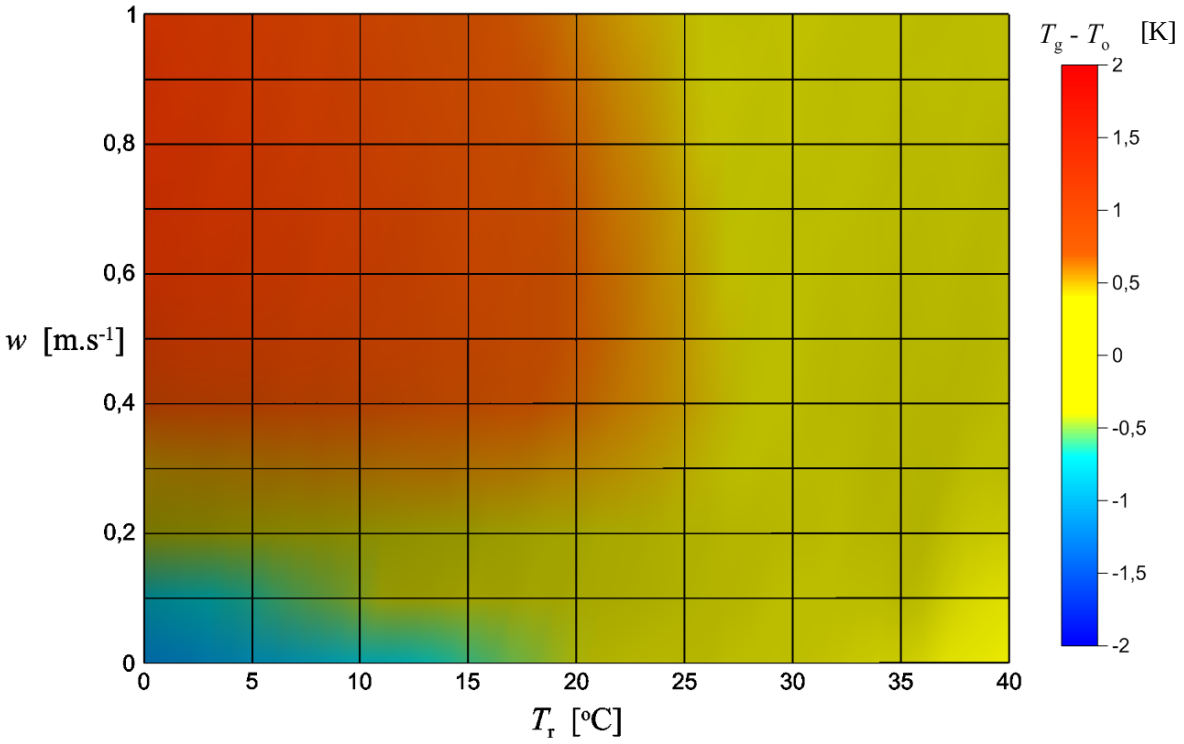

Figure 25. The difference between the globe and the operative temperatures based on the first solution (equation (18)), for constant air temperature T_a = 35 °C

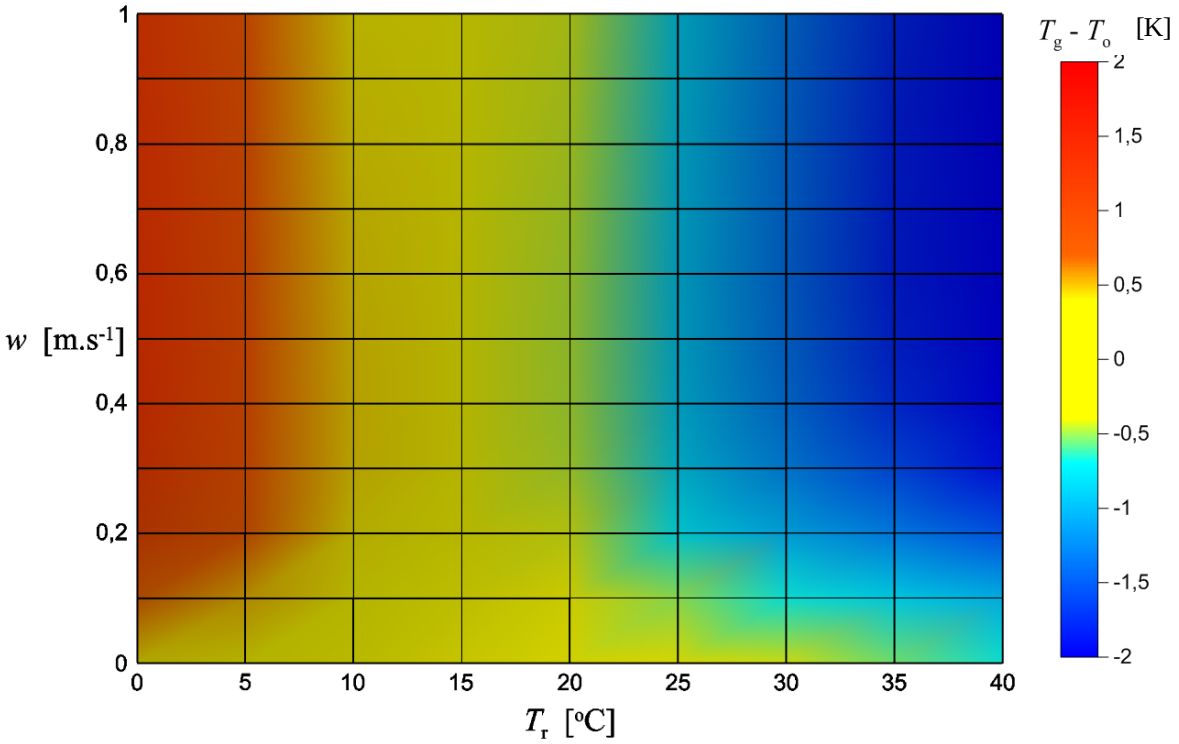

Figure 26. The difference between the globe and the operative temperatures based on the second solution (equation (20)), for constant air temperature T_a = 15 °C

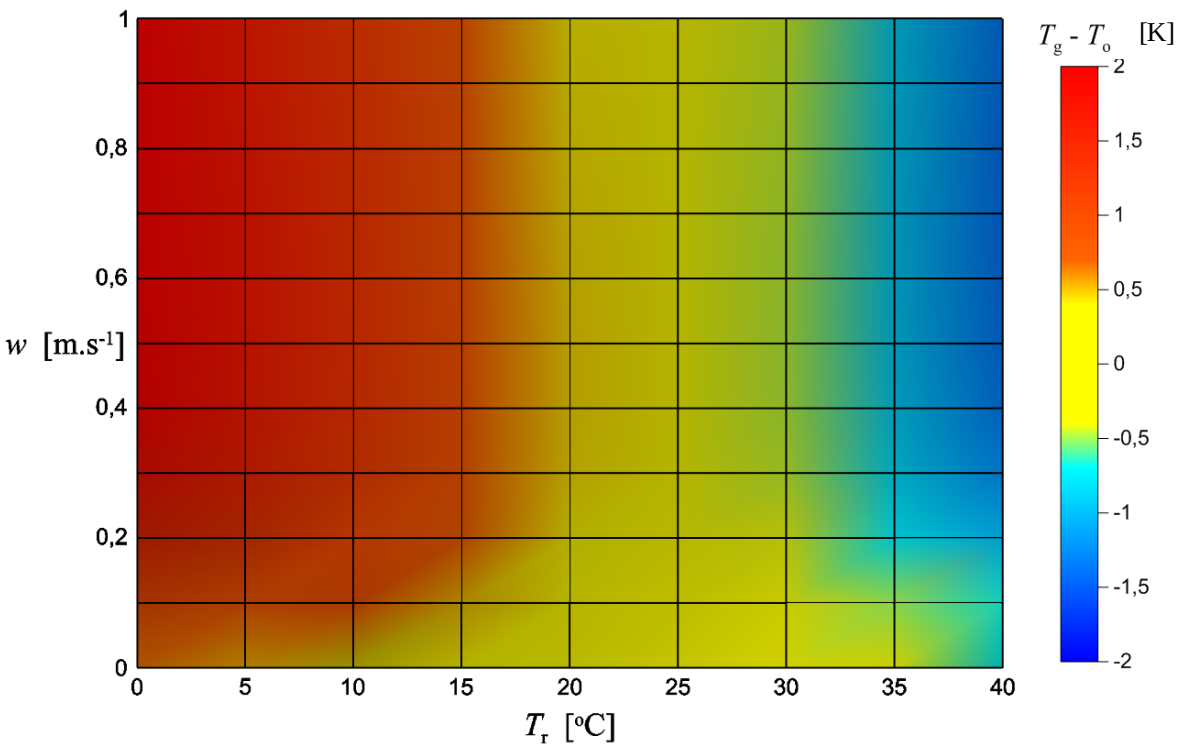

Figure 27. The difference between the globe and the operative temperatures based on the second solution (equation (20)), for constant air temperature T_a = 25 °C

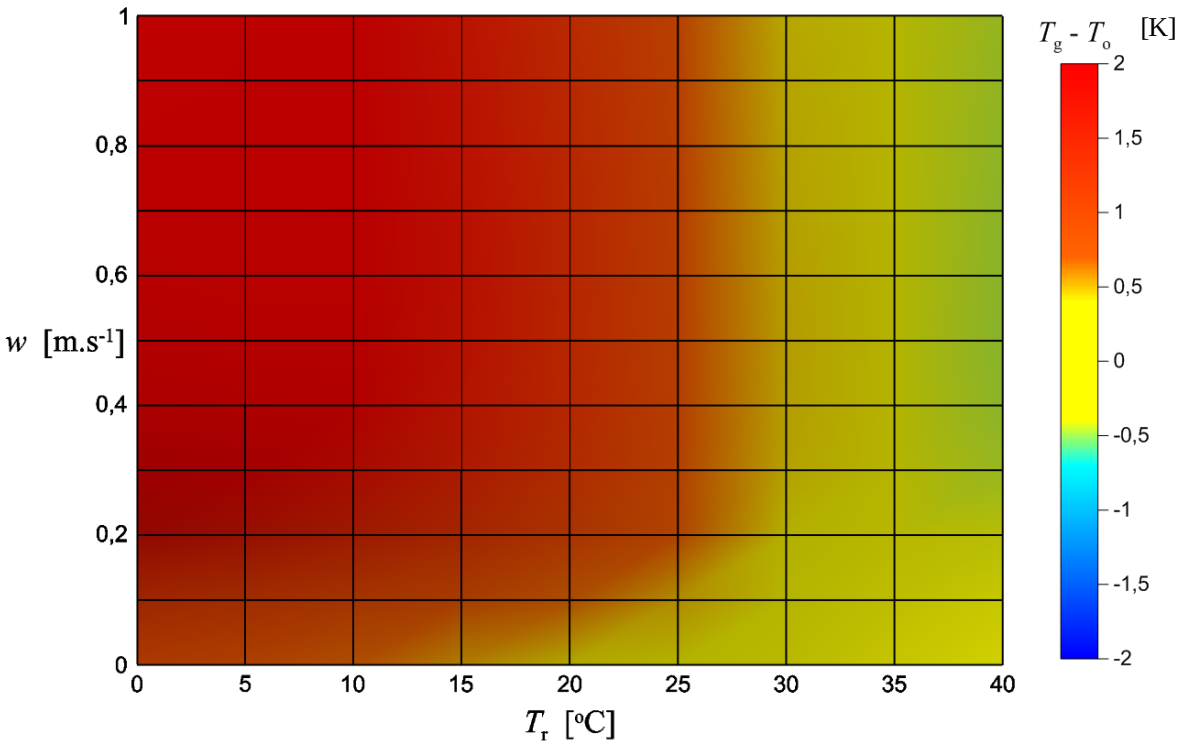

Figure 28. The difference between the globe and the operative temperatures based on the second solution (equation (20)), for constant air temperature T_a = 35 °C

5.1. Discussion of the results

The results of the first theoretical solution based on the equation (18):

From the Figures 35, 36, and 37, it was observed that the difference between the globe and the operative temperatures depends mainly on the difference between the mean radiant and air temperatures ($T_r - T_a$), and further on the air velocity w; where the result can be summarized as following:

- For the range of: $|T_r - T_a| \leq 10$ K, the value of the difference $|T_g - T_o| \leq 0.5$ K.
- For the velocity range of: $w \leq 0.3$ m.s^{-1}, the value of the difference $|T_g - T_o| \leq 0.6$ K.

The results of the second theoretical solution based on the equation (20):

From the Figures 38, 39, and 40, it was observed that the difference between the globe and the operative temperatures depends primarily on the difference between the mean radiant and air temperatures ($T_r - T_a$), also it was seen that the effect of the air velocity w, on the difference between the globe and the operative temperatures is limited; where the result can be summarized as following:

- For the range of: $|T_r - T_a| \leq 8$ K, the value of the difference $|T_g - T_o| \leq 0.5$ K.

The range of ($T_r - T_a$) can be extended by using the air velocity limits, as follow:

- For $|T_r - T_a| \leq 10$ K and $w \leq 0.15$ m.s^{-1}, the value of the difference $|T_g - T_o| \leq 0.5$ K.

The previous results compatible with the *Czech norms*, where according to law (Nařízení vlády 2002), for air velocity less than 0.2 $m.s^{-1}$ it is possible to replace the globe temperature in state of operative temperature.

The Society of Environmental Engineering (Zmrhal et al. 2010), they published article about the same subject, they had opposite result in the range of air velocity (0-0.2) $m.s^{-1}$.

On the other hand the the accuracy in the globe temperature measurement is (±0.5 K) (ISO 7726 1998).

6. Theoretical Solution of Plate Temperature

In practical part of the doctoral study, a plate sensor (Figure 41.) was designed and developed to use as a compact sensor for evaluating the thermal state of an environment.
The construction of plate sensor is descriped in the practical part of the thesis (III/1.).

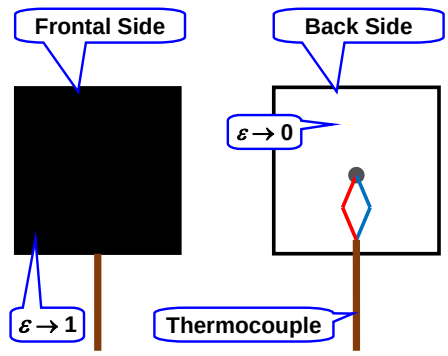

a) Frontal side b) Back Side

Figure 29. The compact plate sensor

The compact plate sensor is designed according to the standards for determining the combined effect of environmental factors (air temperature, air movement, and mean radiant temperature) in a single index, the plate temperature T_p, and for evaluating the thermal state of an interior environment.
The structure of the plate sensor was designed to take in account the low cost of the sensor together with a sufficient accuracy. The structure and the size of the sensor provide flexibility and ease to placement of the sensor in the interior and small spaces. Thuse the designe plate sensor can be used in applications of the heat control (air-conditioned cabins and control rooms).

To determine whether the compact plate sensor can be used to assess the thermal state of an environment, a comparison was done between the temperature measured by the plate sensor (the plate temperature T_p) and the operative temperature index. Thus, theoretical solution of the plate temperature was found.

The work principle of the plate sensor is based on the thermal balance between the radian heat flow and the convective heat flow on the plate sensor. The heat balance equation can be expressed as follow:

$$q_{rp} = q_{cp} \tag{85}$$

The specific radiation heat transfer q_{rp} can be determined from Stefan – Boltzmann's law, and the convection heat transfer q_{cp} is given by Newton's law of cooling.

The convection heat transfer occurs on the both side of the plate sensor, while the radiation heat transfer occurs on the frontal side.

Then the heat balance equation of the globe thermometer can be rewritten as:

$$\sigma\varepsilon\left(T_r^4 - T_p^4\right) = 2h_{cp}(T_p - T_a) \tag{86}$$

where

ε is the emissivity of frontal surface of the plate sensor. For matt black surface (ε = 0.95),

σ is Stefan – Boltzmann's constant, $\sigma = 5.67\times10^{-8}$[W. m^{-2}. K^{-4}],

T_p is the absolute temperatures of plate sensor, K,

T_r is the mean temperatures of surfaces surrounding the plate sensor, K,

h_{cp} is the convection heat transfer coefficient, W.m^{-2} K^{-1},

T_a is the air temperature, K.

The equation (86) characterizes the plate temperature as function of the environmental parameters. The difficulty in this relation is to determine the coefficient heat transfer h_{cp} or the Nusselt number (see equation (4)).

The determination of the heat transfer coefficient (Nusselt number) is difficult and complicated, and it is required to know the type of flow (laminar, turbulent, or mixed) and kind of the convection heat transfer (natural, forced, or combined).

As it has been mentioned earlier, the combined convection heat transfer (forced and natural) has been used to calculate the Nusselt number.

Two separated analysis was used to calculate the Nusselt number:

- ***<u>The first solution</u>*** is based on the comprehensive correlation (18).
- ***<u>The second solution</u>*** is based on the following relation (20).

Both solutions were used:

- For small plate sensor (30 × 30 mm), which is suitable for using on a thermal mannequin.
- For large plate sensor (80 × 80 mm), which is suitable for measuring and controlling the thermal state in the room.

6.1. First Theoretical Solution of Small Plate Temperature

In this chapter, the equation (19) was used to calculate the Nusselt number of combined convection heat transfer. Where:

$$Nu_{comb.} = minNu + \sqrt{Nu_{lam}^2 + Nu_{turb}^2}$$

$$Nu_{lam} = 0.664Re_{comb.}^{0.5}Pr^{1/3}$$

$$Nu_{turb} = \frac{0.037Re_{comb.}^{0.8}Pr}{1 + 2.44Re_{comb.}^{-0.1}(Pr^{2/3} - 1)}$$

$$Re_{comb.} = \sqrt{Re^2 + \frac{Gr}{2.5}}$$

where

$$Re = \frac{Lw}{\nu}$$

$$Gr = \frac{g\beta\left(T_p - T_a\right)L^3}{\nu^2}$$

where

Re is the Reynolds number of flow,
Gr is the Grashof number,
Pr is Prandtl number,
w is the air velocity, m.s^{-1},
g is the gravitational acceleration, m.s^{-2},
β is the coefficient of volume expansion, K^{-1} ($\beta = 1/T$ for ideal gases),
υ is the kinematic viscosity of the fluid, m^2.s^{-1},
T_p is the plate temperature, K,
T_a is the temperature of the air sufficiently far from the globe thermometer, K,
L is the length of the plate sensor, m.

For the plate sensor, the following conditions are applied that the minimum Nusselt number min *Nu* = 0 and the length of the plate sensor *L* = 0.03 m
The convection heat transfer coefficient for the flow over the plate sensor is:

$$h_{cp} = \frac{k}{L}\left[\left(0.664Pr^{1/3}\left(\left(\frac{Lw}{\nu}\right)^2 + \frac{2}{2.5}\frac{g\left(T_p - T_a\right)L^3}{\nu^2\left(T_p + T_a\right)}\right)^{0.25}\right)^2 + \left(\frac{0.037\left(\left(\frac{Lw}{\nu}\right)^2 + \frac{2}{2.5}\frac{g\left(T_p - T_a\right)L^3}{\nu^2\left(T_p + T_a\right)}\right)^{0.4} Pr}{1 + 2.44(Pr^{2/3} - 1)\left(\left(\frac{Lw}{\nu}\right)^2 + \frac{2}{2.5}\frac{g\left(T_p - T_a\right)L^3}{\nu^2\left(T_p + T_a\right)}\right)^{-0.05}}\right)^2\right]^{0.5} \quad (87)$$

The equation (87) represent the convection heat transfer coefficient for the flow over the plate sensor, and it is a function of the environmental factors. By substituting the equation (87) in the equation (86), the plate sensor temperature is written as follow:

$$T_p = \left(T_r^4 - \frac{2h_{cp}}{\varepsilon\sigma}\left(T_p - T_a\right)\right)^{1/4} \quad (88)$$

where T_p, T_r, and T_a in unit of K.

or

$$T_p = \left((T_r + 273)^4 - \frac{2h_{cp}}{\varepsilon\sigma}\left(T_p - T_a\right)\right)^{1/4} - 273 \quad (89)$$

where T_g, T_r, and T_a in unit of ^{o}C.

The equation (89) describes the plate temperature as function of the environmental factors (air temperature, air velocity, and men radiant temperature).

$$T_p = f(T_a, T_r, w)$$

The equation (89) is a transcendental equation, which can be solved using one of the iterative methods, mentioned previous (chapter II/2), and the more suitable methods are Newton-Raphson method and secant method. These two methods are effective in finding the roots of the equation with the least effort and time.

However, The *MATLAB* and *Surfer* programs were used to solve and draw this equation in range of variables:

$$0 \leq T_r \leq 40\ ^{o}C$$

$$0 \leq w \leq 1\ m.\ s^{-1}$$

$$T_a = 15,\ 25,\ \text{and}\ 35\ ^{o}C$$

On Figure 30 and 31 are plotted the three plate temperature surfaces $T_p = f\,(T_a, T_r, w)$, each surface represents the plate temperature function for a constant air temperature.

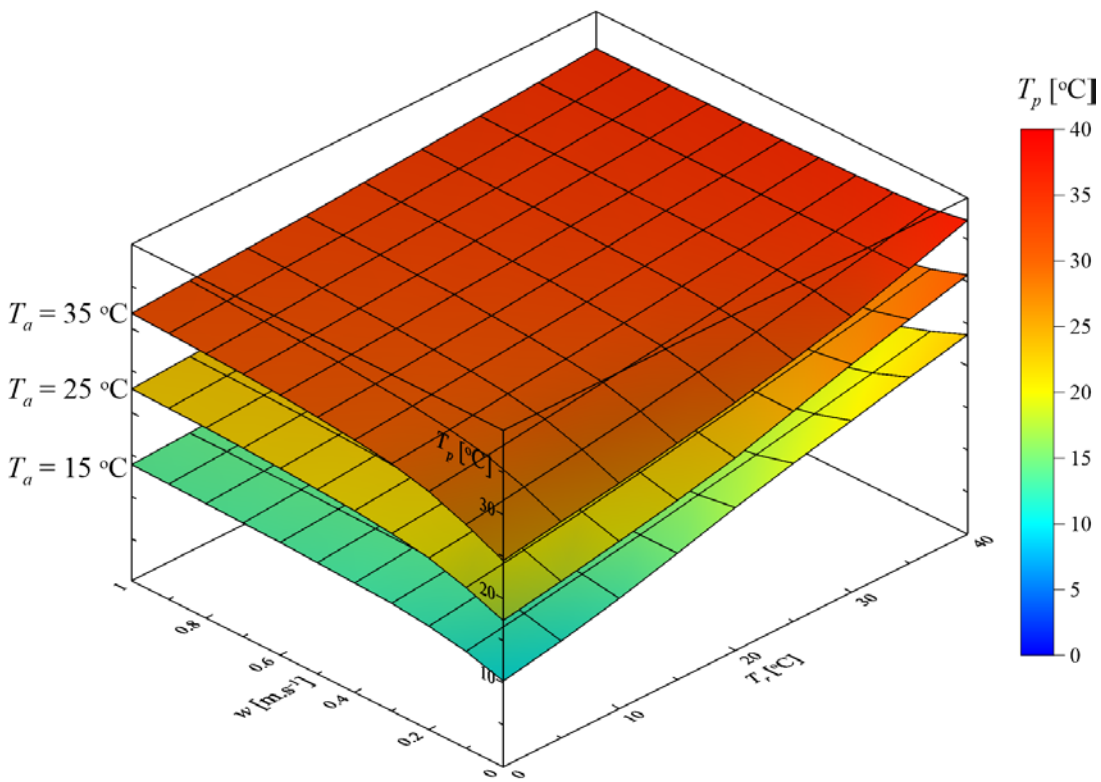

Figure 30. The plate temperature function for constant air temperature – front view

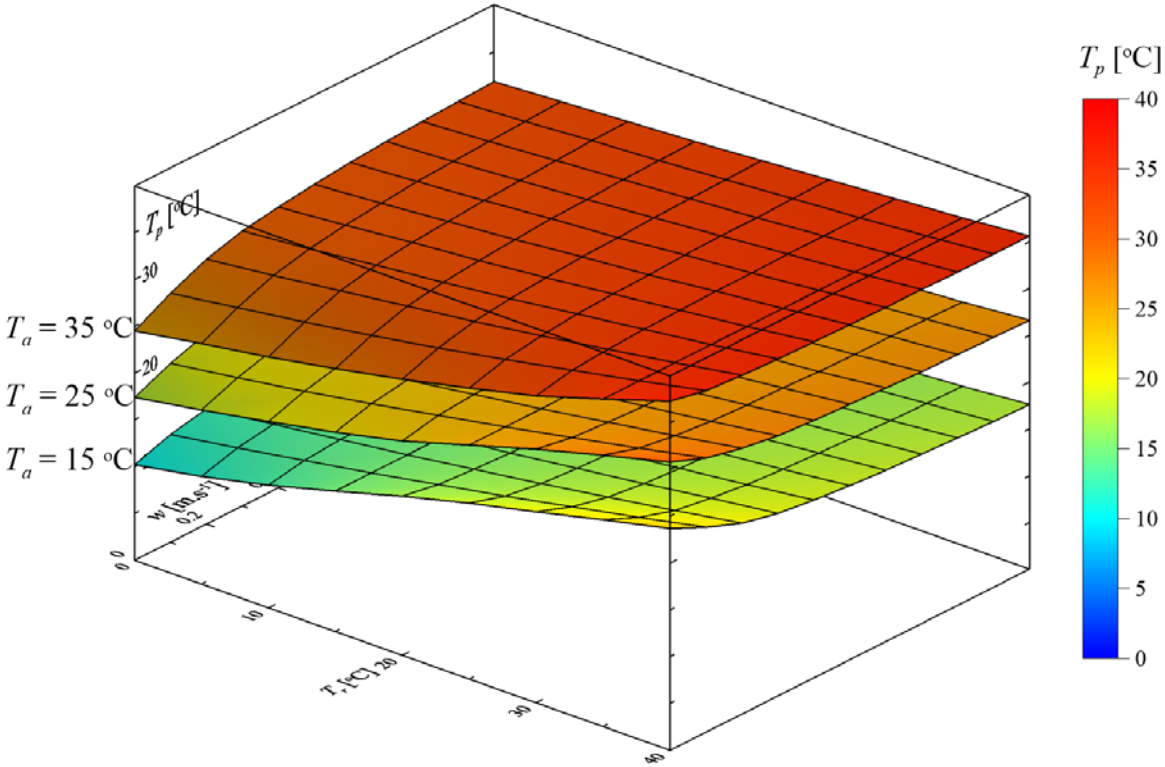

Figure 31. The plate temperature function for constant air temperature – side view

6.2. Second Theoretical Solution of Small Plate Temperature

In this chapter, the equation (20) was used to calculate the Nusselt number of combined convection heat transfer. Where

$$Nu_{comb.} = \left(Nu_{forced}^{n} \pm Nu_{natural}^{n}\right)^{1/n}$$

For the flow over the plate sensor, n = 3, and for assisting and transverse flows the plus sign is used, and for Nu_{forced} and $Nu_{natural}$ the relation (9) and (15), respectively, were used (Çengel 2003; Pohlhausen 1921):

$$Nu_{forced} = 0.664 Re^{0.5} Pr^{1/3}$$

$$Re < 5 \times 10^5 \ \& \ Pr \geq 0.6$$

$$Nu_{natural} = 0.59 Ra^{1/4}$$

$$10^4 \leq Ra \leq 10^9$$

$$Re = \frac{Lw}{\nu}$$

$$Ra = GrPr = \frac{g\beta\left(T_p - T_a\right)L^3}{\nu^2} Pr$$

$$h_{cp} = Nu_{comb.} \frac{k}{L}$$

where

Ra is the Rayleigh number of flow,
w is the air velocity, m.s^{-1},
g is the gravitational acceleration, m.s^{-2},
β is the coefficient of volume expansion, K^{-1},
υ is the kinematic viscosity of the fluid, m^2. s^{-1},
T_p is the globe temperature, ^{o}C,
T_a is the temperature of the air sufficiently far from the globe thermometer, ^{o}C,
L is the length of the plate sensor, m.

For plate sensor: the length of the plate L = 0.03 m and the volumetric thermal expansion coefficient $\beta = 2 / (T_p + T_a)$, K^{-1}. Thus, the coefficient of convection heat transfer for air flow over the plate sensor can be expressed as follow:

$$h_{cp} = \frac{k}{D}\left[\left(0.664\left(\frac{Lw}{\nu}\right)^{0.5} Pr^{1/3}\right)^3 + \left(0.59\left(\frac{2g\left(T_p - T_a\right)L^3}{\nu^2\left(T_p + T_a\right)} Pr\right)^{1/4}\right)^3\right]^{1/3} \tag{90}$$

By substituting the equation (90) in the equation (86), the plate temperature is written as follow:

$$T_p = \left((T_r + 273)^4 - \frac{2h_{cp}}{\varepsilon\sigma}(T_p - T_a)\right)^{1/4} - 273 \tag{91}$$

where T_g, T_r, and T_a in unit of ^{o}C.

The equation (91) describes the plate temperature as function of the environmental factors (air temperature, air velocity, and men radiant temperature).

$$T_p = f(T_a, T_r, w)$$

The equation (91) is a transcendental equation, which can be solved using one of the iterative methods, mentioned previous (chapter II/2), and the more suitable methods are Newton-Raphson method and secant method.
However, The *MATLAB* and *Surfer* programs were used to solve and draw this equation in range of variables:

$$0 \le T_r \le 40\ ^o\text{C}$$

$$0 \le w \le 1\ \text{m. s}^{-1}$$

$$T_a = 15, 25, \text{and } 35\ ^o\text{C}$$

On Figure 32 and 33 are plotted the three plate temperature surfaces $T_p = f(T_a, T_r, w)$, each surface represents the plate temperature function for a constant air temperature.

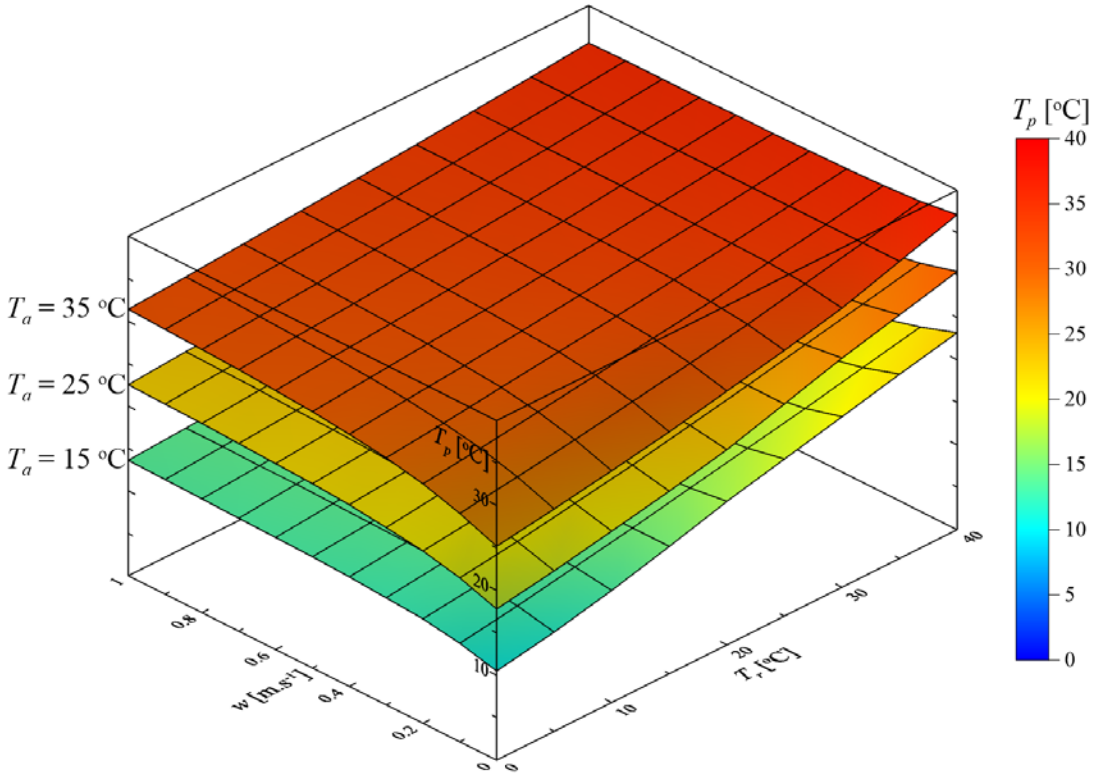

Figure 32. The plate temperature function for constant air temperature – front view

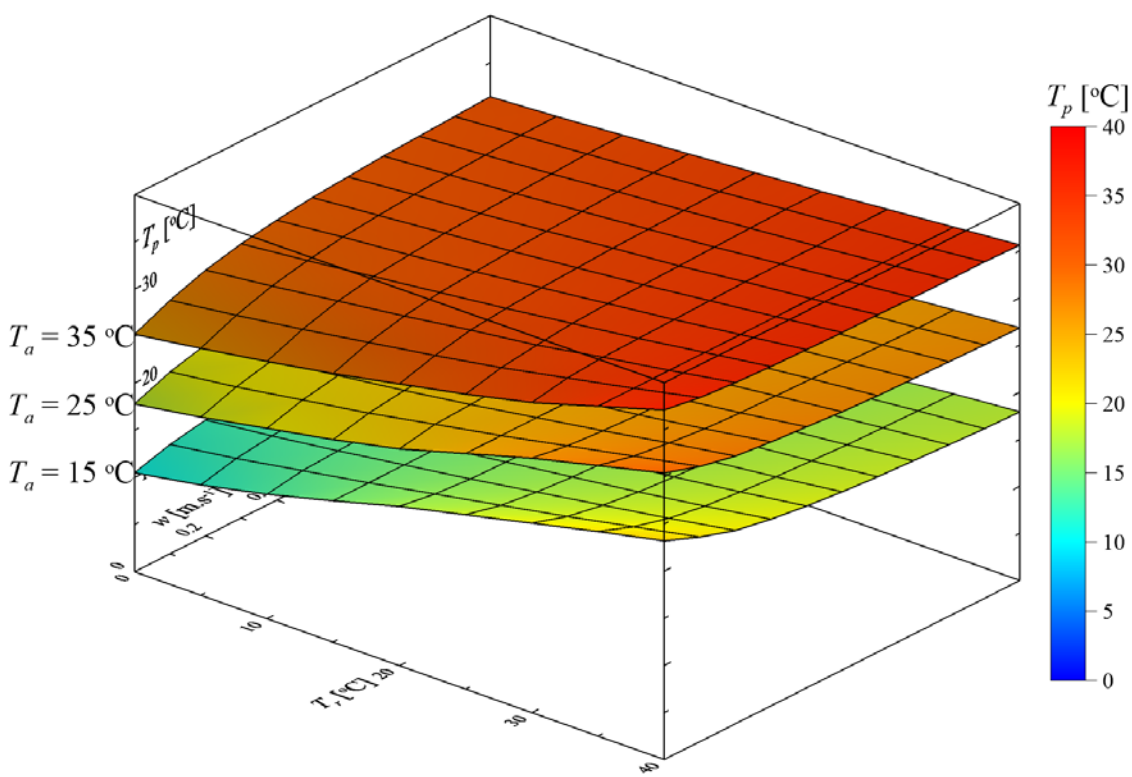

Figure 33. The plate temperature function for constant air temperature – side view

7. Comparison Between Plate and Operative Temperatures

In the previous sections, the plate and operative temperatures was written as functions of the environmental factors (air temperature, air velocity, and mean radiant temperature), these functions were as results of the theoretical solution of the combined convection heat transfer based on the equations (18) and (20). The difference between these two functions (plate and operative temperatures) represents the difference between the plate and the operative temperatures; this difference is also function of the environmental factors as follow:

$$T_p - T_o = f(T_a, w, T_r) \tag{92}$$

$$T_p - T_o = f_1(T_a, w, T_r) \tag{93}$$

where

f_1: is function based of the theoretical solution of the equation (18)
f_2: is function based of the theoretical solution of the equation (20)

The difference between the plate and the operative temperatures was plotted on Figures 34, 35, and 36 for the function f_1, and on Figures 37, 38, and 39 for the function f_2.

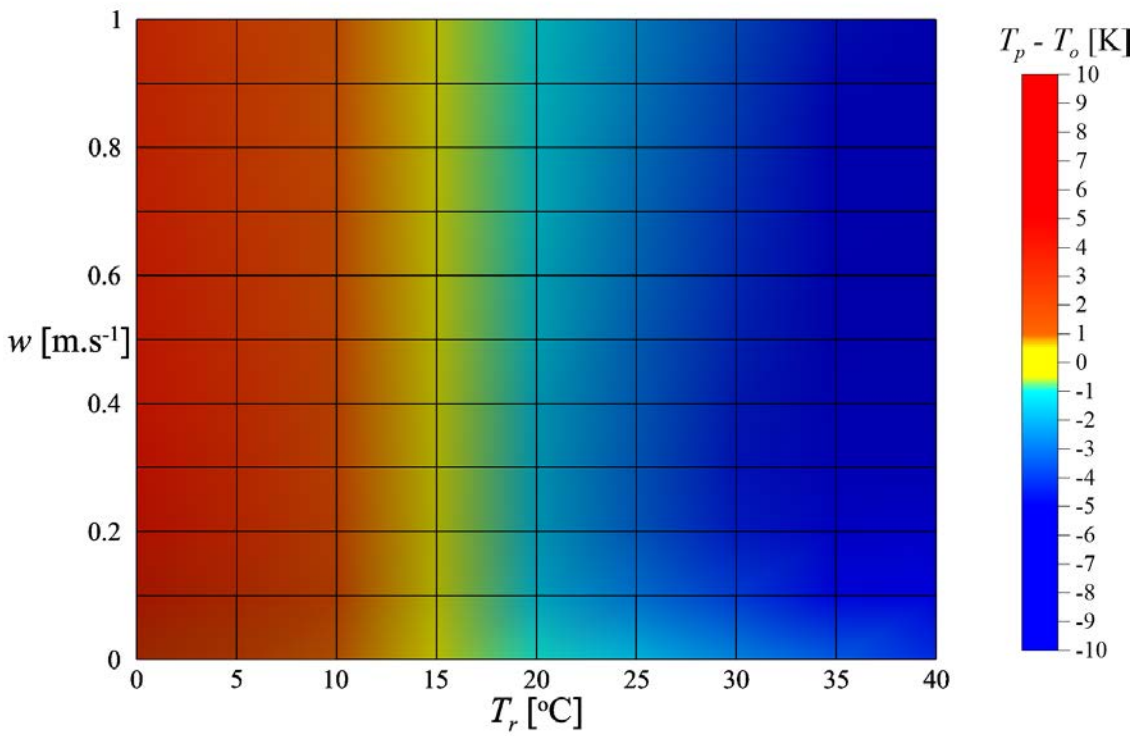

Figure 34. The difference between the plate and the operative temperatures based on the first solution (equation (18)), for constant air temperature T_a = 15 °C

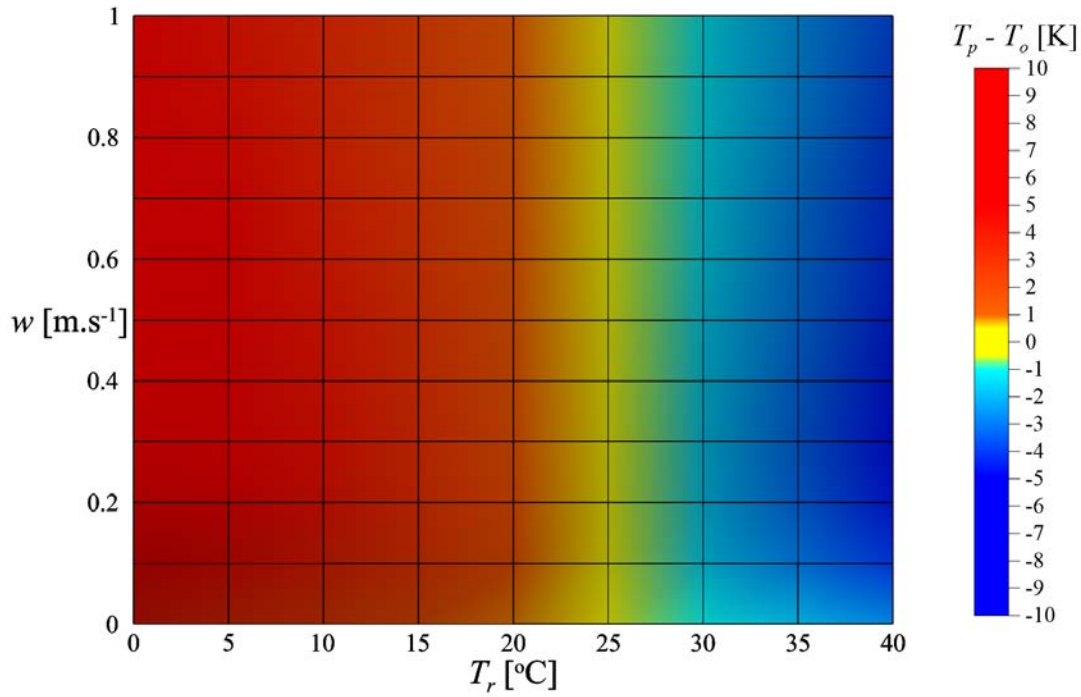

Figure 35. The difference between the plate and the operative temperatures based on the first solution (equation (18)), for constant air temperature T_a = 25 ºC

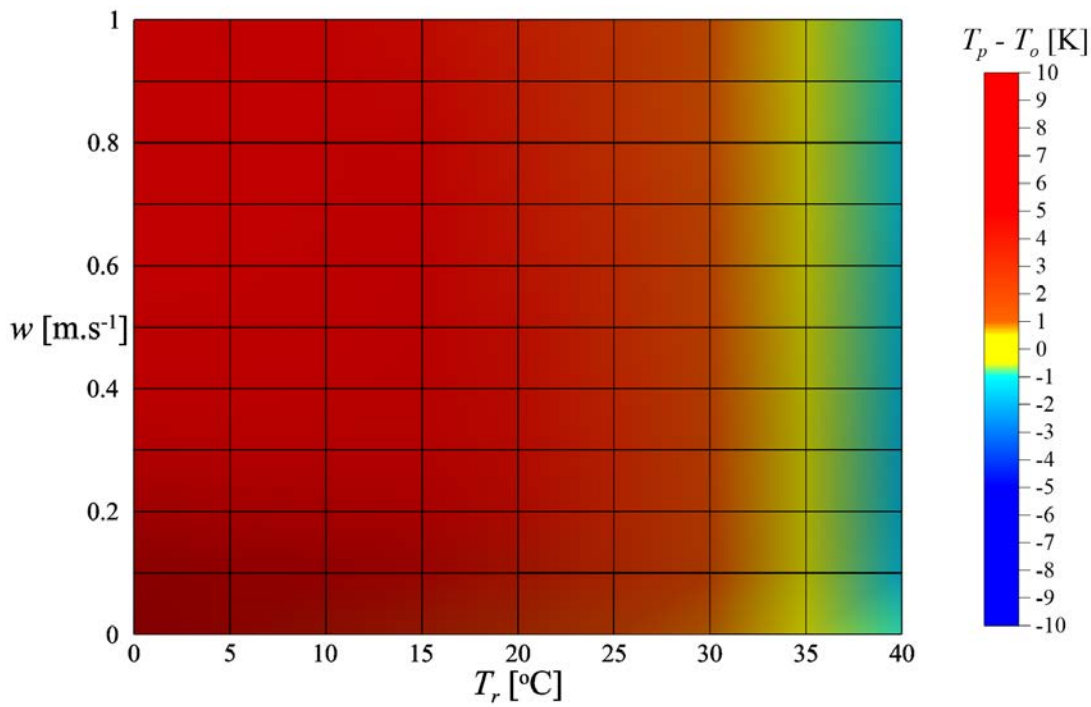

Figure 36. The difference between the plate and the operative temperatures based on the first solution (equation (18)), for constant air temperature T_a = 35 ºC

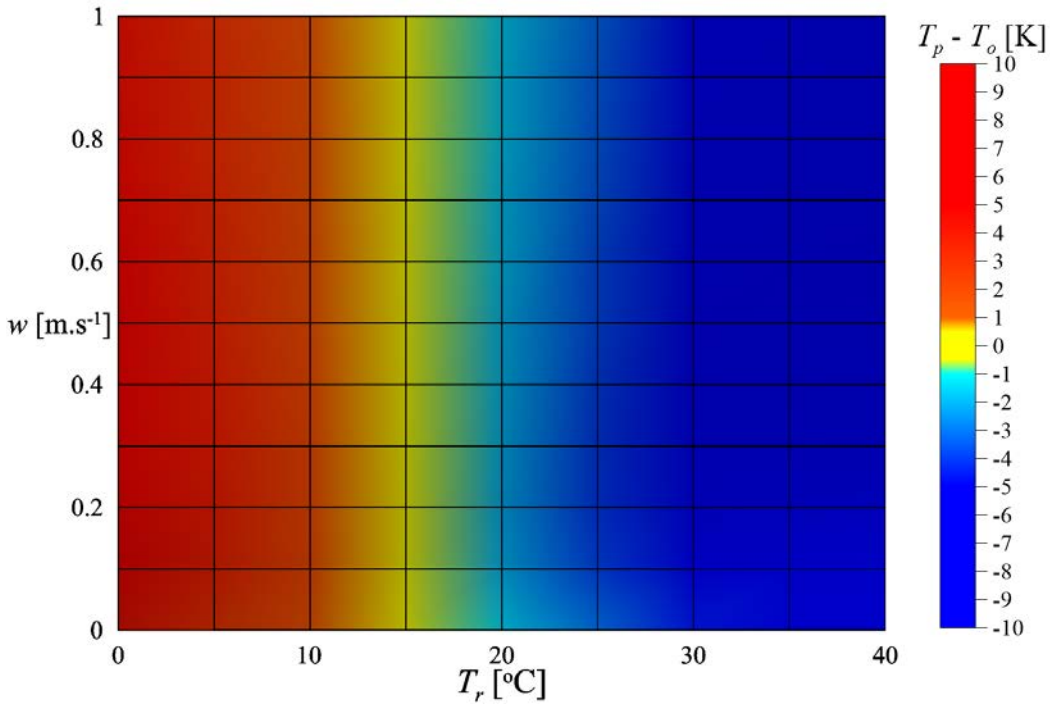

Figure 37. The difference between the plate and the operative temperatures based on the second solution (equation (20)), for constant air temperature T_a = 15 °C

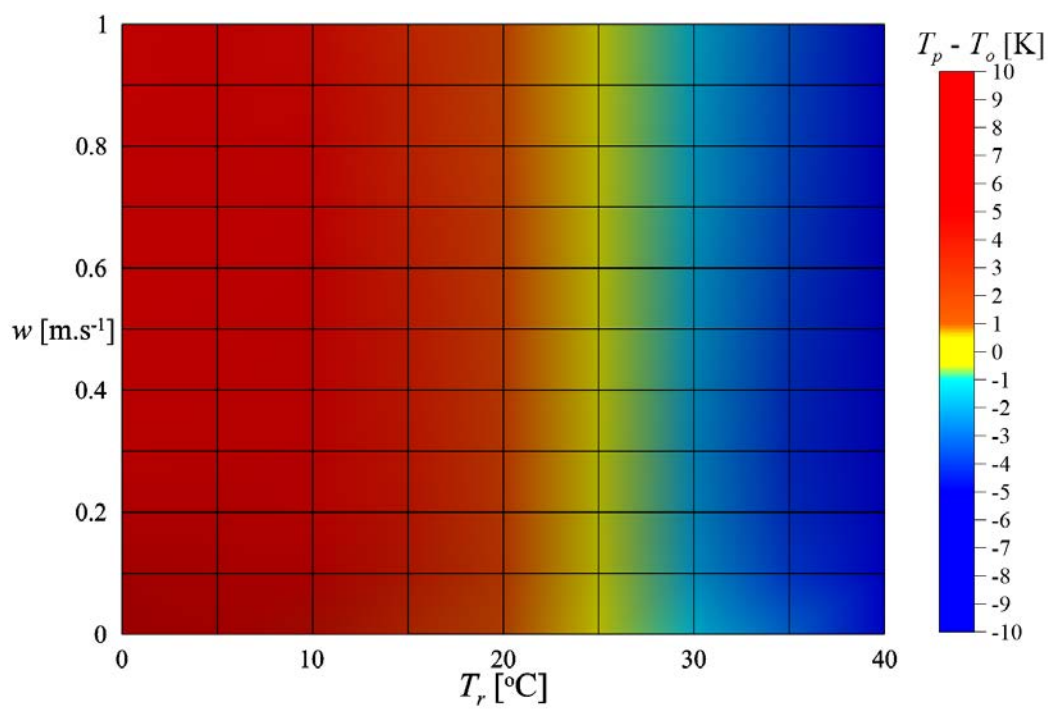

Figure 38. The difference between the plate and the operative temperatures based on the second solution (equation (20)), for constant air temperature T_a = 25 °C

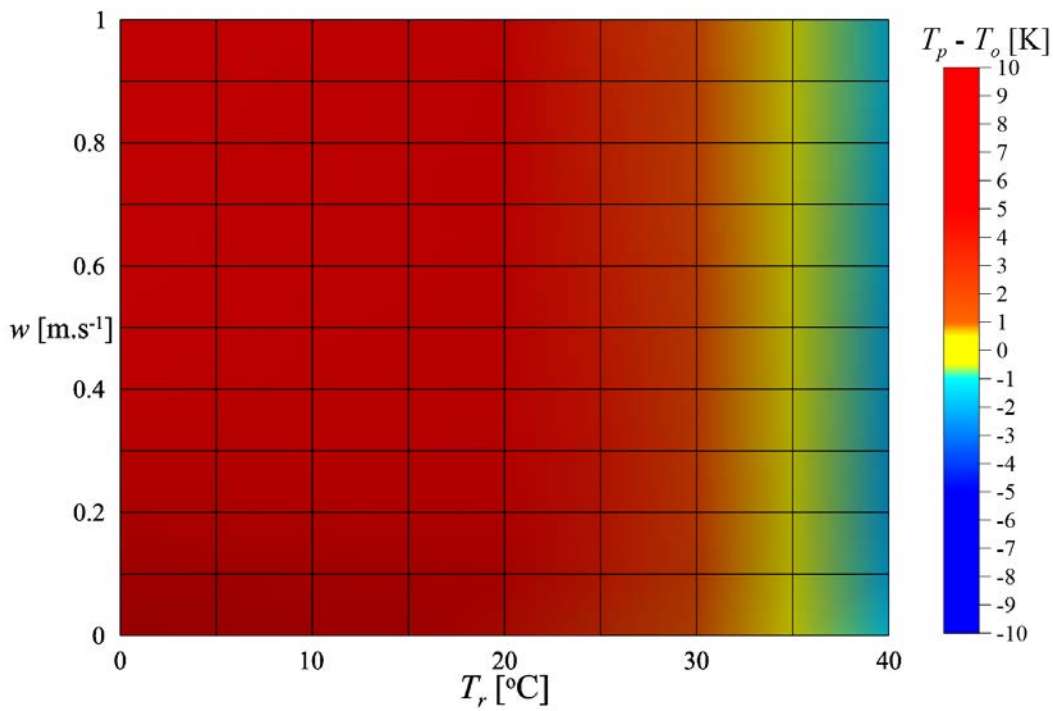

Figure 39. The difference between the plate and the operative temperatures based on the second solution (equation (20)), for constant air temperature T_a = 35 °C

7.1. Discussion of the results:

From the Figures 34, 35, 36, 37, 38 and 39, it can be seen that the results based on the equation (18) is very close from the one based on the equation (20). Where it can be observed that the difference between the plate and the operative temperatures depends on the difference between the mean radiant and air temperatures ($T_r - T_a$), where the result can be summarized as following:

- For the range of: $|T_r - T_a| \leq 1$ K, the value of the difference $|T_p - T_o| \leq 0.7$ K.

Thus, it can be seen that there is a high difference between the operative temperature and the temperature measured by the plate sensor. And the range, in which the difference between the temperatures les than 0.5 K, is very small.

To improve the rsults, a correction for the values of the temperature measured by the plate sensor is performed. For the correction, it is possible to use another environment parameter, which can be measured as simple as possible (eg. air temperature T_a), then the sensor needed to measure this parameter to be added to the plate compact sensor. To use the plate compact sensor in the non-uniform radiant temperature environment, the designed sensor will also need to be explored for this effect.

The purpose of correcting the values of plate temperature is to find a relation which representes the operative temperature as function of the plate temperature. By droping the data of the plate and operative temperatures on the chart (T_a - T_p, T_p - T_o) and using the mean square method to analysing the data. Figure 58.

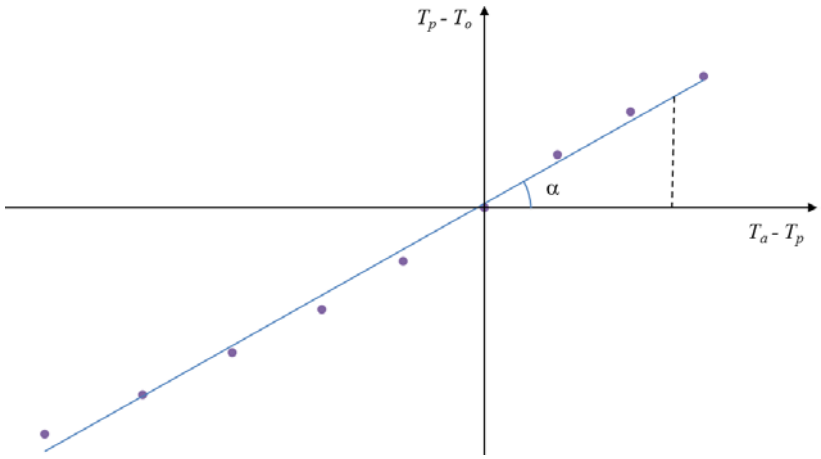

Figure 40. The correction of plate temperature

The slope of the line (T_p - T_o) is given by the followin relation :

$$\tan \alpha = \frac{T_p - T_o}{T_a - T_p} \tag{94}$$

or

$$T_o = T_p - (T_a - T_p)\ \mathrm{tng}\alpha \tag{95}$$

The corrected plate temperature is given as follow:

$$T_{pc} = T_p - c\ \left(T_p - T_a\right) \tag{96}$$

where

c is the correction factor.

The correction factor c dependes on the air temperature and its value can be determined from the following equation:

$$c = 1.82\ T_a^{-0.121} \tag{97}$$
$$c = 2.54\ T_a^{-0.145} \tag{98}$$

where

The equation (97) is based on the data of the first theoretical solution of the plate temperature
The equation (98) is based on the data of the first theoretical solution of the plate temperature.

The difference between the corected plate temperature T_{pc} and operative temperaure T_o are ploted on the Figures 40, 41, 42, 43, 44, and 45.

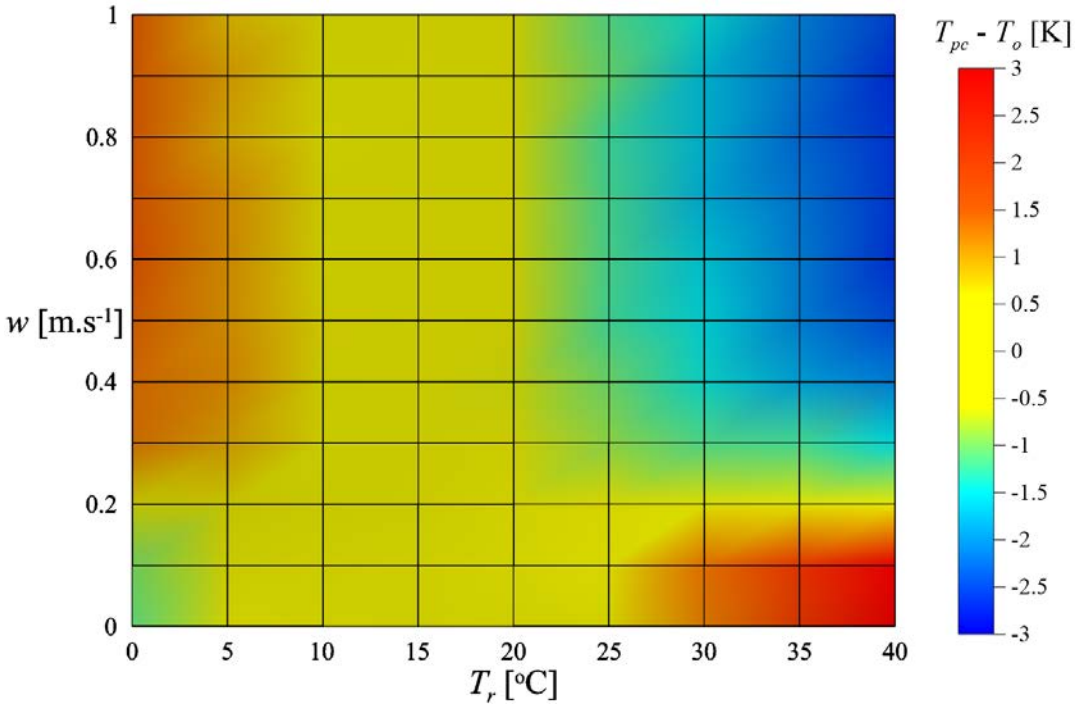

Figure 41. The difference between the corrected plate and the operative temperatures based on the first theoretical solution, for constant air temperature (T_a =15 °C)

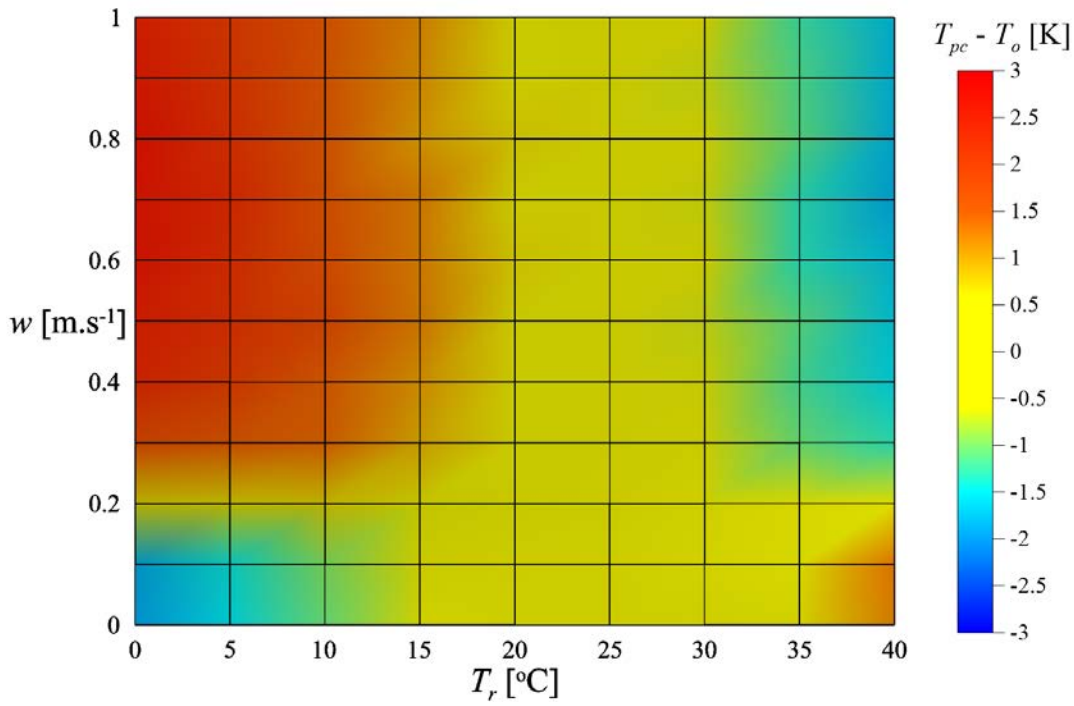

Figure 42. The difference between the corrected plate and the operative temperatures based on the first theoretical solution, for constant air temperature (T_a =25 °C)

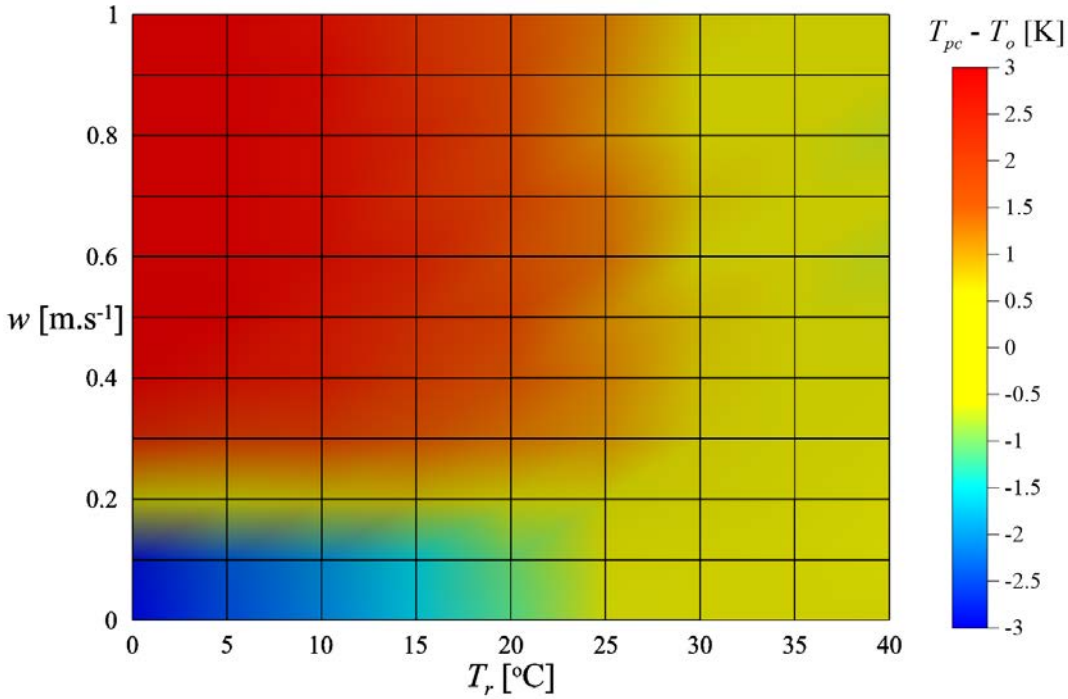

Figure 43. The difference between the corrected plate and the operative temperatures based on the first theoretical solution, for constant air temperature (T_a =35 °C)

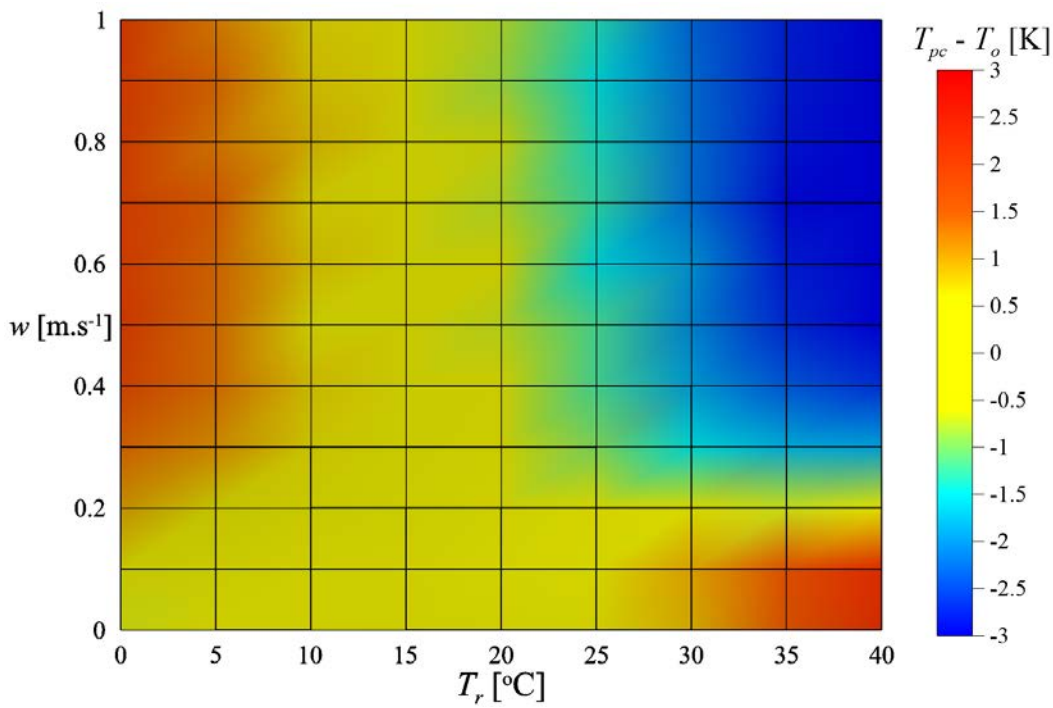

Figure 44. The difference between the corrected plate and the operative temperatures based on the second theoretical solution, for constant air temperature (T_a =15 °C)

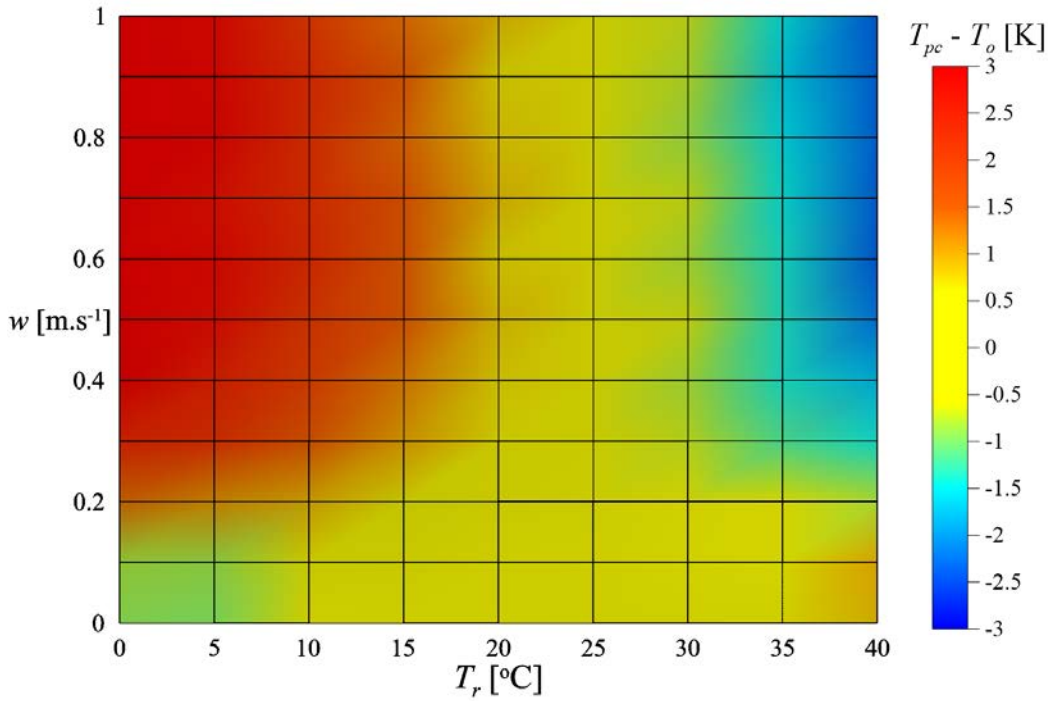

Figure 45. The difference between the corrected plate and the operative temperatures based on the second theoretical solution, for constant air temperature (T_a =25 °C)

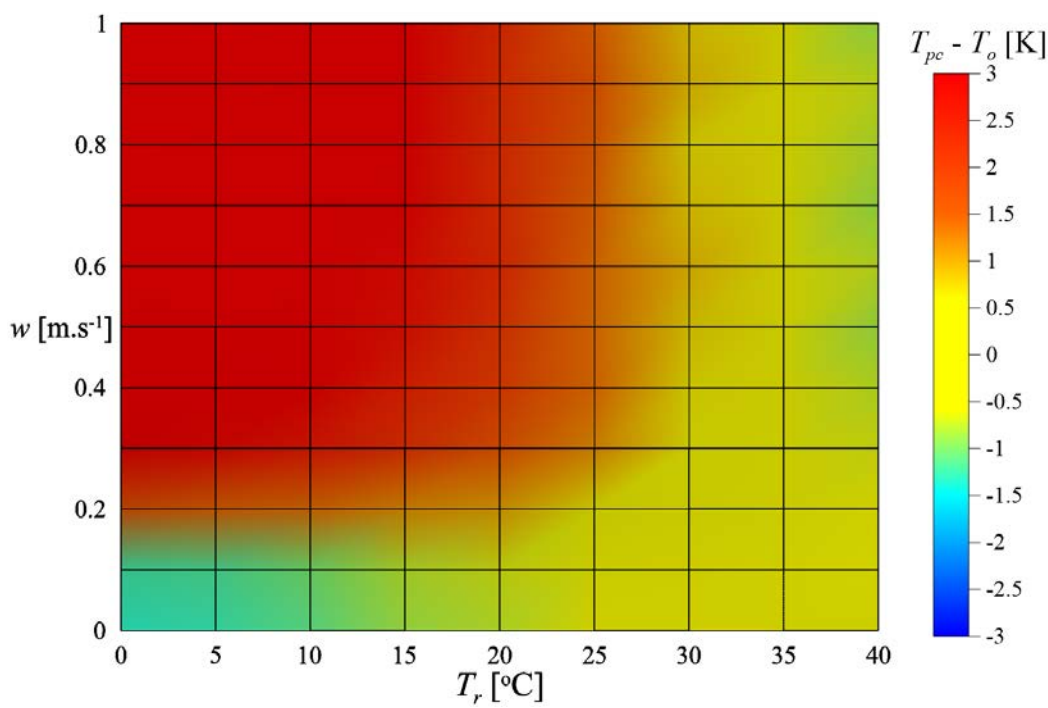

Figure 46. The difference between the corrected plate and the operative temperatures based on the second theoretical solution, for constant air temperature (T_a =35 °C)

From the Figures, it can be observed that the difference between the corrected plate and the operative temperatures depends primarily on the difference between the mean radiant and air temperatures ($T_r - T_a$), also it can be seen that the effect of the air velocity w, on the difference is limited; where it can be noticed that:

- For the range of $| T_r - T_a | \leq 5$ K, the value of the difference $|T_{pc} - T_o| \leq 0.6$ K.

The range of $| T_r - T_a |$ can be extended by using the air velocity limits, as follow:

- For $| T_r - T_a | \leq 10$ K and $w \leq 0.2$ m.s^{-1}, the value of the difference $|T_{\mathrm{pc}} - T_{\mathrm{o}}| \leq 0.5$ K.

Thus, under the previous conditions the operative temperature can be replaced by the corrected temperature measured by the new designed plate sensor T_{pc}, and according to these results it can consider the plate sensor as a compact sensor.

8. Theoretical Solution of Large Plate Sensor

For the purpose of determining the thermal state of the environment especially for the purpose of regulation, it is required to expand the range of $|T_r - T_a|$ in which the plate temperature can be used instead of the operative temperature.

In this part of the thesis a large compact plate sensor (80 × 80 mm) was studied. the same equations, which were used for small plate sensor, are used for finding the plate temperature as function of the environmental parameters (air temperature, air velocity, and mean radiant temperature). The difference between the plate temperature T_p of the big plate sensor and the operative temperaure T_o are ploted on the Figures 47, 48, and 49.

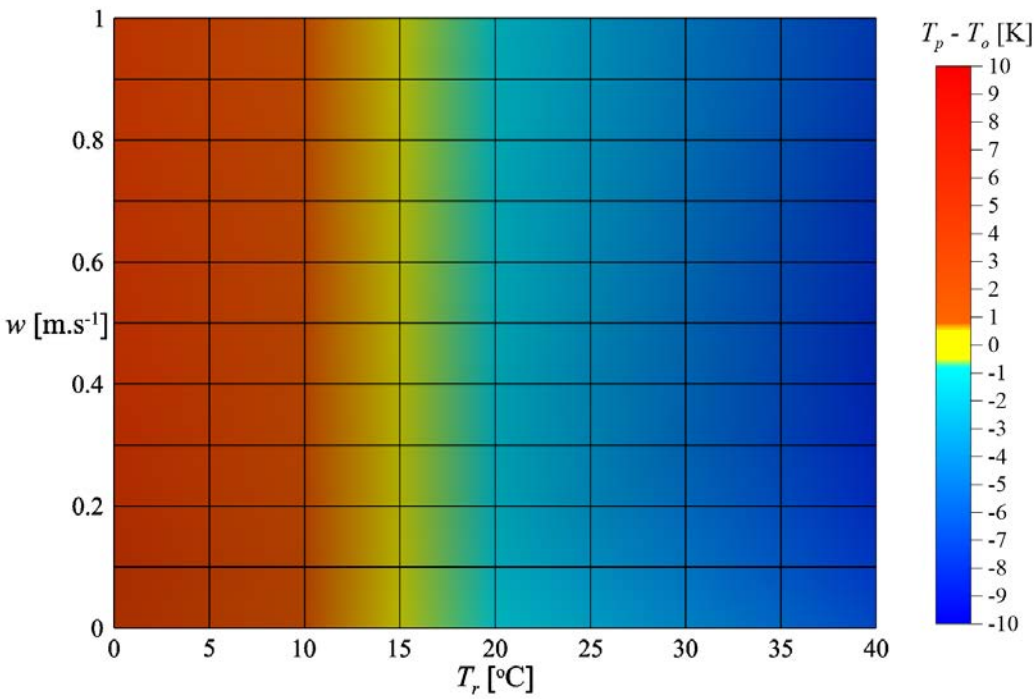

Figure 47. The difference between the plate and the operative temperatures based on the second theoretical solution, for constant air temperature (T_a =15 °C)

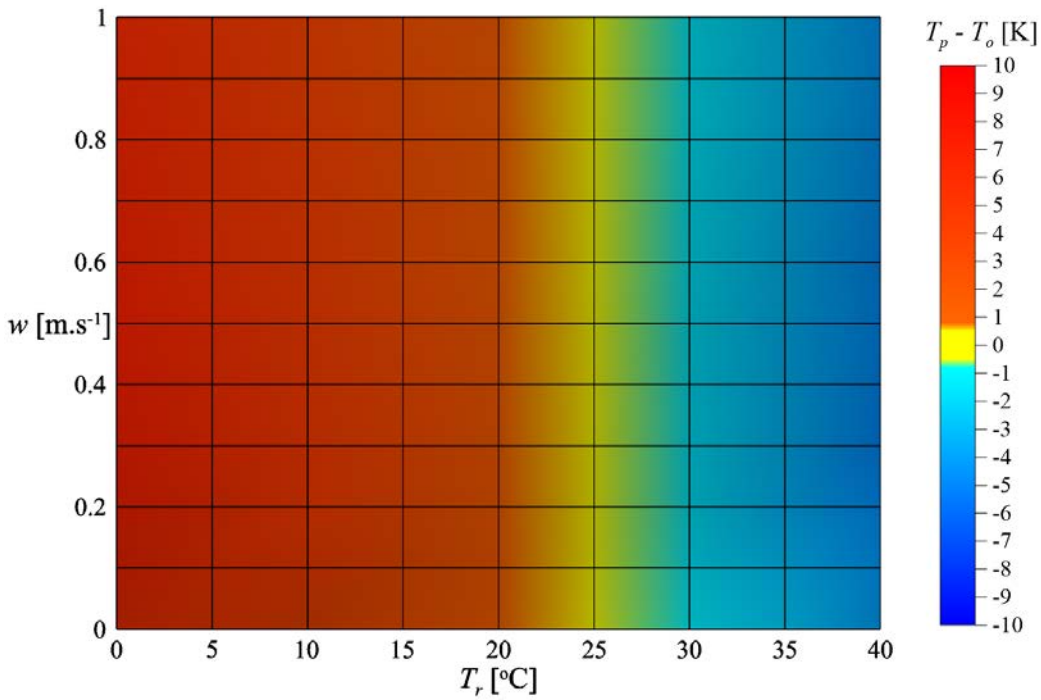

Figure 48. The difference between the plate and the operative temperatures based on the second theoretical solution, for constant air temperature (T_a =25 °C)

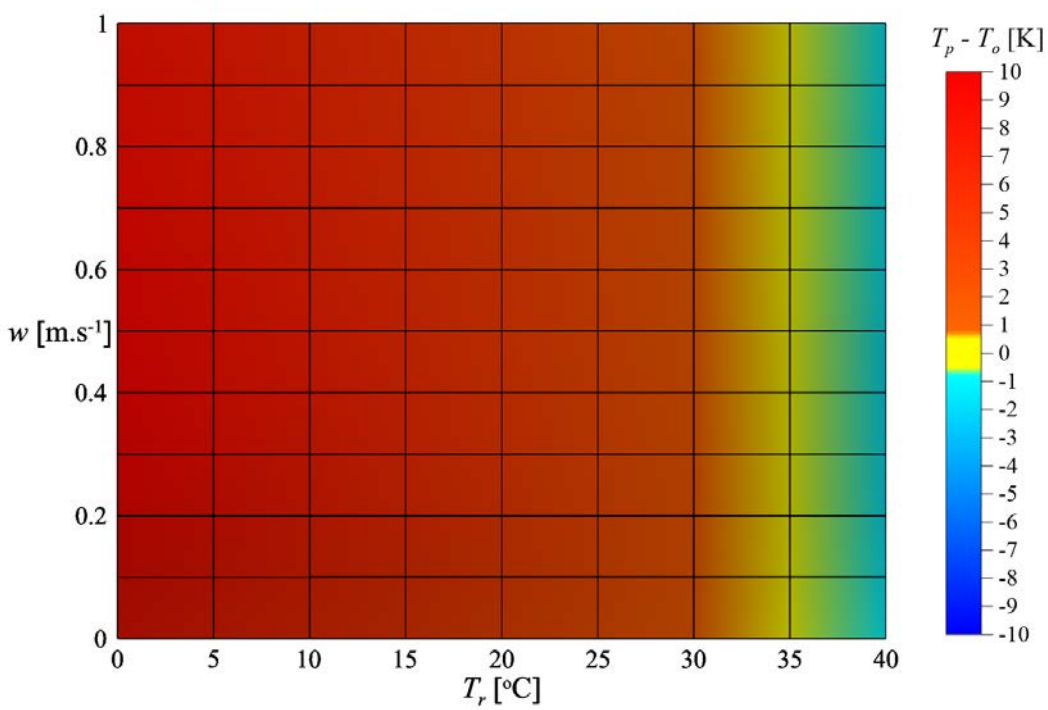

Figure 49. The difference between the plate and the operative temperatures based on the second theoretical solution, for constant air temperature (T_a =35 °C)

From the Figures 47, 48, and 49, it can be observed that the difference between the plate and the operative temperatures depends on the difference between the mean radiant and air temperatures ($T_r - T_a$), where the result can be summarized as following:

- For the range of: $|T_r - T_a| \leq 2$ K, the value of the difference $|T_p - T_o| \leq 0.6$ K.

Thus, it can be seen that the results of the big plate sensor are better than that of the small plate sensor, but still these results are not sufficient for purpose of measuring and regulating the thermal state of the environment.

To improve the results, a correction for the values of the temperature measured by the large plate sensor is performed (in the same way as the small plate sensor).

The difference between the corected the plate temperature T_{pc} for large sensor and the operative temperaure T_o are ploted on the Figures 50, 51, and 52.

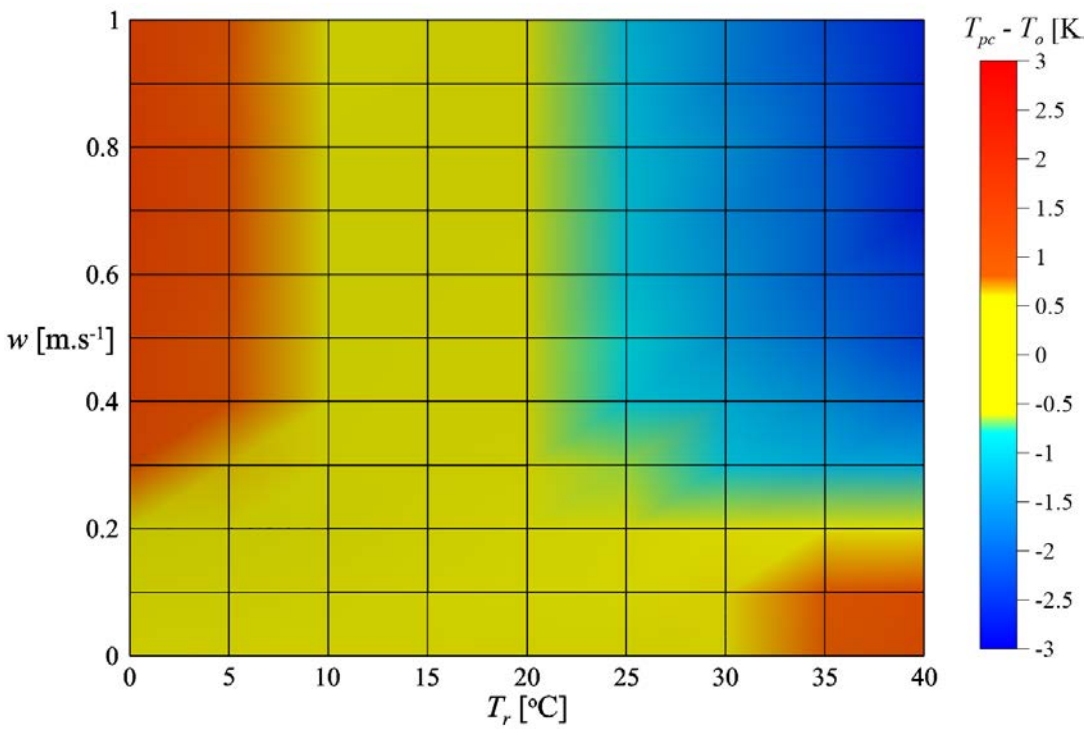

Figure 50. The difference between the corrected plate and the operative temperatures based on the second theoretical solution, for constant air temperature (T_a =15 °C)

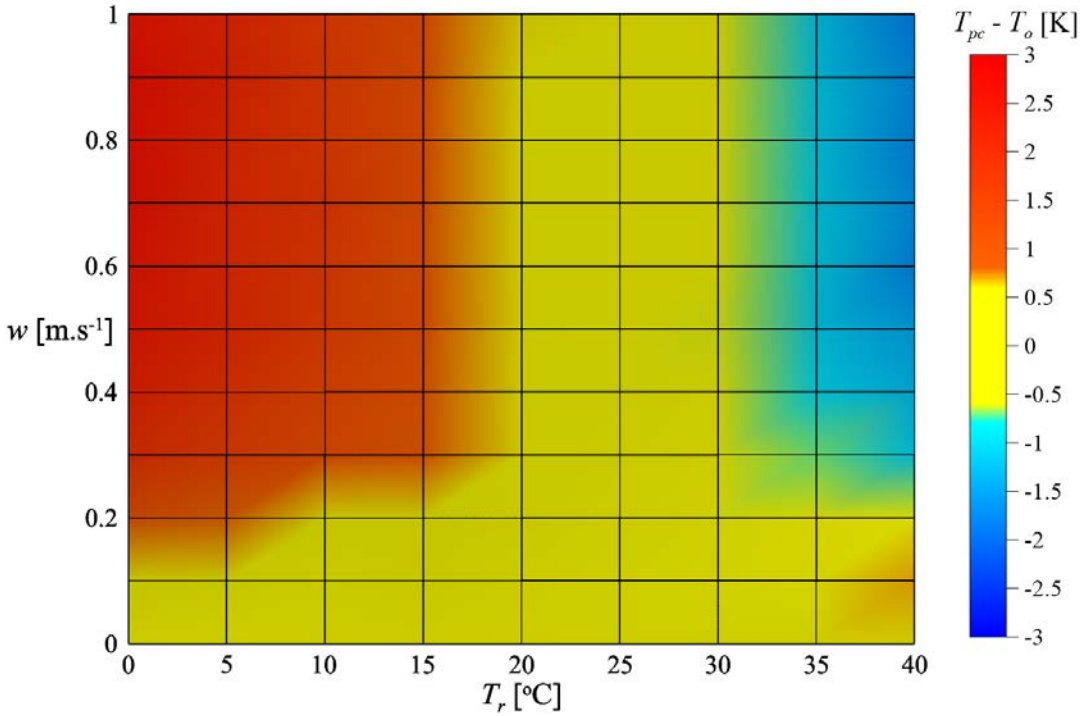

Figure 51. The difference between the corrected plate and the operative temperatures based on the second theoretical solution, for constant air temperature (T_a =25 °C)

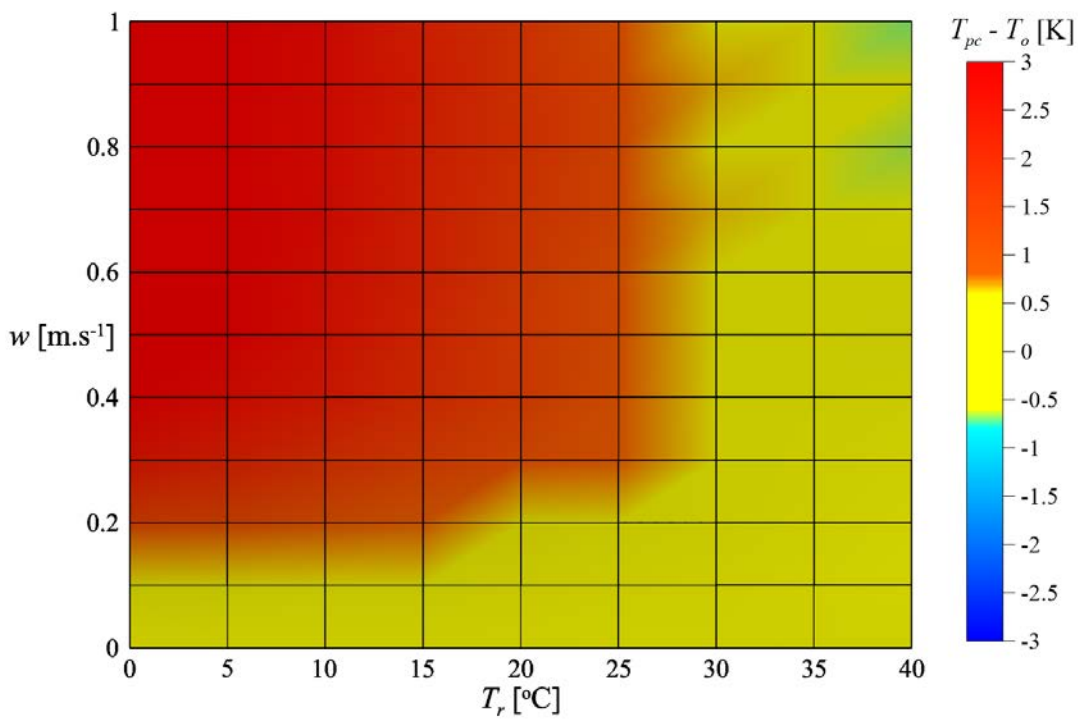

Figure 52. The difference between the corrected plate and the operative temperatures based on the second theoretical solution, for constant air temperature (T_a =35 °C)

From the Figures 50, 51, and 52, it can be observed that the difference between the corrected plate temperature and the operative temperature depends primarily on the difference between the mean radiant and air temperatures ($T_r - T_a$), also it can be seen that the effect of the air velocity w, on the difference is limited; where it can be noticed that:

- For the range of $| T_r - T_a | \leq 7$ °C, the value of the difference $|T_{pc} - T_o| \leq 0.6$ °C.

The range of $| T_r - T_a |$ can be extended by using the air velocity limits, as follow:

- For $| T_r - T_a | \leq 15$ °C and $w \leq 0.2$ m.s^{-1}, the value of the difference $|T_{\mathrm{pc}} - T_{\mathrm{o}}| \leq 0.5$ °C.

Thus, by using the large size of plate sensor the range of $| T_r - T_a |$, in which the plate temperature can be used instead of the operative temperature, extended.

III. PRACTICAL PART

1. Construction of Plate Compact Sensor

The compact plate sensor (Figure 41) consists of a metallic plate of zinc ($A \times A$ mm), the frontal surface of the sensor is painted with black matt paint with high emissivity, the back side has small emissivity, and on the center of this face a thermocouple is fixed by welding. Another thermocouple, for measuring the air temperature, is fixed on the plate sensor as it is shown on Figures 53 and 54. The sensor can be placed on plastic base (Figure 53) with small emissivity or placed on small holder (Figure 54). In this work, the dimension of the plate sensor A, was considered 30 mm for small sensor and 80 mm for large plate sensor.

The plate sensor with small holder is stronger, with small influence of conduction and slightly obstructed convection. While plate sensor with plastic base is not so sturdy, but practically without the influence of conduction and without the obstruction of convection. Both of them enable easy to install the sensor on all surfaces.

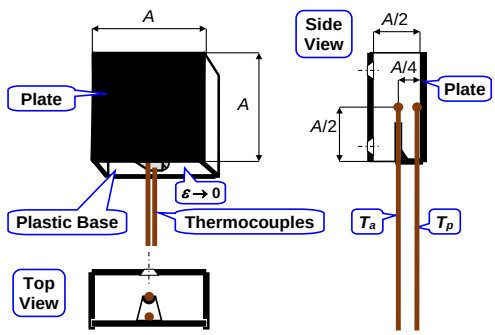

Figure 53. The construction of Plate compact sensor with plastic base

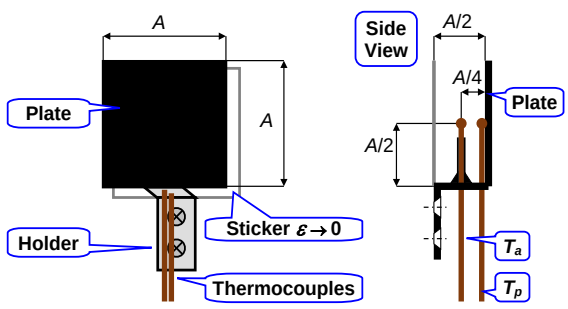

Figure 54. The construction of plate compact sensor with small holder

The distance A/4, at which the thermocouple for measuring the air temperature is fixed on the plate sensor, is determined according to the thikness of the thermal boundary layer over the plate sensor. The temperature distibutions over the plate sensor can be evaluated from dimensionless temperature θ as following (Ostrach 1952):

$$\theta = \frac{T_{x,y} - T_a}{T_p - T_a} = f(\eta) \tag{99}$$

$$\eta = \left(\frac{Gr_x}{4}\right)^{1/4} \frac{y}{x} \tag{100}$$

where

$T_{x,y}$ is the absolute temperature of fluid at the coordinate (x,y), K,

T_a, T_p are the air and plate temperature, respectively, K,

η is the similarity variable,

Gr_x is Grashof number based on x,

x is the distance alonge the plate sensor,m,

y is the distance from the surace of the plate sensor, m.

The temperature distributions as given by equation (99) is presented in Figure 55 as function of the similarity variable η for Prandtl number $Pr = 0.72$.

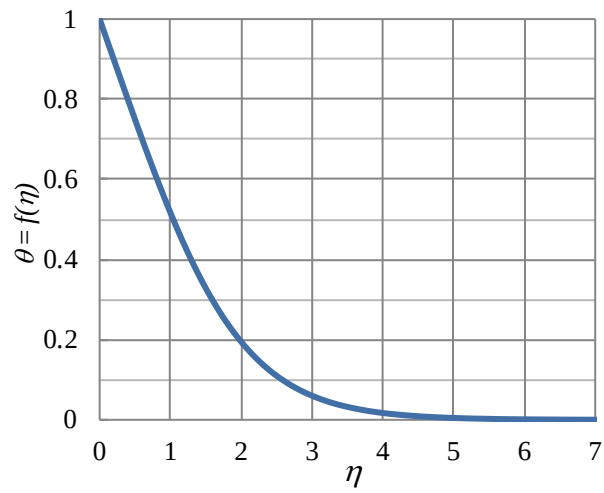

Figure 55. The dimensionless temperature distribution for Prandtl number of 0.72 (Ostrach 1952)

For small plate sensor (30 × 30 mm) the distance $y = A/4 = 0.0075$ m, and $x = A/2 = 0.015$ m at this distances and for $Pr = 0.72$ it is possible to calculate the similarity variable η from equation (100) then from the Figure 55, the values of dimensionless temperature θ can be determined. Then the relation between $T_{x,y} - T_a$ and $T_p - T_a$ can be plot on figure 56.

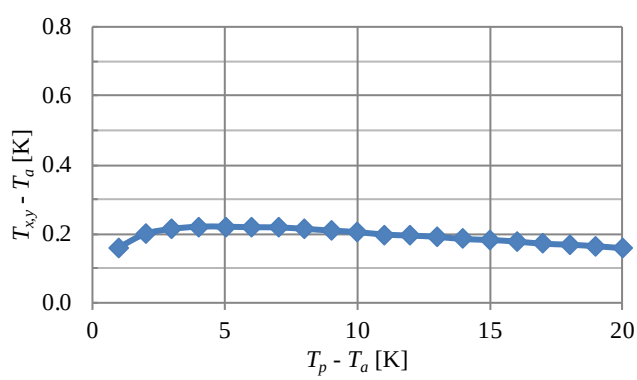

Figure 56. The difference between the thermocouple temperature at the location (x,y) and the air temperature as function of the difference T_p - T_a

The plate temperature T_p measured by the new sensor, where its thermocouple is connected to ADAM- 4018 8-channel Analog Input Module (Advantech 2017) (Fingure 57).

The ADAM-4018 uses a 16-bit microprocessor-controlled sigmadelta A/D converter to convert sensor voltage or current into digital data. The digital data is then translated into engineering units. When prompted by the host computer, the module sends the data to the host through a standard RS-485 interface.

Figure 57. *The ADAM-4018 unit*

The small plate sensor (30 × 30 mm) is suitable for using on a thermal mannequin Figure 58.

Figure 58. The plate sensor placed on thermal mannequin

2. Experimental Equipment

2.1. Testing Chamber

The testing chamber (Figure 59) is chamber for experimenting sensors of the thermal comfort. It has been designed for the purpose of experiment the developed sensors by comparing with expensive laboratory sensors. The chamber minimizes the thermal effects of surrounding and creates a relatively homogeneous environment.

Figure 59. The testing chamber

The testing chamber consists of four stands; these stands are connected by plastic tubes. The walls are curtains of black textile, which provide uniform mean radiant temperature. The curtains are about 10 cm above the floor to allow the air flows. On the top of the chamber four regulating ventilators are placed to force the air to flow with different velocities. The Chamber has been designed so that it is possible to change all its three dimensions, which provides a testing space about 6-15 m^3. Scheme of test chamber is shown in Figure 60 (Košíková et al. 2011).

Basic technical parameters:

- Dimensions (width x length x height):
  Minimum: 1.7 x 1.7 x 2.2 m - Maximum: 2.25 x 2.25 x 3.1 m
- Material used:
  - *Stand* (×4): OMNITRONIC aluminum, Max load: 18 kg, min. Height: 1.4 m, max. height: 2.1 m.
  - Tubes: plastic pipe *PN* 20, Ø 32x5.4 mm
  - Ventilator (×4): SOMOGYI ELEKTRONIC, floor fan type *PVR* 35. The specifications:
    Power supply: 220 V AC / 50 Hz,
    Input power: 60 W,
    Maximum air speed 6 $m.s^{-1}$
    Blade diameter: 35 cm.
    Weight: 2.6 Kg
- Curtains: a black matt textile is fixed on the structure of the chamber to form the walls of the testing chamber.

The four ventilators provide a relatively steady uniform distribution of air flow in the testing chamber. The air flow velocity in the testing chamber can be controlled through control the power supply to the fans.

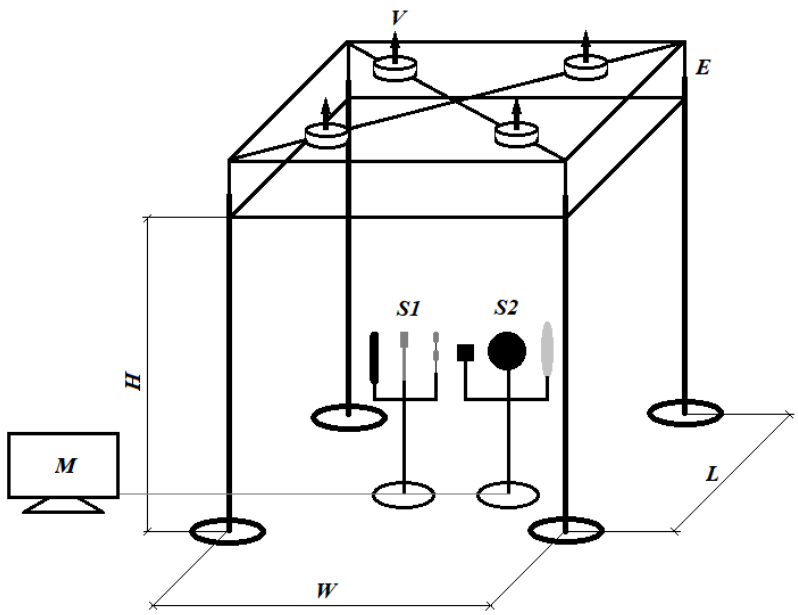

Figure 60. *Scheme of test chamber: S1 – Set of sensors to measuring humidity, velocity, and temperature of the air; S2 – Set of thermal comfort sensors; V – ventilators with adjustable flow; M – monitor; Chamber Dimensions (W - width, L - length, H- High)*

2.2. Calibration Chamber

The calibration chamber is a compact mobile chamber for calibration of the developed thermal comfort sensors. The chamber has been designed to calibrating the thermocouples, operative temperature, and black plate sensors types. The calibrated sensors are placed in the center of the chamber, and the thermal state of wall and the inner spas of the chamber are monitored.

The surface area of sensors inside the chamber is required to be at least fifty times smaller than the surface of the inner walls of the chamber. In such an arrangement, it is possible to consider the radiation conditions on the surfaces of the sensors as a small body in a large space.

The chamber has been designed to use a large set of sensors (such as globe thermometer with a diameter of 100 mm or 150 mm) for measuring the thermal environment according to ISO 7726 (ISO 7726 1998).

The chamber walls consist of three layers (Figure 61), the Upper layer is the frame of the chamber and has a protection function. The second layer has an insulating function and contains a component of heating elements. The third layer is the inner structure and it is made of aluminum sheets of 3 mm thick, which are painted by matt black paint to provide a surface emissivity $\varepsilon = 0.98$ (Janečka et al. 2011)

<u>*Basic technical parameters:*</u>

- Outside dimensions: 780 mm x1100 mm x1100 mm
- Inside dimensions: 580 mm x 820 mm x 820 mm
- Range of temperature adjustment: (0 – 50) °C
- Setting of temperature step: 0.1 K
- Setting of required temperature hysteresis: (0.01 – 1.5) K

- Uncertainty of temperature measurement: 0.2 K
- Range air velocity measurement: (0 – 2) m. s^{-1}
- Measurement uncertainty air velocity: 0.05 m. s^{-1}

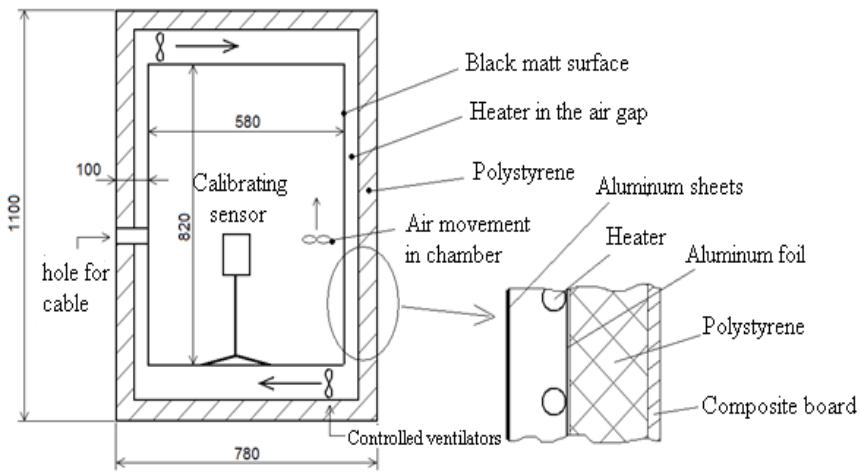

Figure 61. Scheme of calibration chamber (Janečka et al. 2011)

2.3. INNOVA System for Measurement the Thermal Comfort

For calibration and thermal comfort measurement is used mobile measuring system (Figure 62) by INNOVA function by employing sensors to assess thermal comfort in residential spaces, working spaces and vehicles under either laboratory or operational conditions. It enables to carry out simultaneous measurement at three positions within the space (head, abdomen and ankle levels usually). The system consists of the Thermal Comfort Data logger INNOVA 1221, a set of 28 sensors with tripod stands (Figures 63), and a laptop with measuring software. (LumaSense Technologies 2007)

Figure 62. Portable data logger INNOVA and a laptop

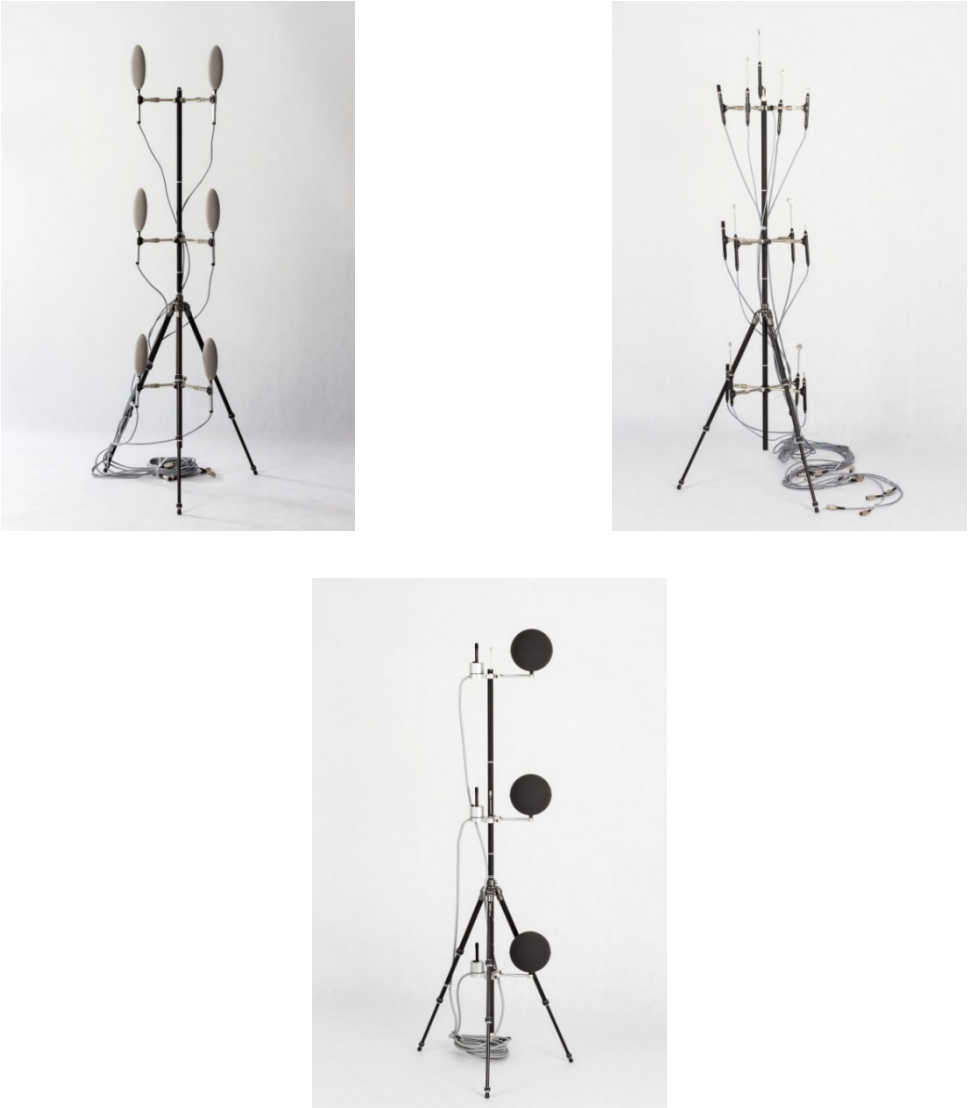

Figure 63. Arrangement of sensor for different measurement types

<u>*The system application:*</u>

- ✓ Assessment of the thermal environment state based on measurement many quantities (air temperature, surface temperature, radiant temperature, radiant temperature asymmetry, air velocity, turbulence intensity and air humidity).
- ✓ Assessment of the thermal environment state based on a single quantity measurement (measurement of the operative temperature or the equivalent temperature, determination of dry heat loss, and determination of indices *PMV* and *PPD*)
- ✓ Measurement and assessment of workers' heat load in hot environments (measurement of the air temperature, globe temperature, and naturally ventilated wet bulb temperature, and determination of the *WBGT*-index Wet Bulb Globe Temperature).

- ✓ Calibration measurement (when developing simple thermal comfort sensors which may be employed in field of measurement, thermal comfort control etc.)
- ✓ Measurement in research on suitable parameters for objective assessment of thermal comfort of several types of the environment.

The measuring ranges and accuracy as well as methods of the measured quantities treatment follow standards listed below:

- ✓ ISO 7726 Thermal environments (ISO 7726 1998).
- ✓ ISO 7730 Moderate Thermal Environments—Determination of the *PMV* and *PPD* indices and specification of the conditions for thermal comfort (ISO 7730 1994).
- ✓ ISO 7243 Hot environments. Estimation of the heat stress on working man, based on the *WBGT*-index (wet bulb globe temperature) (ISO 7243 1982).
- ✓ ISO 7933 Hot Environments—Analytical determination and interpretation of thermal stress using calculation of required sweat rate. (ISO 7933 1989)

2.3.1. List of The INNOVA Sensors Used in Doctoral Measurements

Wet Bulb Globe Temperature (WBGT) Sensor – INNOVA MM0030:

The WBGT-index is the most widely used heat stress index and is standardized in ISO7243. The index is a single value which enables you to evaluate the level of heat stress caused by an environment (LumaSense Technologies 2007).

The *WBGT* sensor (Figure 64) includes three separate sensors, which provide the necessary parameters to calculate the *WBGT*-index. All three sensors are based on resistance temperature sensing elements of platinum (Pt100).
The three Sensors are (LumaSense Technologies 2007):

Wet Bulb Temperature sensor:
The wet bulb temperature simulates the effect evaporative heat loss, by having an unshielded bulb covered with a wet cotton sock or wick. The evaporation from the wick cools the sensor in the same way that sweat cools the body.

Globe thermometer:
This thermometer primary uses to determine the radiation effect of an environment. The sensor consists of a Pt100 temperature element situated at the center of the globe (150 mm in diameter). Size and construction of the globe are defined by ISO7243.

Air Temperature thermometer:
The sensor consists of platinum (Pt100) sensor which is radiantly shielded, where it is surround by an open-ended aluminum-foil cylinder.

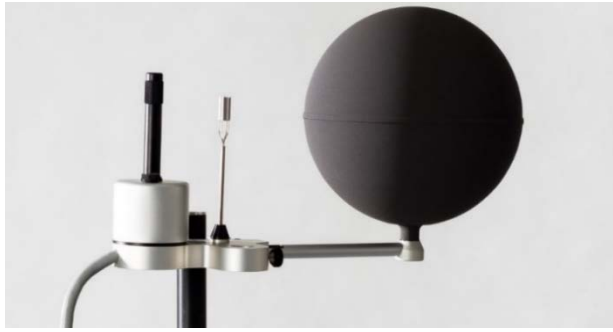

Figure 64. The Wet Bulb Globe Temperature (WBGT) Sensor

Air Temperature Sensor – INNOVA MM0034

The MM0034 measures the air temperature with minimal thermal radiation interference from hot or cold objects. It consists of a Pt100 resistor sensor, which is surrounded by an open ends aluminum-foil cylinder to reduce the thermal radiation effect from surrounding. The cylinder, with its open ends, enables a free flow of air around the sensor (Figure 65). (LumaSense Technologies 2007)

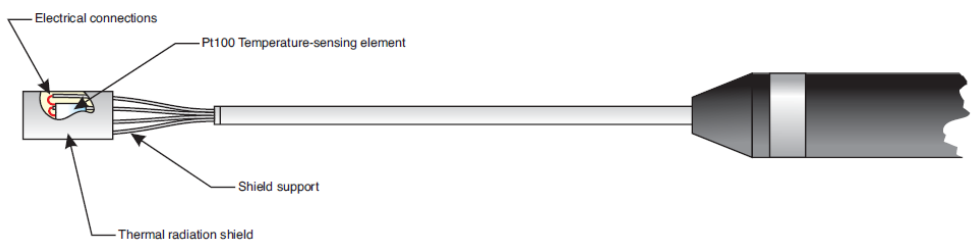

Figure 65. The Air Temperature Sensor – INNOVA MM0034

Radiant Temperature Asymmetry Sensor – INNOVA MM0036

It consists of two identical faces (*A* and *B*) Figure 66, that independently measure the net incident radiation on each plane surface (the plane radiant temperature) T_{rA} and T_{rB}.
Each face of the sensor consists of a reflective gold-plated element and a black-painted element of the same size. Both elements are connected to a centre block via thermopiles.
The work principle of the sensor based on that the gold plated loses or gains heat entirely by convection whereas the black plate loses or gains heat both by convection and radiation.
Thus the resultant difference voltage produced across the thermopiles is a function of the net heat transfer by radiation between the black plate and the environment. Both sets of elements are covered with polyethylene shields. These prevent air velocity from influencing the results. (LumaSense Technologies 2007)
By measuring plane radiant temperature in several directions the mean radiant temperature can also be calculated as following:

$$T_r = (T_{rA} + T_{rB})/2$$

and the asymmetry of the radiant temperature:

$$\Delta T_r = |T_{rA} - T_{rB}|$$

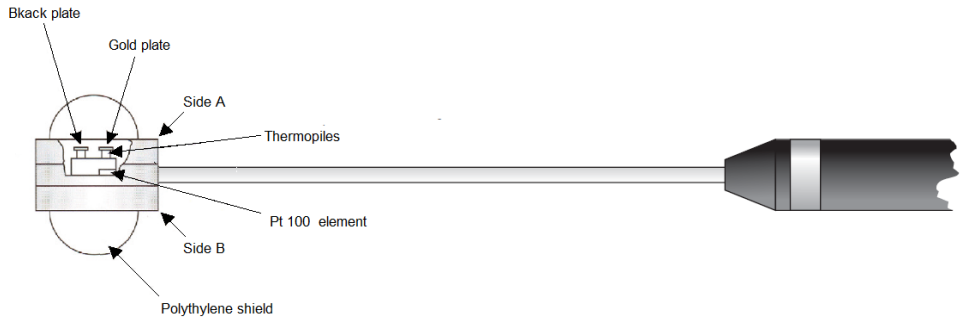

Figure 66. The Radiant Temperature Asymmetry Sensor – INNOVA MM0036

Air Velocity Sensor – INNOVA MM0038

The Air Velocity Sensor MM0038 (Figure 67) is designed to measure omnidirectional air velocities in indoor climates (lower velocities).

The measurement principle of the sensor is based on the constant temperature difference anemometer principle. Where the sensor consistes of two sensor elements, one of which is heated electrically, are plased in two plastic foam ellipsoids on a single shaft. The heated sensor contains three heated coils. The controlled electrical heating maintains a constant temperature difference of 15°C, independent of the air temperature, between the two sensors.

The smallish sphere at the end of the shaft prevents errors occurring if the air-flow is parallel to the shaft. (LumaSense Technologies 2007)

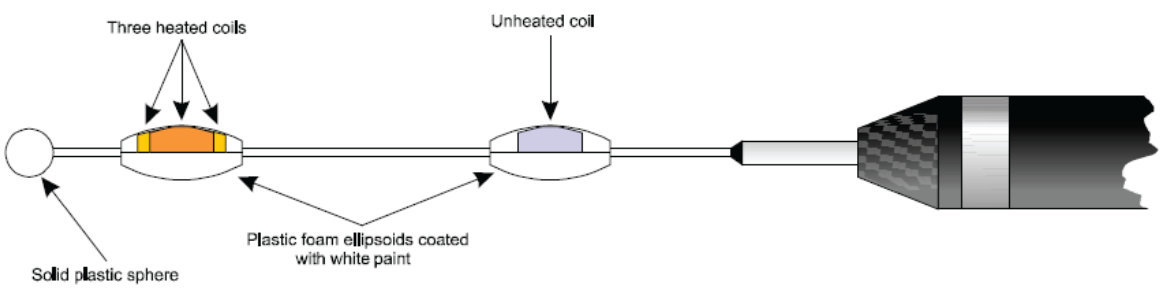

Figure 67. Air Velocity Sensor – INNOVA MM0038

Operative Temperature Sensor – INNOVA MM0060

Four major factors were taken into consideration during the design of the operative temperature sensor, Figure 68 (LumaSense Technologies 2007):

- Size: The size has been chosen so that the ratio between heat loss by radiation and by convection is similar to that of the human body.
- Shape: The ellipsoid shape provides the same angle factor to the individual room enclosures as for a human being.
- Color: The sensor's Color and emission coefficient have been chosen so that the longwave radiation absorbed by the sensor is the same as that of both a naked and a dressed person. The grey Color chosen simulates both naked people and people dressed in light colored clothing.

- Orientation: The sensor has three settings: vertical, 30° from the vertical, and horizontal, which represent the body in the standing, sitting and lying positions respectively.

Figure 68. The Operative Temperature Sensor – INNOVA MM0060

3. Experimental Measurements

3.1. Comparison Between Globe and Operative Temperatures in The Testing Chamber

In this experiment is presented the results of measurements of the thermal state of the chamber environment. The measurements include the environmental parameters (air temperature T_a, air velocity w, and men radiant temperature T_r) and indexes of thermal comfort (Globe temperature T_g and operative temperature T_o). The length of the experiment was three hours, and it was divided into three periods in each one the air velocity was controlled and the globe and the operative temperatures were observed.

<u>Experiment set-up:</u>

The four fans are located on the top of the chamber to provide a uniform air flow in the chamber, by adjusting the power supply the air velocity can be controlled.

The air temperature, air velocity, and mean radiant temperature were measured with the Innova sonsors MM0034, MM0038, and MM0036, respectivlly. The globe and the operative temperatures were measured by the Innova sonsors MM0030 and MM0060, respectivlly. The sensors were located on the center of the chamber at high of 0.6 m from the floor. The Figure 69 presentes the sensors used in the experiment.

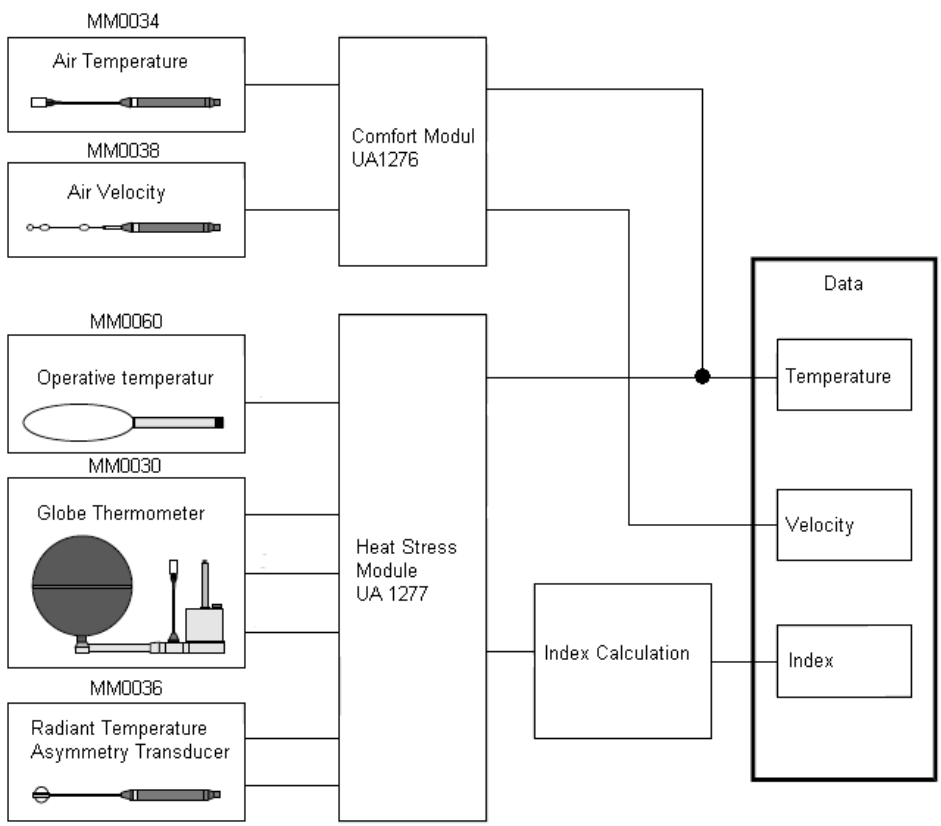

Figure 69. Overview of sensors types used in experiment

Measurement conditions:

1- ***The first part of the experiment (Figure 70):***
The duration of this part was one hour. The ventilators were adjusted to provide air velocity of 0.9 m. s^{-1} at the first half hour then the velocity is reduced to 0.65 m. s^{-1}. The air temperature in the chamber at the beginning of the experimental was 18.5 ^{o}C. There wasn't source of radiation in the chamber.

2- ***The second part of the experiment (Figure 71):***
The length of the second part of the experiment was about one hour. The four ventilators were adjusted to provide air flow velocity of (0.7 ÷ 0.8) m. s^{-1}. The air temperature in the chamber at the beginning of the experimental was 19 ^{o}C. There wasn't source of radiation in the chamber.

3- ***The last part of the experiment (Figure 72):***
The duration of this part of the experimental was about one hour. The ventilators were adjusted to provide air flow velocity of 0.6 m. s^{-1} at the first half hour then the velocity is reduced to 0.5 m. s^{-1}. The air temperature in the chamber at the beginning of the experimental was 18.3 ^{o}C. There wasn't source of radiation in the chamber.

Results of the experiment:

The results are shown on the Figures 70, 71, and 72. The air temperature T_a, air velocity w, mean radiant temperature T_r, globe temperature T_g, and operative temperatures (T_{o1} and T_{o2}) are plotted by time. Where T_{o1} is the operative temperature measured by Innova sonsor MM0060, and T_{o2} is the operative temperature calculated from equation (51) as function of air temperature, air velocity, and mean radiant temperature.

During the experiment, the air temperature was higher than the radiant temperature and the difference between them varies from 0.9 K up to 1.5 K.

From the figures 70, 71, and 72, can be notice that the operative temperature T_{o1} measured via Innova sonsor MM0060 is matching to that (T_{o2}) calculated from equation (51).

The difference between the globe and the operative temperatures is very small during the all experiment and didn't exceed 0.2 K, that agree with the theoretical solution of the globe and operative temperatures, and compatible the accuracy of the globe and operative temperature measurement (±0.5 K) according to the norms ISO 7726.

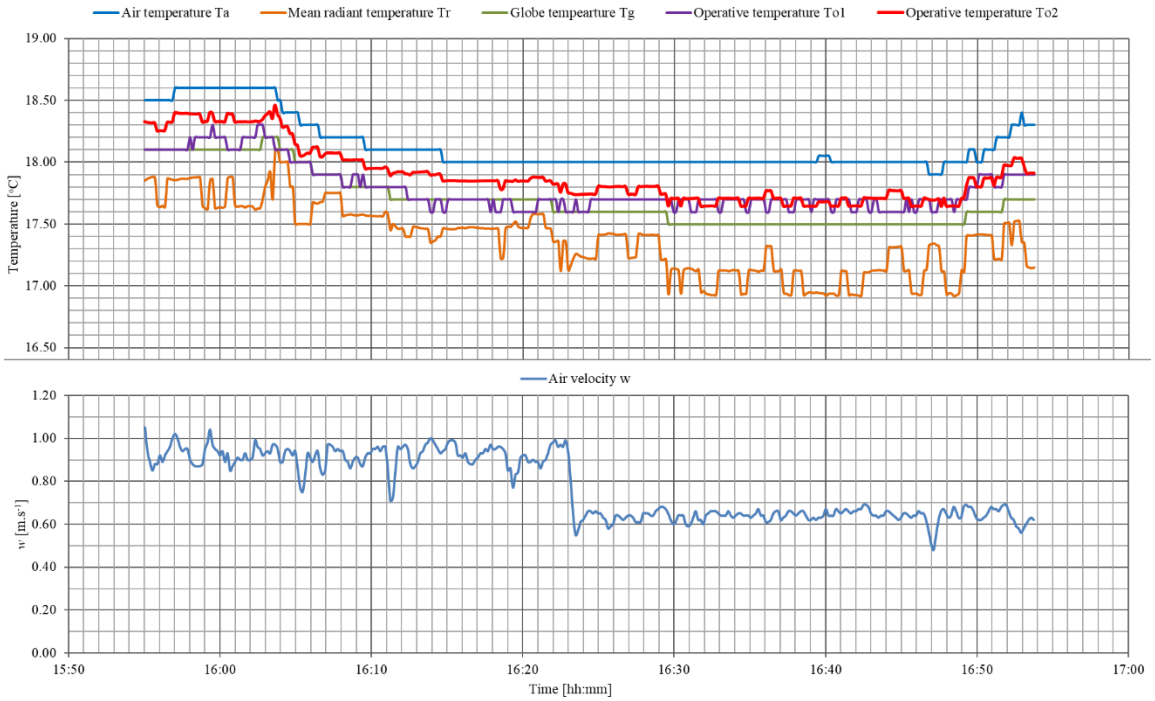

Figure 70. Comparison between the globe and operative temperatures in the testing chamber (first period)

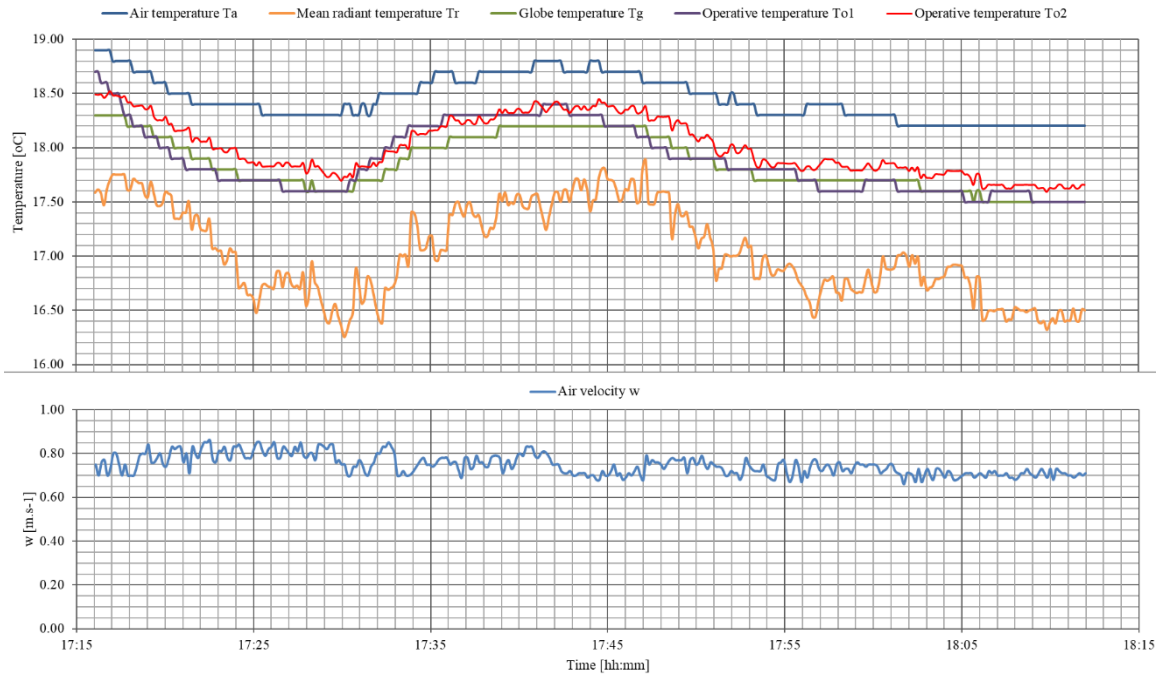

Figure 71. Comparison between the globe and operative temperatures in the testing chamber (second period)

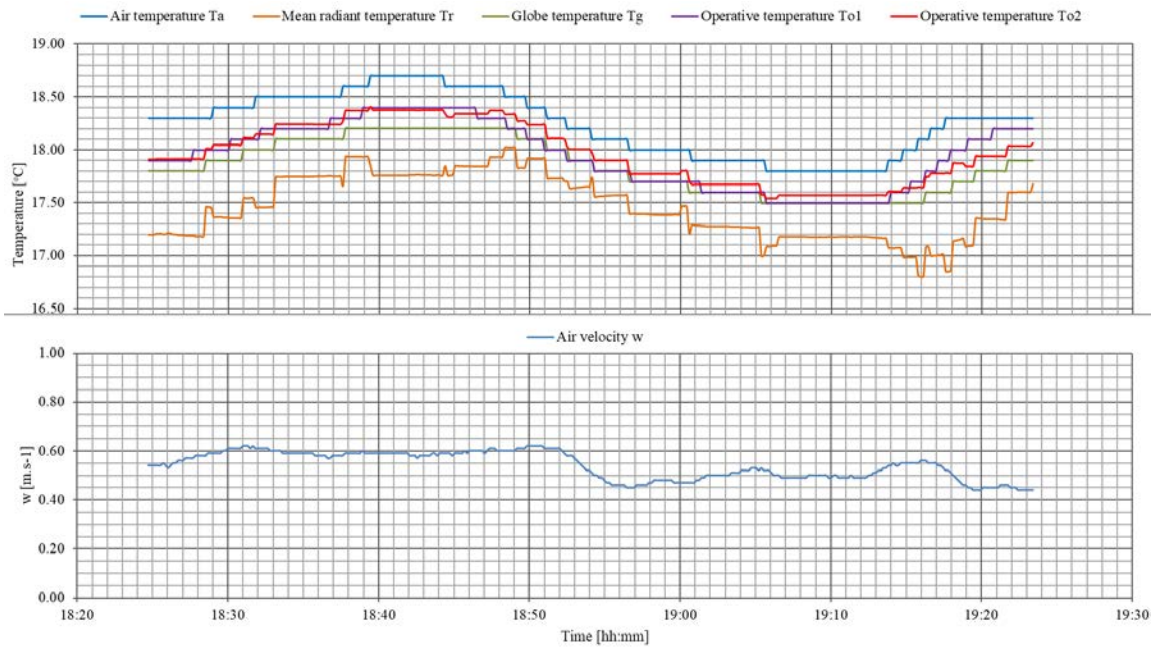

Figure 72. Comparison between the globe and operative temperatures in the testing chamber (third period)

3.2. Testing the Designed Plate Sensor

The aim of this experiment is to examine the designed small plate sensor (30 × 30 mm), and to determine if it is possible to use it in the evaluating the thermal state of an environment for different air velocity.

In this experiment the plate temperature T_p, globe temperature T_g, and operative temperature T_o were measured as function of the environmental parameters of the testing chamber. The measurements of plate, globe, and operative temperatures were observed and plotted on Figures 73 and 74 by the time.

The experiment divided into two periods, the first period had four hours length and the second one three hours.

<u>Experiment set-up:</u>

The four fans are located on the top of the chamber to provide a uniform air flow in the chamber, by controlling the power supply the air velocity can be adjusted.

The air temperature, air velocity, and mean radiant temperature were measured with the Innova sensors MM0034, MM0038, and MM0036, respectivlly. The globe and the operative temperatures were measured with the Innova sensors MM0030 and MM0060, respectivlly. The plate temperature measured by the new sensor, where its thermocouple is connected to ADAM- 4018 8-channel Analog Input Module.

The sensors were located on the center of the chamber at high of 0.6 m from the floor. The chamber in this experimental wasn't include sours of radiation.

Measurement conditions:

1- ***The first part of the experiment (Figure 73):***
The duration of the measurement was four hours. The ventilators were adjusted during this period of the experiment to provide air velocity of 0, 0.2, 0.4, 0.6, and 1 m. s^{-1}. The air temperature in the chamber at the beginning of the experiment was 18.50 °C and it remained almost constant during the measurement. There weren't heat or radiation source in the chamber.

2- ***The second part of the experiment (Figure 74):***
The measurement lasted three hours. The ventilators were adjusted to provide air flow velocity of 1, 0.8, and 0.6 m. s^{-1}. The air temperature in the chamber at the beginning of the experiment was 19.9 °C and it gradually rises due to air velocity dropping.

Results of the experiment:

The air temperature, globe temperature, operative temperature, plate temperature, mean radiant temperature, and air velocity are plotted on the Figures 73 and 74 by time.

The thermal indexes (globe and the operative temperatures) and the plate temperature were almost the same during the all experiment and the maximum difference didn't exceed 0.2 K, that agree with the theoretical solution of the globe and operative temperatures and compatible the accuracy of the globe and operative temperature measurement (±0.5 K) according to the norms ISO 7726.

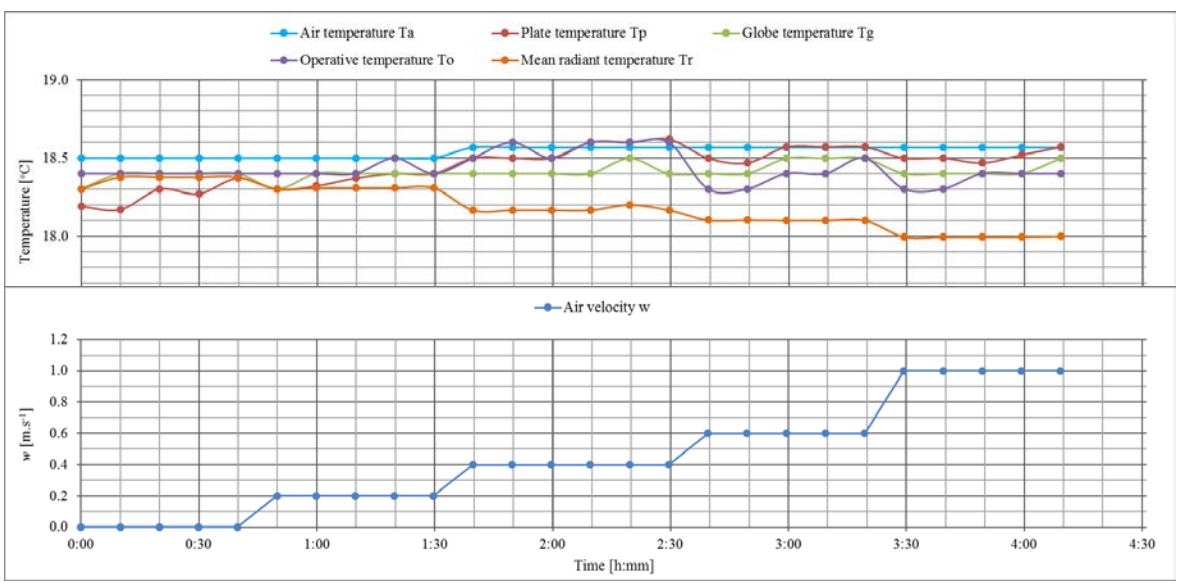

Figure 73. Testing the New Plate Sensor (first period)

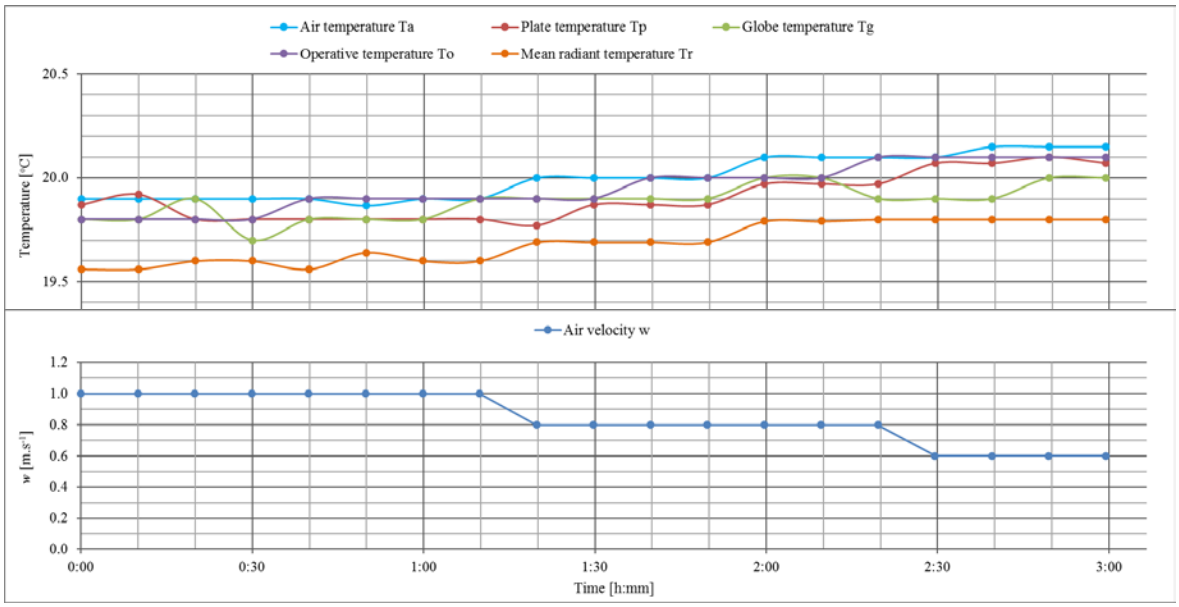

Figure 74. Testing the New Plate Sensor (second period)

3.3. Impact of The Directional Radiation on The Testing Sensors

The purpose of this experiment is to determine the impact of the directional radiation on the designed plate sensor (30 × 30 mm). The experiment is taken place in the testing chamber, a radiation source (lamp) is applied in the testing chamber, where it located at various angle from the sensors, Figure 75.

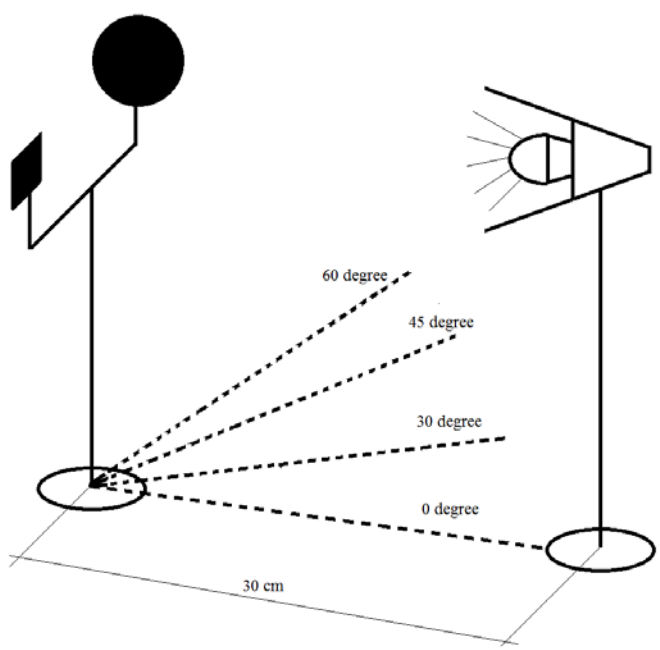

Figure 75. Scheme of the radiant impact experiment

Experiment set-up:

The plate sensor and globe thermometer are fixed in the center of the testing chamber at high of 0.6 m from the floor. The radiation steady state source (lamp 75 W) is located at the distance of 30 cm from the plate and globe sensors, with possibility to change the angle of the lamp as it shown on Figure 75.

The experiment was without ventilators, the air temperature was measured with the Innova sensor MM0034. The globe temperature was measured with the Innova sensor MM0030. The plate temperature measured with the new sensor, where its thermocouple is connected to ADAM- 4018 8-channel Analog Input Module.

Measurement conditions:

The experiment was lasted for four hours. The ventilators were turned off and the source of radiation at the angle 0 degree. The air temperature in the chamber at the beginning of the experimental was 18.50 °C and it increased by time till 19.10 °C at the end.

The experiment is repeated for the same condition except the angle of the radiation source where it is changed (30, 45, and 60 degree).

Results of the experiment:

The plate temperature and globe temperature were plotted on the Figures 76 and 77, respectively, by time.

From the results, the impact of the radiation source angle on the plate temperature is significant. While this impact is small for the globe temperature as it shown on Figure 78.

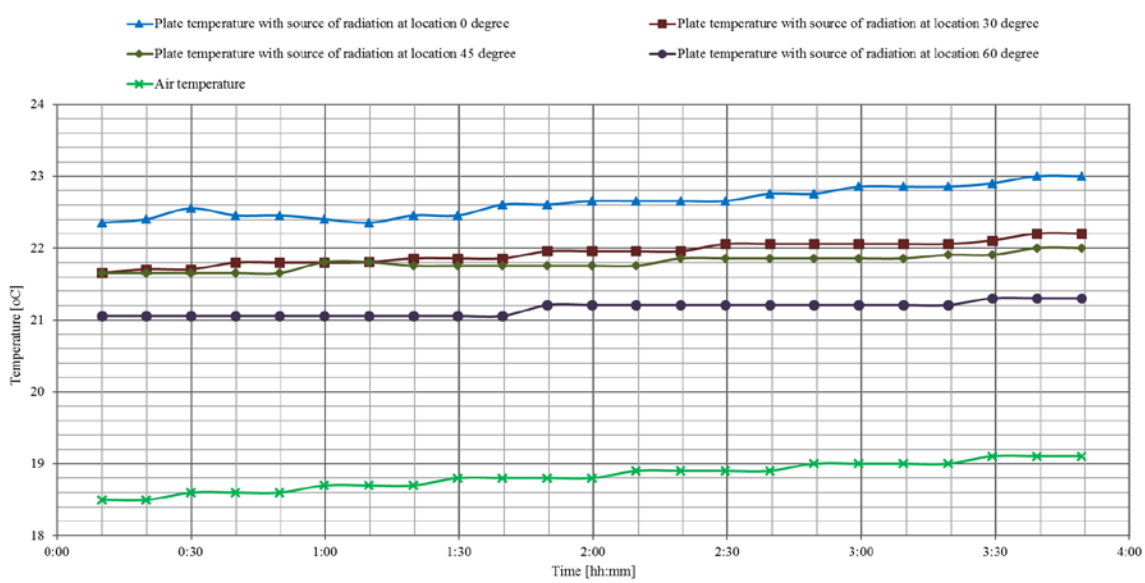

Figure 76. The impact of the radiation on the plate temperature

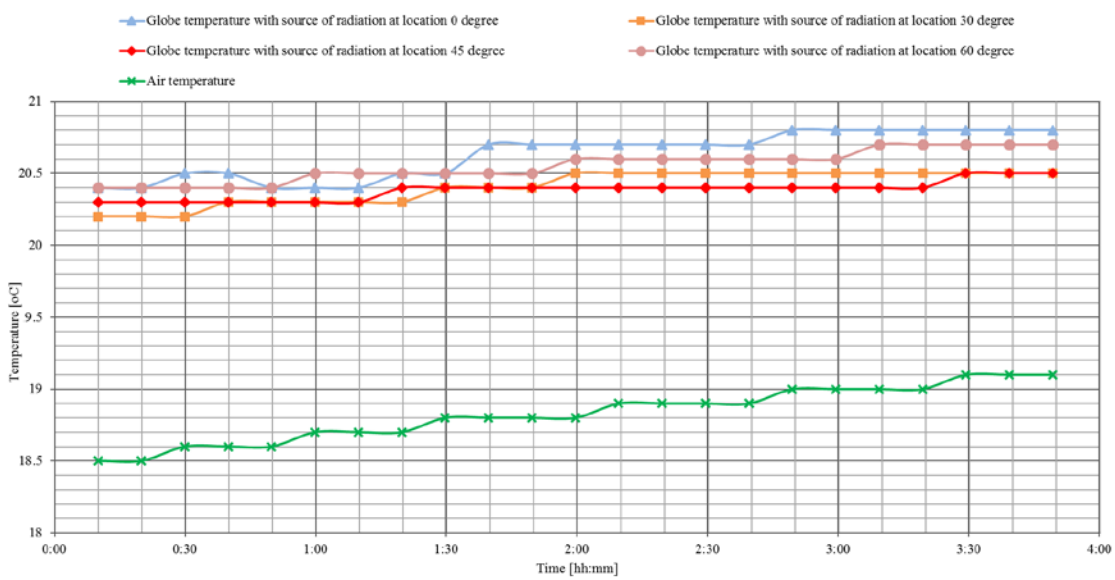

Figure 77. The impact of the radiation on the globe temperature

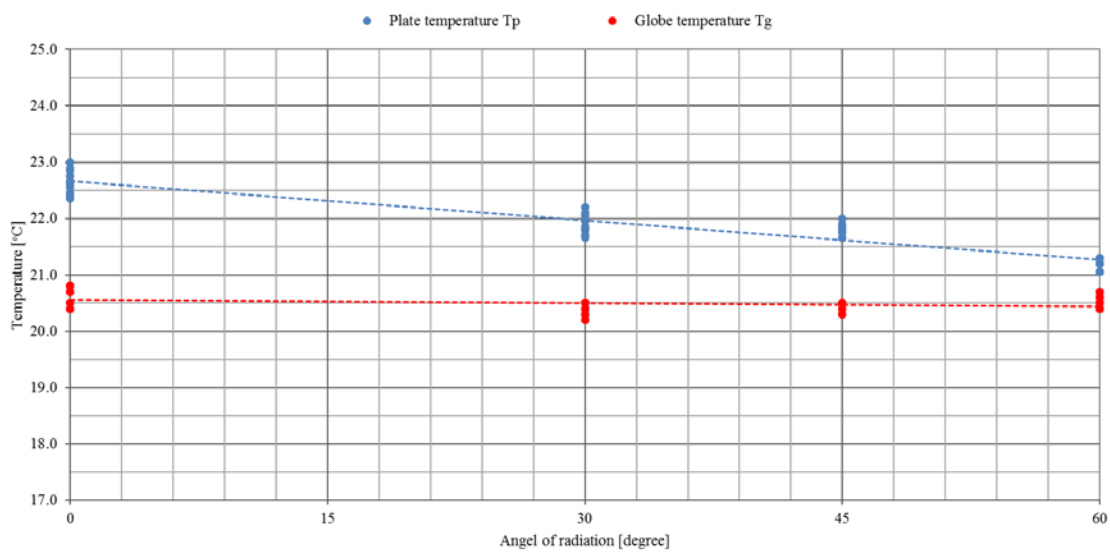

Figure 78. The impact of the radiation on the plate and globe temperature

From the Figure 78, it is noticed that for the angle of radiation in range of ± 20° the difference in plate temperature $\Delta T \approx 0.5$ K. This compliant with the norms ISO 7726. For this reason, it is necessary to place the plate sensors with respect to the large radiation source at this angle.

From this experiment, it is obvious that temperature measured by the designed plate sensor T_p is dependent on the direction of the radiation. When the plate sensor is installed in room with a non-homogeneous radiation, it is needed to consider if we want to take in account the effect of directional radiation (as in case of the thermal manikin) or we will not (measuring the thermal state in the environment, where the average radiant temperature is required).

CONCLUSION

The basic plan of my work during the doctoral study was presented in this thesis. The thesis is divided into three parts.

In the first part of the thesis the literature survey has been achieved, which include a brief introduction of heat transfer, an overview of the thermal comfort, the heat balance equation of human body, and the thermal comfort indices.

The theoretical solution was the second part of the thesis, where in this part the globe and operative temperature were selected as thermal comfort indexes to assess the thermal state of an environment. The effect of the environmental factors on the globe and operative temperatures was studied, and the relations between the environmental vectors (mean radiant temperature, air temperature, and air velocity) and each of globe temperature and operative temperature were funded. Then a theoretical solution for these relations was funded. The comparison between globe and operative temperature was carried out using own theoretical solution of operative and globe temperatures in a wide range of environmental parameters.

The theoretical solution was based on two different equations of the combined heat transfer (forced and natural). The results based on the two equations were close and can be summarized as follow:

The difference between the globe and the operative temperatures depends mainly on the difference between the mean radiant and air temperatures $|T_r - T_a|$, *and further on the air velocity w, as following:*

- For the range of: $|T_r - T_a| \leq 8$ K, the value of the difference $|T_g - T_o| \leq 0.5$ K.

The range of $(T_r - T_a)$ can be extended by using the air velocity limits, as follow:

- For $|T_r - T_a| \leq 10$ K and $w \leq 0.15$ m.s^{-1}, the value of the difference $|T_g - T_o| \leq 0.5$ K.

Later in the second part, new designed plate sensor was presented. The developed sensor was designed as compact sensor for continuous and effective measurement of parameters of local thermal environment, which enable to evaluate the local thermal comfort. The temperature measured by the new plate sensor is called the plate temperature T_p. As it in the globe and operative temperatures, the relation between the environmental parameters (air temperature, air velocity, and mean radiant temperature) and plate temperature was derived. Then a theoretical solution for this relation was funded.

The main purpose was to make comparison between plate and operative temperatures, which is carried out using own theoretical solution of operative and plate temperatures in a wide range of environmental parameters. The theoretical solution was based on two different equations of the combined heat transfer (forced and natural). The results can be summarized as follow:

The difference between the plate and the operative temperatures depends on the difference between the mean radiant and air temperatures $|T_r - T_a|$; *where:*

- *For the range of:* $| T_r - T_a | \leq 2$ K, *the value of the difference* $|T_g - T_o| \leq 0.6$ K.

Thus, it can be seen that there is a big difference between the operative temperature and the temperature measured by the plate sensor, and the range, in which the difference between the temperatures les than 0.5 K, is very small.
In order to improve the rsults, a correction for the values of the temperature measured by the plate sensor was performed.

The following form of the corection was suggested:

$$T_{pc} = T_p + c(T_p - T_a)$$

where:

c: is the correction factor and its value depende on the air temperature and can be determined from the equations (97) and (98).
The using of the correction form the difference between the corrected plate and the operative temperatures is decreased; where:

- For the range of $| T_r - T_a | \leq 5$ K, the value of the difference $|T_{pc} - T_o| \leq 0.6$ K.

The range of $| T_r - T_a |$ can be extended by using the air velocity limits, as follow:

- For $| T_r - T_a | \leq 10$ K and $w \leq 0.2$ m.s^{-1}, the value of the difference $|T_{pc} - T_o| \leq 0.5$ K.

Consequently, under the previous conditons of the environmental factors it is possible to use the corrected plate temperature as an index of thermal state in state of the operative temperature. Also it can be seen from the form of the corection that the corrected plate temperature is function of air temperature and temperature measured by the plate sensor. Thus, if the plate sensor is provided with simple air temperature sensor (thrmocouple) then the plate sensor it could be considered as a compact sensor for evaluating the thermal state of the environment.

In the last part of the thesis is presented the practice of the study. The experimental equipments used in this work is:

- Testing chamber: in which the comparative measurement was achieved.
- Calibration chamber for calibration of the sensors.
- INNOVA system: which includes the set of the sensors for evaluating the thermal state of an environment.

These equipments were developed in the framework of this dissertation, and the cooperation with other PhD students.

The measurements achieved in the testing chamber were:

1- *<u>The comparison between the globe and operative temperatures in the testing chamber:</u>* The measurements was included the environmental parameters (air velocity, air temperature, and men radiant temperature) and indexes of thermal comfort (Globe temperature T_g and operative temperature T_o) of the environment in the testing chamber. The results of the measurement are shown that the globe and the operative temperatures are almost the same during the all experiment and the maximum difference between them didn't exceed 0.2 °C, that agree with the theoretical solution of the globe and operative temperatures.

2- *Testing the new plate sensor:* in this experiment the plat, globe, and operative temperatures were measured as function of the environmental parameters of the testing chamber (air temperature, mean radiant temperature, and air velocity).
   The results of the measurement are shown that the thermal indexes (globe and the operative temperatures) and the plate temperature are very close during the all experiment and the maximum difference didn't exceed 0.2 ^{o}C, that agree with the theoretical solution of the globe, operative, and plate temperatures.
3- *Impact of the directional radiation on the testing sensors:* The purpose of this experiment was to determine the impact of the directional radiation on the designed plate sensor. Where the results are shown that the impact of the radiation source angle on the plate temperature is significant. While this impact is small for the globe temperature.

The research presented in this text is financially supported by the project GAČR 101/09/H050 "Research on energy efficient systems to reach indoor environment comfort".

LIST OF THE IMPORTANT SYMBOLS

A_D	[m^2]	Du Bois surface area
A_r	[m^2]	effective radiative area of the body
C	[W.m^{-2}]	specific rates of heat loss from the body by convection
c_p	[J.kg^{-1}. K^{-1}]	specific heat capacity
C_{res}	[W.m^{-2}]	rate of heat loss by convection from respiration
D	[m]	diameter of globe thermometer
D_o	[m]	equivalent diameter of human body
E	[W.m^{-2}]	specific rates of heat loss from the body by evaporation
$e_b(T)$	[W. m^{-2}]	specific radiation energy emitted by a blackbody per unit time and per unit surface area at absolute temperature T
E_{res}	[W.m^{-2}]	specific rate of heat loss by evaporation from respiration
E_{sk}	[W.m^{-2}]	specific rate of total heat loss by evaporation from the skin
f_{cl}	[-]	clothing area factor
F_{ij}	[-]	fraction of the radiation leaving surface i that strikes surface j
g	[m.s^{-2}]	acceleration due to Earth's gravity
Gr	[-]	Grashof number
H	[W.m^{-2}]	total production of the metabolic heat of the human
h	[W. m^{-2}. K^{-1}]	combined (convection and radiation) heat transfer coefficient
h_c	[W. m^{-2}. K^{-1}]	convective heat transfer coefficient
h_{cg}	[W. m^{-2}. K^{-1}]	coefficient of heat transfer around the globe thermometer
h_{co}	[W. m^{-2}. K^{-1}]	convection heat transfer coefficient between air and human
h_{cp}	[W. m^{-2}. K^{-1}]	convection heat transfer coefficient over the plate sensor
h_e	[W.m^{-2}. Pa^{-1}]	evaporative heat transfer coefficient
h_r	[W. m^{-2}. K^{-1}]	linear radiative heat transfer coefficient
I_{cl}	[clo]	dry thermal insulation of clothing
K	[W.m^{-2}]	rates of heat loss from the body by conductive
k	[W.m^{-1}·K^{-1}]	thermal conductivity of the fluid
L	[m]	characteristic length of a surface

M	[W.m^{-2}]	metabolic heat rate
min Nu	[-]	minimum Nusselt number
Nu	[-]	Nusselt number
Nu_{forced}	[-]	Nusselt number for forced heat transfer
$Nu_{lam.}$	[-]	Nusselt number for laminar flow
$Nu_{natural}$	[-]	Nusselt number for natural heat transfer
$Nu_{turb.}$	[-]	Nusselt number for turbulent flow
P_a	[Pa]	water vapor pressure in the ambient air
Pe	[-]	Peclet number
PMV	[-]	Predicted Mean Vote
PPD	[-]	Predicted Percentage Dissatisfied
Pr	[-]	Prandtl number
$P_{sk,s}$	[Pa]	saturated water vapor at skin temperature
Q_c	[W]	convection heat transfer
q_c	[W. m^{-2}]	specific heat by radiation
Q_{con}	[W]	conduction heat transfer
Q_r	[W]	radiation heat transfer
q_r	[W. m^{-2}]	specific heat by radiation
Q_{res}	[W.m^{-2}]	total rate of heat loss through respiration
Q_{sk}	[W.m^{-2}]	total rate of heat loss from the skin
R	[W.m^{-2}]	rates of heat loss from the body by radiation
Ra	[-]	Rayleigh number
R_{cl}	[m^2. K. W^{-1}]	thermal resistance of clothing
Re	[-]	Reynolds number
$R_{e,cl}$	[m^2. Pa. W^{-1}]	evaporative heat transfer resistance of the clothing layer
Re_{comb}	[-]	Reynolds number for combined (forced and natural) flow
Re_{cr}	[-]	critical Reynolds number
RH	[%]	Relative Humidity
T_∞	[^{o}C]	temperature of the fluid sufficiently far from the surface
T_a	[^{o}C]	air temperature

T_{ce}	[°C]	corrected effective temperature
T_{cl}	[°C]	mean temperature over the clothed body
T_{db}	[°C]	dry-bulb temperature
T_{Dp}	[°C]	Dew Point Temperature
T_e	[°C]	effective temperature
T_{eq}	[°C]	equivalent temperature
T_f	[°C]	film temperature
T_g	[°C]	globe temperature
T_o	[°C]	operative temperature
T_p	[°C]	plate temperature
T_{pc}	[°C]	corrected plate temperature
T_r	[°C]	mean radiant temperature
T_s	[°C]	temperature of the surface
T_{sk}	[°C]	mean skin temperature
T_{wb}	[°C]	wet-bulb temperature
w	[m. s^{-1}]	air velocity
W	[W.m^{-2}]	mechanical work performed by the human body
$WBGT$	[°C]	wet bulb globe temperature
WBT	[°C]	Wet Bulb temperature
w_r	[m. s^{-1}]	relative air velocity against the human body
α	[m^2. s^{-1}]	thermal diffusivity,
β	[K^{-1}]	coefficient of volume expansion
ε	[-]	emissivity of a surface
μ	[N. s. m^{-2}]	dynamic viscosity of the fluid
ρ	[kg.m-^{3}]	density of the fluid
σ	[W. m^{-2}. K^{-4}]	Stefan – Boltzmann's constant
υ	[m^2. s^{-1}]	kinematic viscosity of the fluid

REFERENCES

ADVANTECH. *Data acquisition modules ADAM*, user's manual. Available from: http://www.advantech.com/

ANANTHANARAYANAN, P.N., 2013. *Basic refrigeration and air conditioning*. 4th ed. New Delhi: McGraw-Hill Education (India). ISBN 1259062708.

ARENS, E. and ZHANG, H., 2006. The Skin's Role in Human Thermoregulation and Comfort. *Thermal and Moisture Transport in Fibrous Materials*. Gibson, Woodhead Publishing Ltd, p. 560-602.

ASHRAE, 1966, Thermal comfort conditions, ASHRAE standard 55.66, New York.

ASHRAE, 1981: Thermal environmental conditions for human occupancy, Atlanta, American Society for Heating, Refrigerating and Air Conditioning Engineers.

ASHRAE, 1989. Ventilation for acceptable indoor air quality. ANSI/ASHRAE standard 62, Atlanta.

ASHRAE, 1989a. Physiological principles, comfort and health, in Fundamentals Handbook, Atlanta.

ASHRAE, 1993. Physiological principles and thermal comfort, ASHRAE Handbook of Fundamentals, Chapter 8, Atlanta, USA.

ASHRAE, 1997. Thermal comfort, ASHRAE Handbook of Fundamentals, Chapter 8, Atlanta, USA.

ASHRAE, 2004. User's manual, *thermal environmental conditions for human occupancy*. Atlanta.

ASIMAKOPOULOS, D., SANTAMOURIS, M., ed., 2013. *Passive Cooling of Buildings: BEST (Buildings Energy and Solar Technology)*. New York: Routledge. ISBN 9781134254828.

BALAGURUSAMY, E, 2012. *Numerical methods*. 32nd edition. New Delhi: McGraw-Hill Education. ISBN 0074633112.

BEDFORD, T. and WARNER, C.G., 1934. The globe thermometer in studies of heating and ventilation, *Journal of Hygiene*. Vol. 34, no. 4, p. 458–473.

BEDFORD, T., 1946. Environmental warmth and its measurement. *Medical Research Memorandum*. London: HMSO.

BEDFORD, T., 1951. Equivalent temperature, what it is, how it's measured. *Heating, Piping, Air conditioning*. Aug. p.87-91

BLAIR, Byron E. and A. H. MORGAN, ed., 1972. *Precision measurement and calibration: selected NBS papers on Frequency and time*. Washington: U.S. Department of Commerce. NBS special publication 300, 5.

BLAXTER, K. L., 1989. *Energy metabolism in animals and man*. New York: Cambridge University Press. ISBN 0521369312.

BOBENHAUSEN, William, 1994. *Simplified design of HVAC systems*. New York: Wiley. ISBN 0471532800.

BOHS, 1990. *The Thermal Environment*, British Occupational Hygiene Society Guide No. 8, by Youle, A., Collins, K.J., Crockford, G.W., Fishman, D.S., Parsons, K.C. and Sykes, J., Science Reviews Lid with H and H Scientific Consultants Ltd, Leeds.

BROOKS, G. A., FAHEY, T. D., and WHITE, T. P., 1996. Exercise Physiology, Human Bioenergetics and Its Applications, *Mountain View*, Ca, Mayfield.

BURTON, Alan C. and O. G. EDHOLM, 1955. *Man in a cold environment: physiological and pathological effects of exposure to low temperatures*. London: E. Arnold.

ÇENGEL, Yunus A., c2003. *Heat transfer: a practical approach*. 2nd ed. Boston: McGraw-Hill. ISBN 0072458933.

CHURCHILL, S. W. and CHU, H. S., 1975. Correlating Equations for Laminar and Turbulent Free Convection from a Horizontal Cylinder. *International Journal of Heat Mass Transfer*. Vol. 18, p. 1049.

CHURCHILL, S. W., 1983. *Free Convection Around Immersed Bodies*. In *Heat Exchanger Design Handbook*, ed. E. U. SCHLÜNDER. Section 2.5.7. New York: Hemisphere.

CHURCHILL, S. W., 1998. *Combined Free and Forced Convection Around Immersed Bodies*. Begell House, New York.

CLARK M. BLATTEIS., 1998. *Physiology and pathophysiology of temperature regulation*. Singapore: World Scientific. ISBN 9810231725.

DE DEAR, R.J. and BRAGER, G.S., 1998. Developing an adaptive model of thermal comfort and preference. *ASHRAE Transactions*, Atlanta, USA.

DJONGYANG, Noël, RENÉ, Tchinda, and DONATIEN, Njomo, 2010. "Thermal Comfort: A Review Paper." *Renewable and Sustainable Energy Reviews*. Vol. 14, no. 9, p. 2626-2640.

DOMAT control system. Manufacturer of small globe thermometers. Available from: http://domat-int.com/

Du BOIS, D. and E.F. Du BOIS. 1916. A formula to estimate approximate surface area, if height and weight are known. *Archives of Internal Medicine*. Vol. 17, p. 863–871.

DUFTON, A. F., 1929. The eupatheostat, *Journal of Scientific Instruments*. Vol. 6, p. 249–251.

DUFTON, A. F., 1932. *Equivalent temperature of a room and its measurement*, B R Technical Paper 13. HMSO

EDHOLM, O. G. a J. S. WEINER, 1981. *The principles and practice of human physiology*. New York: Academic Press. ISBN 0122316509.

EDWARDS, D. K., c1981. *Radiation heat transfer notes*. Washington: Hemisphere Pub. ISBN 0891162313.

FANGER, P. O., 1967. Calculation of thermal comfort: introduction of a basic comfort equation, *ASHRAE Transactions*, 73, Part 2.

FANGER, P. O., 1970. *Thermal comfort: analysis and applications in environmental engineering*. Copenhagen: Danish Technical Press. ISBN 8757103410.

FANGER, P. O., 1982. *Thermal comfort: analysis and applications in environmental engineering*. Malabar, Fla.: R.E. Krieger Pub. Co. ISBN 0898744466.

FANGER, P. O., 1994. How to apply models predicting thermal sensation and discomfort in practice. In: Oseland, N.A. and Humphreys, M.A. (eds) *Proceedings Thermal Comfort, Past, Present and Future*, Garston, 11–17.

FIŠER, J., BADER, V., and THOMSCHKE, C., 2014. Impact of convective plume around human body on T_{EQ} measured by equivalent temperature sensors. In *Proceedings of Ambience14& 10i3m*. Proceedings of Ambience, Scientific Conference for Smart Textiles. Tampere, Finlad: Tampere University of Technology. p. 100-104. ISBN: 978-952-15-3269- 6.

GAGGE, A. P., 1937. A new physiological variable associated with sensible and insensible perspiration, *American Journal of Physiology*. Vol. 120, p. 277–287.

GAGGE, A. P., BURTON, A. C., and BAZETT, H. C. A, 1941. Practical System of Units for the Description of the Heat Exchange of Man with his Environment. *Science*. Vol. 94, no. 2445, p. 428-430.

GAGGE, A. P., G.M. RAPPE and J.D. HARDY, 1967. The effective radiant field and operative temperature necessary for comfort with radiant heating, *ASHRAE Journal*. Vol. May, p. 63.

GANONG, William F., 1991. *Review of medical physiology*. 15th ed. Norwalk: Appleton and Lange. Lange medical book. ISBN 0838584187.

GUYTON, Arthur C., 1974. *Function of the human body*. 4th ed. Philadelphia: Saunders. ISBN 0721643779.

HAVENITH, G., HOLMÉR, I., PARSONS, K., 2002. Personal factors in thermal comfort assessment: clothing properties and metabolic heat production. *Energy and Buildings*. Vol. 34, no. 6, p. 581-591.

HENSEN, J.L.M., 1990. Literature review on thermal comfort in transient conditions, *Build. Environ*mental. Vol. 25, p. 309–316.

HOFFMAN, Joe D., 1992. *Numerical methods for engineers and scientists*. New York: McGraw-Hill Book Company. ISBN 0071129626.

HOLMAN, J.P., 2001. *Heat transfer*. 8th SI metric ed. London [etc.]: McGraw-Hill Book Co. ISBN 0070083002.

HOOF, Joost Van, MITJA, Mazej, and HENSEN, Jan, 2010. "Result Filters." National Center for Biotechnology Information. U.S. National Library of Medicine.

HOUGHTON, F. C. and YAGLOGLOU, C.P., 1923. Determining equal comfort lines, *Journal of ASHVE*. Vol. 29, p. 165–176.

HOUGHTON, F. C. and YAGLOGLOU, C.P., 1924. Cooling effect on human beings produced by various air velocities, *Journal of ASHVE*. Vol. 30, p. 193.

HOWELL, John R., c1982. *A catalog of radiation configuration factors*. New York: McGraw-Hill Book Co. ISBN 0070306060.

HUMPHREYS, M. A., and NICOL, J. F., 1995. An adaptive guideline for UK office temperatures. In *Standards for Thermal Comfort*. P. 190–195. Windsor, UK: E & FN Spon.

INCROPERA, Frank P., c2007. *Fundamentals of heat and mass transfer*. 6th ed. Hoboken, NJ: John Wiley. ISBN 0471457280.

INGRAM, D. L. and L. E. MOUNT, 1975. *Man and animals in hot environments*. New York: Springer-Verlag. ISBN 0387068651.

ISO 7243. *Hot environments—estimation of the heat stress on working man, based on the WBGT-index (wet bulb globe temperature)*, 1982. Geneva: International Standards Organization.

ISO 7726. *Ergonomics of the thermal environment. Instruments for measuring physical quantities*, 1998. Geneva: International Standards Organization.

ISO 7730. *Moderate Thermal Environments—Determination of the PMV and PPD indices and specification of the conditions for thermal comfort*, 1994. Geneva: International Standards Organization.

ISO 7933. *Hot Environments—Analytical determination and interpretation of thermal stress using calculation of required sweat rate*, 1989. Geneva: International Standards Organization.

ISO 8996. *Ergonomics of the Thermal Environment: Estimation of metabolic heat production*, 1990. Geneva: International Standards Organization.

JANEČKA, J., MLČÁK, R., KAZKAZ, M., KOŠÍKOVÁ, J., VDOLEČEK, F., and PAVELEK, M., 2011. Komora pro kalibraci senzorů tepelné pohody. FSI VUT. Available from: http://www.energetickeforum.cz/fsi-vut-v-brne/komora-pro-kalibraci-senzoru-tepelne-pohody.

KAZKAZ, M.; PAVELEK, M., 2013. OPERATIVE TEMPERATURE AND GLOBE TEMPERATURE. Engineering Mechanics, N. 3/ 4, P. 319-326. ISSN: 1802- 1484.

KAZKAZ, M.; SATTOUF, M., 2014. Effects of Air Temperature, Mean Radiant Temperature and Air Velocity on The Globe Temperature and Operative Temperature. international journal of energy and environment, N. 8, P. 74-80. ISSN: 2308- 1007.

KERSLAKE, D. McK., 1972. *The Stress of Hot Environments*. London: Cambridge University Press. ISBN 0521083435.

KOŠÍKOVÁ, J., KAZKAZ, M., JANEČKA, J., VDOLEČEK, F., and PAVELEK, M., 2011. Testovací komora pro porovnávání snímačů tepelné pohody. FSI VUT. Available from: http://www.energetickeforum.cz/fsi-vut-v-brne/testovaci-komora-pro-porovnavani-snimacu-tepelne-pohody.

KREITH, Frank, ed., 2000. *The CRC handbook of thermal engineering*. Springer Science & Business Media. ISBN 9783540663492.

KWOK, G. Alison and RAJKOVICH, B. Nicholas, 2010. "Addressing Climate Change in Comfort Standards." *Building and Environment*. Vol. 45, no. 1, p. 18–22.

LECHER, N., 1991. *Heating, Cooling, Lighting: design methods for architects.* New York, John Wiley & Sons. ISBN 0471628875.

LIENHARD, John H., c2011. *A heat transfer textbook*. 4th ed. Mineola, N.Y.: Dover Publications. ISBN 0486479315.

LumaSense Technologies A/S, 2007. *Thermal comfort data logger INNOVA 1221*, user manual. Ballerup, Denmark. Available from: http://www.lumasenseinc.com/

MACPHERSON, R. K., 1962. The Assessment of the Thermal Environment. A Review. *Occupational and Environmental Medicine*. Vol. 19, no. 3, p. 151–64.

MADSEN, T.L., B.W. OLESEN, and N.K KRISTENSEN, 1984. Comparison between operative and effective temperature under typical indoor conditions, *ASHRAE Transaction.* Vol. 90, p. 1077 - 1090.

Mc CULLOUGH, E. A., JONES, B. W., and HUCK, J., 1985. A comprehensive data base for estimating clothing insulation. *ASHRAE Transactions*. Vol. 91 (2A), p. 29–47.

Mc CULLOUGH, E.A. and JONES, B.W., 1984. A comprehensive database for estimating clothing insulation. *Institute for Environmental Research*. Kansas State University, IER Technical Report 84–101, December.

Mc INTYRE D. A. and GRIFFITHS I. S., 1972. 'Radiant temperature and thermal comfort'. *Symposium; Thermal Comfort and Moderate Heat Stress*, CIB Commission W45, BRE, Watford, England.

Mc INTYRE, D.A., 1980. *Indoor Climate*, London: Applied Science.

MITCHELL, D., 1974. Convective heat loss from man and other animals, in J. L. Monteith and L. E. Mount, *Heat Loss from Animals and Man*, London: Butterworths.

MODEST, M. F., c1993. *Radiative heat transfer*. New York: McGraw-Hill. ISBN 0070426767.

MURGATROYD, P. R.; SHETTY, P. S.; PRENTICE, A. M., 1993. Techniques for the measurement of human energy expenditure: a practical guide. *International journal of obesity and related metabolic disorders: journal of the International Association for the Study of Obesity*. Vol. 17, no. 10, p. 549–568.

MUTHAYYA, NM, 2010. *Human physiology*. Fully rev. 4th ed. New Delhi: Jaypee Bros. ISBN 8184487363.

NAŘÍZENÍ VLÁDY, 2002, kterým se mění nařízení vlády č. 178/2001 Sb., kterým se stanoví podmínky ochrany zdraví zaměstnanců při práci. Nařízení vlády č. 523/2002 Sb. Sbírka zákonů ČR.

NAŘÍZENÍ VLÁDY, 2012, kterým se mění nařízení vlády č. 361/2007 Sb., kterým se stanoví podmínky ochrany zdraví při práci, ve znění nařízení vlády č. 68/2010 Sb. Sbírka zákonů ČR.

NIKOLAOS GKIKAS., 2013. *Automotive ergonomics driver-vehicle interaction*. Online-Ausg. Boca Raton: CRC Press. ISBN 9781439894279.

OLESEN, B.W. and DUKES-DUBOS, F.N., 1988, International standards for assessing the effect of clothing on heat tolerance and comfort, in S. Z. Mansdorf, R. Sager and A. P. Nielson (Eds), *Performance of Protective Clothing*, Philadelphia: ASTM, p. 17–30.

OSTRACH, S., 1952. An analysis of laminar free-convection flow and heat transfer about a flat plate parallel to the direction of the generating body force. United States.

PARSONS, K. C., 2003. *Human thermal environments: the effects of hot, moderate, and cold environments on human health, comfort, and performance*. 2nd ed. New York: Taylor & Francis. ISBN 0415237920.

POHLHAUSEN E., 1921. Der Wärmeaustausch zwischen festen Körpern und Flüssigkeiten mit kleiner Reibung und kleiner Wärmeleitung. *Z angew Math Mech*. Vol. 1, p. 115–121.

POSUDIN, Jurij Ivanovič, 2014. *Methods of measuring environmental parameters*. Hoboken: John Wiley. ISBN 9781118686935.

SALVENDY, Gavriel. 2006. *Handbook of Human Factors and Ergonomics*. Hoboken, NJ: J. Wiley.

ANKARA K. RAO., 2007. *Numerical methods for scientists and engineering*. 3rd ed. New Delhi: Prentice Hall of India. ISBN 8120332172.

SCHLICHTING, H., 1951. *Grenzschicht-Theorie*, 3rd edn. Verlag G. Braun, Karlsruhe.

SCHLÜNDER, Ernst-Ulrich, 1975. *Einführung in die Wärme- und Stoffübertragung Skriptum für Maschinenbauer, Verfahrenstechniker, Chemie-Ingenieure, Chemiker, Physiker ab 4. Semester*. 2. Wiesbaden: Springer-Verlag. ISBN 3322855414.

SIEGEL, Robert and John R. HOWELL, c1992. *Thermal radiation heat transfer*. 3rd ed. Washington, D.C.: Hemisphere Pub. ISBN 0891162712.

SMITH, B.J., G.M. PHILLIPS, and M.E. SWEENEY, 1983. *Environmental science*. London: Longman. ISBN 0582416205.

SONG, Guowen., 2011. *Improving comfort in clothing*. Philadelphia: Woodhead Pub. Woodhead publishing in textiles, no. 106. ISBN 1845695399.

SPARROW, E. M. and R. D. CESS, c1978. *Radiation heat transfer*. Augmented ed. Washington: Hemisphere Pub. ISBN 0070599106.

Spektrum. Manufacturer of small globe thermometers. Available from: http://spektrum-ams.cz/.

SRIVASTAVA, A.C. and P.K. SRIVASTAVA, 2011. *Engineering Mathematics: Volume III*. PHI Learning. ISBN 9788120342934.

THORSSON, Sofia, FREDRIK, Lindberg, INGEGÄRD, Eliasson, and BJÖRN Holmer, 2007. "Different Methods for Estimating the Mean Radiant Temperature in an Outdoor Urban Setting." *International Journal of Climatology*. Vol. 27, no.14, p. 1983–1993.

TROTT, A. R. a T. C. WELCH, 1999. *Refrigeration and Air Conditioning*. 3. Butterworth-Heinemann: Technology & Engineering. ISBN 9780080540436.

VERNON, H.M. and WARNER, C.G., 1932. The influence of the humidity of the air on capacity for work at high temperatures. *Journal Hygiene Cambridge*. Vol. 32, p. 431–462.

VERNON, H.M., 1930. The measurement of radiant heat in relation to human comfort, *Journal of Physiology*. Vol. 70, no. 15.

VERNON, Rose, and Barbara COHRSSEN, 2011. *Patty's Industrial Hygiene*. 6th edition. New Jersey: John Wiley. ISBN 9780470769539.

WEBB, P., 1995. The physiology of heat regulation, *Am. J. Physiol Regul Integr Comp Physiol*. Vol. 268, p. 838–850.

WHITAKER S., 1972. Forced Convection heat transfer correlations for flow in pipes, past flat plates, single cylinders, single spheres, and for slow in packed beds and tube bundles. *AIChE J.*, 18:361.

WILSON, John R. and SHARPLES Sarah, 2015. *Evaluation of Human Work*. Boca Raton, FL: CRC, Taylor & Francis Group. ISBN 1466559624.

WINSLOW, C.E. A., HERRINGTON, L.P. and GAGGE, A.P., 1936, A new method of partitional calorimetry, Ibid., 116, 669.

YAGLOU, C. P. and MINARD, D., 1957. Control of heat casualties at military training centers. *American Medical Association Archives of Industrial Health*. Vol. 16, p. 302–316.

YGLOU, C. P., 1947. A method of improving the effective temperature indices, *ASHRAE Transactions*. Vol. 53, p. 307.

ZMRHAL, V., DRKAL, F., MATHAUSEROVA, Z., 2010. Operativní teplota v praxi. *Směrnice Společnost pro Techniku Prostředí*. Prague.

AUTHOR'S PUBLICATIONS

KAZKAZ, M.; PAVELEK, M., 2013. OPERATIVE TEMPERATURE AND GLOBE TEMPERATURE. Engineering Mechanics, N. 3/ 4, P. 319-326. ISSN: 1802- 1484.

KAZKAZ, M.; SATTOUF, M., 2014. Effects of Air Temperature, Mean Radiant Temperature and Air Velocity on The Globe Temperature and Operative Temperature. international journal of energy and environment, N. 8, P. 74-80. ISSN: 2308- 1007.

JANEČKA, J.; MLČÁK, R.; KAZKAZ, M.; KOŠÍKOVÁ, J.; VDOLEČEK, F.; PAVELEK, M.: KOMKAL 2; Komora pro kalibraci senzorů tepelné pohody. FSI VUT; C3/ 0003. URL: http://ottp.fme.vutbr.cz/vysledkyvyzkumu/. (funkční vzorek)

KAZKAZ, M.; PAVELEK, M. Operative temperature and globe temperature. In Sborník příspěvků 31. mezinárodní konference Setkání kateder mechaniky tekutin a termomechaniky. Brno: Vysoké učení technické v Brně, 2012. s. 89-92. ISBN: 978-80-214-4529- 1.

KAZKAZ, M.; WEISMANOVÁ, J. ASSESSMENT OF THE THERMAL COMFORT: THE OPERATIVE TEMPERATURE. In Sborník příspěvků Mezinárodní Masarykovy konference pro doktorandy a mladé vědecké pracovníky 2012. Hradec Králové: MAGNANIMITAS, 2012. s. 2870-2877. ISBN: 978-80-905243-3- 0.

KOŠÍKOVÁ, J.; KAZKAZ, M.; JANEČKA, J.; VDOLEČEK, F.; PAVELEK, M.: TESTKOM 1; Testovací komora pro porovnávání snímačů tepelné pohody. FSI VUT, C3/ 0003. URL: http://ottp.fme.vutbr.cz/vysledkyvyzkumu/. (funkční vzorek)

WEISMANOVÁ, J.; KAZKAZ, M. BUILDING DYNAMIC SIMULATIONS USING STATE-SPACE METHOD. In Sborník příspěvků Mezinárodní Masarykovy konference pro doktorandy a mladé vědecké pracovníky 2012. Hradec Králové: MAGNANIMITAS, 2012. s. 2878-2884. ISBN: 978-80-905243-3- 0.